Competitive Adsorption of Silicic Acid and Arsenite on Goethite

Todd Peter Luxton

Thesis submitted to the Faculty of the Virginia Polytechnic Institute and State University in partial fulfillment of the requirements for the degree of

Master of Science
in
Soil Chemistry

Matthew J. Eick (Chair)
Lee W. Daniels
Christopher J. Tadanier
Lucian W. Zelazny

Keywords: Competitive Adsorption, Surface Complexation Modeling, CD-MUSIC Model, Fe-hydroxide, Goethite, Arsenite, Silicic Acid

Copyright © December 28, 2002 by Todd Luxton

Competitive Adsorption of Silicic Acid and Arsenite on Goethite

Todd Peter Luxton

Thesis Abstract

The adsorption behavior of silicic acid and arsenite alone and competitively on goethite over a broad pH range (3-11) at environmentally relevant concentrations was investigated utilizing pH adsorption data and zeta potential measurements. Both addition scenarios (Si before As(III) and As(III) before Si) were examined. The results of the adsorption experiments and zeta potential measurements were then used to model the single ion and competitive ion adsorption on goethite with the CD-MUSIC model implemented in the FITEQL 4.0 computer program. Silicic acid adsorption was reduced by the presence of arsenite for all but one of the adsorption scenarios examined, while in contrast silicic acid had little effect upon arsenite adsorption. However, the presence of silicic acid, regardless of the addition scenario, dramatically increased the arsenite equilibrium solution concentration over the entire pH range investigated. The CD-MUSIC model was able to predict the single ion adsorption behavior of silicic acid and arsenite on goethite. The modeled zeta potential data provided further evidence of the CD-MUSIC model's ability to describe the single anion adsorption on goethite. Our model was also able to collectively describe adsorption and zeta potential data for the low Si-arsenite adsorption scenario quite well however, our model under-predicted silicic acid adsorption for the high Si-arsenite competitive scenario.

Authors Acknowledgements

The number of people that should be mentioned in this section is staggering. I have been blessed to have had the opportunity to work with and befriend countless members of the Virginia Tech community who have helped to make this an incredible experience. First and foremost, I would like to thank my advisor Dr. Matthew Eick. Matt has been a continual source of knowledge and wisdom, I couldn't have had a better mentor and advisor. His understanding nature of my sometimes clumsy hands has also been a wonderful asset. Next I would like to thank the rest of my committee: Dr. Christopher Tadanier, Dr. Lucian Zelazny, and Dr. Lee Daniels for their time, wisdom and patience. Chris helped to push and pull me through the dreaded learning curve associated with surface complexation modeling and the CD-MUSIC model. I am very grateful that through all of my stumbling he never through me out of his office or attempted to strangle me, even though I begged him at times. Dr. Zelazny has helped to provided me with a firm foundation in soil chemistry and mineralogy, and a wonderful appreciation for the complexity of soils. I am very grateful the willingness of Lee to become a member of my committee, and for his support throughout the last summer. I cannot thank him enough for helping me to remain at Virginia Tech. Finally I need to thank my fellow graduate students in the CSES department and Hubert Walker and W.T. Price who helped to keep me smiling and laughing throughout the whole process.

Besides the support I have received at Virginia Tech, I would also like to express my deepest gratitude to my parents, Pete and Linda, and my brother, Matt, for their support, words of encouragement, phone calls and visits. I am very blessed to be a part of this family. I also want to thank Michele for her continued support, words of wisdom, thoughts, and friendship. Finally, I would like to thank Natalie for everything she does and everything she is.

Last but not least I would like to thank God for providing me with this opportunity, and seeing me through it.

Table of Contents

List of Figures

List of Tables

1. Chapter Theoretical Background

Abstract—Modeling adsorption of aqueous ions by naturally occurring colloidal particles, in an attempt to better understand the underlying physiochemical properties governing the bioavailability of contaminants and nutrients in the biosphere, is of primary interest in environmental soil and geochemistry. The use of surface complexation models (SCM) to elucidate potential surface chemical species and bonding mechanisms from ion adsorption data has become a useful tool in determining the fate of environmental contaminants and nutrients. Surface complexation models describe the adsorption of aqueous ions onto mineral surfaces utilizing a thermodynamic approach where surface reactions are described through a series of mass law and material balances. All SCM's are comprised of an adsorption model that defines the type(s) and reactivity of surface adsorption sites, and an electrostatic model that describes the placement of ions into discrete electrostatic planes that define the electric double layer, and mathematical relationships between charge and potential at the mineral-water interface. The recently developed charge-distribution multi-site ionic composition (CD-MUSIC) model has improved upon existing SCM's by: i) incorporating mineral crystallographic parameters into the description of mineral surface sites in the adsorption model, and ii) allowing for the distribution of charge, due to specifically adsorbing ions, between electrostatic planes making it one of the most fundamentally complete SCM. Both the TLM and the CD-MUSIC model were used to describe silicic acid adsorption on goethite. Both models were able to accurately describe silicic acid adsorption; however the CD-MUSIC model provided a more accurate description of zeta potential data collected for silicic acid adsorption on goethite.

The surface and colloid chemistry of soils and sediments is largely determined by two properties: surface area and the presence of a surface electrical potential (Gast, 1977). The development and magnitude of the surface potential controls several physical and chemical properties pertinent to soils including ion exchange, particle-particle interactions, ion adsorption, single and multiple ion activity measurements, mineral precipitation, and redox potential (Gast, 1977; McBride, 1994; Sparks, 1999; Sposito, 1989; Zelazny et al., 1996). Extensive efforts have been put forth by soil and surface scientists to measure and model surface charge and ion adsorption in order to better understand and predict the chemical and physical properties of soils and sediments. This information is critical for understanding the potential bioavailability of contaminants and nutrients in the environment.

Surface Charge

Charge on soil colloids is a result of one of two phenomenon; structural imperfections in the mineral lattice and chemical reactions of surface ionizable groups (Gast, 1977; McBride, 1994; Sparks, 1999; Sposito, 1989; Zelazny et al., 1996). Structural imperfections resulting in the development of mineral surface charge are the result of isomorphous substitution and/or site vacancies within the crystal lattice - isomorphous substitution is a common occurrence in phyllosilicates and zeolites. Surface charge developed in this manner exhibits a constant or permanent charge (σ_{CC}) that is independent of the surrounding environmental conditions, including pH, ionic strength, and solution ion composition (Davis and Kent, 1990; Gast, 1977; Sparks, 1999; Sposito, 1989).

Colloidal surface charge developed from dissociation at or preferential adsorption of ions by surface ionizable functional groups is termed variable charge in colloids and is characteristic of oxides, organic matter, (oxy)hydroxides, carbonates, silicates, and the edges of phyllosilicates and zeolites (Davis and B., 1990; Sparks, 1999; Sposito, 1989).

The most abundant surface functional group associated with hydrated metal oxides, hydroxides, oxyhydroxides, clay minerals, and amorphous hydroxides is the hydroxyl group (OH) (Sposito, 1989). Typically, more than one type of hydroxyl group can be identified at mineral surfaces based on the number of coordinating cations (McBride, 1994; Parks, 1990; Sparks, 1999; Sposito, 1989; Stumm, 1992a). The variation in the type of surface functional groups can be explained using goethite as an example.

The goethite structure is comprised of double chains of $FeO_3(OH)_3$ octahedra that run parallel to the c-axis as shown in Fig. 1.1. The oxygen or hydroxide ligand may be coordinated to one, two, or three Fe atoms in the goethite structure termed singly, doubly, or triply coordinated surface groups, respectively (Fig. 1.1b). Research has shown that each OH group exhibits different affinities for water, protons, and aqueous ions (Hiemstra et al., 1989b; Hiemstra et al., 1989a; Hiemstra and Van Riemsdijk, 1999; McBride, 1994; Schwertmann and Cornell, 1996; Sparks, 1999; Sposito, 1984; Stumm, 1992a; Tadanier and Eick, 2002). Because ionization of surface hydroxyls on goethite is strongly pH-dependent the surface charge is also very dependent upon pH.

A

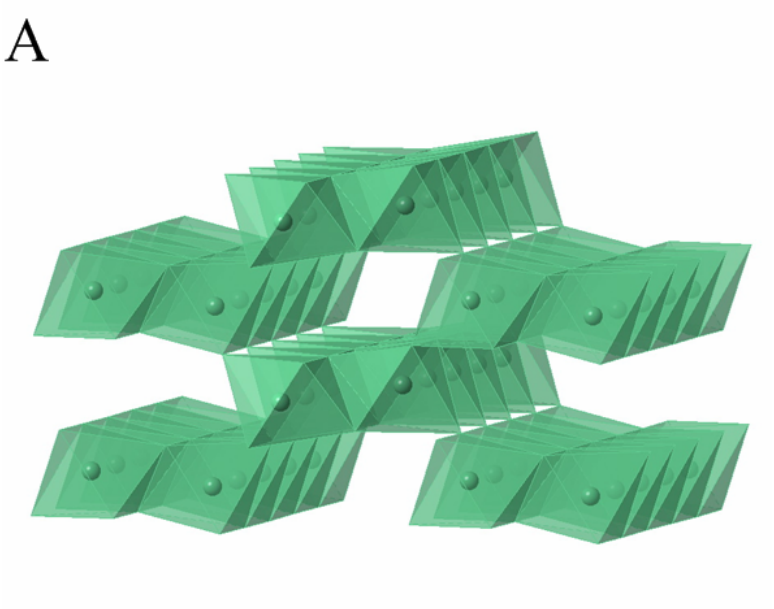

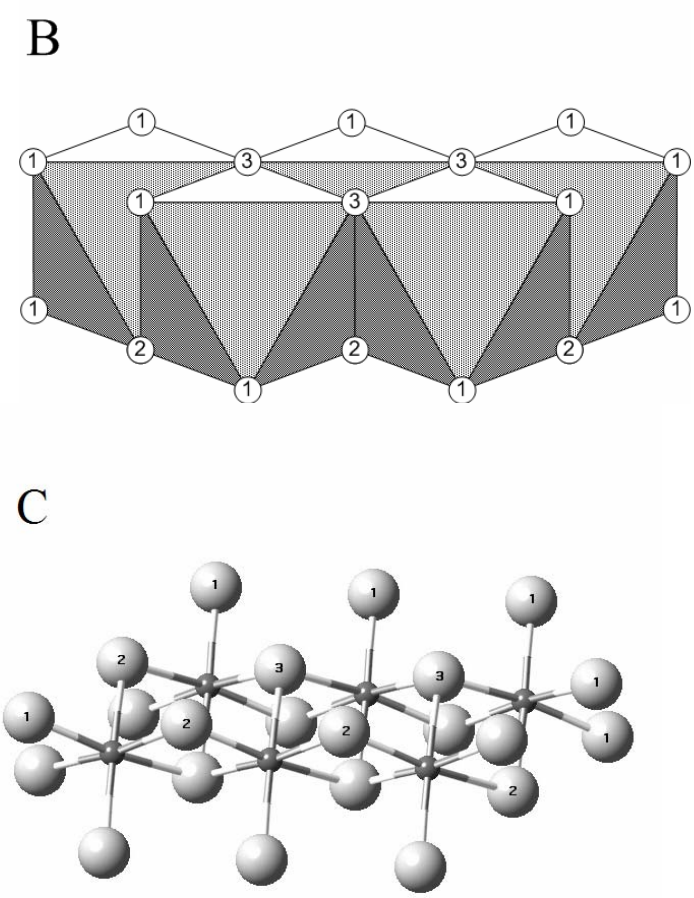

Figure 1.1. A) Polyhedral model of goethite superstructure. B) Polyhedral model indicating the number Fe atoms that surface oxygens are coordinated with. C) Ball and stick model indicating the number of Fe atoms that oxygen is coordinated with.

The term *surface acidity* is used to describe the surface ionization reactions responsible for amphoteric behavior of oxide and hydroxide minerals (Dzombak and Morel, 1990; Hiemstra et al., 1989a; Hiemstra and Van Reinsdijk, 1996; Hiemstra and Van Riemsdijk, 1999; Sposito, 1989; Stumm, 1992a; Westall, 1980; Zelazny et al., 1996). The protonation of amphoteric surface ligands can be described in a two step process, as depicted in Eq. 1, with two association constants (Eq. 2 and 3).

$$\equiv XO^- + H^+ \overset{K_1^S}{\leftrightarrow} \equiv XOH^0 + H^+ \overset{K_2^S}{\leftrightarrow} \equiv XOH_2^+ \qquad \textbf{(1)}$$

$$K_1^S = \frac{(\equiv XOH^0)}{(\equiv XO^-)(H^+)} \quad \textbf{(2)}$$

$$K_2^S = \frac{(\equiv XOH_2^+)}{(\equiv XOH^0)(H^+)} \quad \textbf{(3)}$$

where

K^S = surface association constant

X = the bulk mineral cation

( ) = activity.

Particle charge then depends on the extent of surface protonation/deprotonation and other surface coordinated ions (Stumm, 1992a; Zelazny et al., 1996). At low ionic strengths when the correction for solution ion activity is minimal, molar concentrations may be substituted for activity. Surfaces generally exhibit a positive charge at low pH and negative charge at high pH values based upon the protonation of surface functional groups (Sposito, 1989; Stumm, 1992a; Zelazny et al., 1996).

General Aspects of Ion Adsorption

Ion adsorption is the net accumulation of matter at the interface between a particle surface and the solution phase (Sposito, 1989). Ion adsorption can be separated into two categories; specific (inner-sphere) and non-specific (outer-sphere) adsorption (Fig. 1.2).

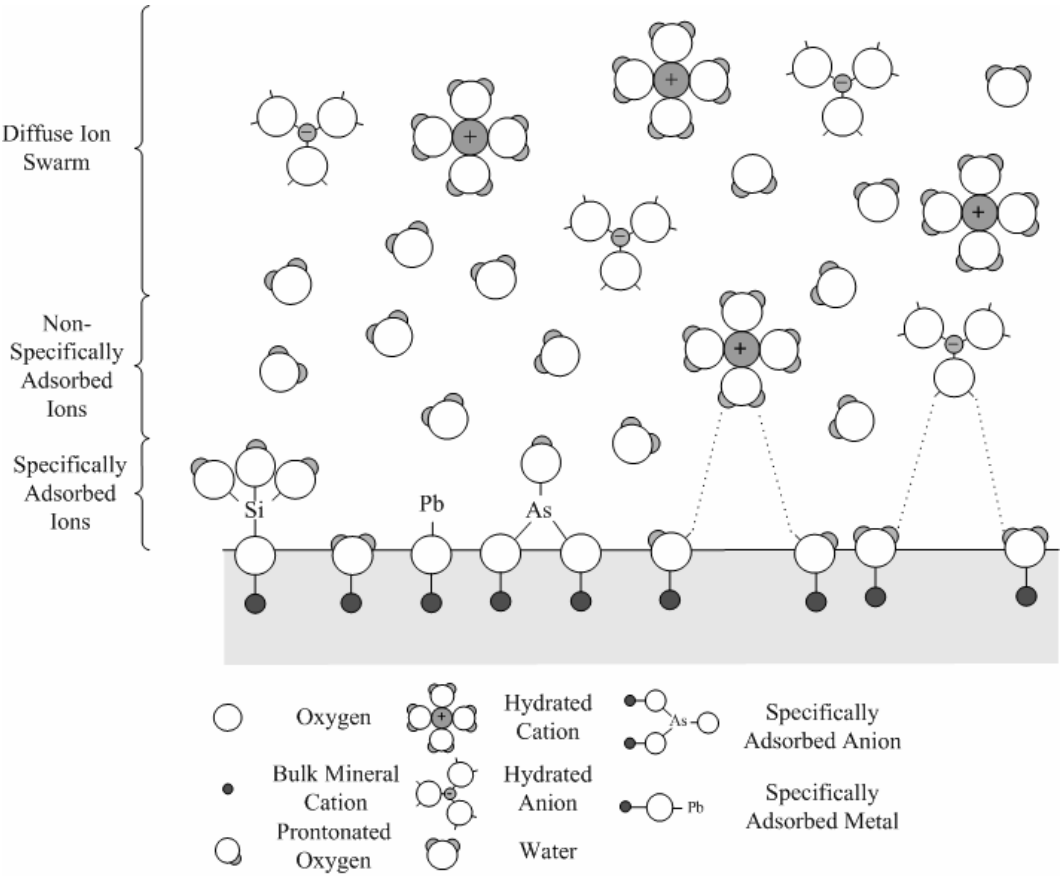

Figure 1.2. Mechanisms of ion adsorption.

Non-specific adsorption refers to solvated ions that form a weakly bound complex with specific surface groups. The weakly bound complex interacts with surface functional groups forming an outer-sphere complex, as represented in the following equations

$$\equiv XO^- + Na^+ \leftrightarrow \equiv XO^- \cdots Na^+ \quad \textbf{(4)}$$

$$\equiv XO^- + NO_3^- \leftrightarrow \equiv XO^- \cdots NO_3^- \quad \textbf{(5)}$$

where the dotted line indicates a weak molecular interaction (e.g. hydrogen, electrostatic, and van der Waals bonding) in Equations 4 and 5 and Figure 1.2 (Sposito, 1989; Stumm, 1992b; Zelazny et al., 1996). Ions located in the diffuse ion swarm balance the remaining surface charge in a delocalized sense (Fig. 1.2).

Specific adsorption refers to solution ions that form a complex with a specific charged surface functional group(s) (Sposito, 1989; Stumm, 1992b). Typically, ions that are specifically adsorbed form more stable surface complexes than non-specifically adsorbed ions, due to the formation of ionic and/or covalent bonds between the ion and the surface. During the formation of cation inner-sphere complexes (e.g. Pb^{2+} and Cu^{2+}) the surface hydroxyl groups act as charge donors and increase the overall electron density of the coordinated metal, altering many of its chemical properties (Eq. 6 Fig. 1.2).

$$\equiv XOH + Pb^{+2} \rightarrow \equiv XOPb^{+} + H^{+} \quad \textbf{(6)}$$

During the formation of anion inner-sphere complexes (e.g. CrO_4^{2-} and AsO_3^{3-}), mineral cations act as Lewis acids exchanging the electrons of the surface OH group(s) with those of the adsorbate. The process of anion inner-sphere complex formation (Eq. 7, Fig. 1.2) is referred to as a ligand exchange reaction; anions that possess electron donating coordination groups are often referred to as ligands (McBride, 1994; Stumm, 1992a).

$$\equiv XOH + AsO_3^{-3} \rightarrow \equiv XOAsO_2^{-2} + OH^{-} \quad \textbf{(7)}$$

Equations 6 and 7 describe the formation of monodentate mononuclear surface species. This notation indicates the formation of one bond from the adsorbate to the adsorbent (monodentate) and that the oxygen shared by the adsorbate and the mineral cation is bound to only one cation within the mineral structure (mononuclear) (Fig. 1.3).

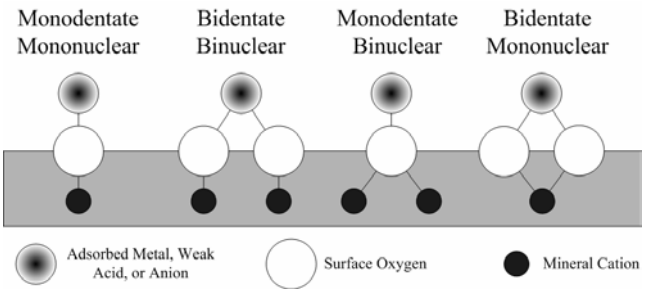

Figure 1.3. Diagram of different types of surface complexes on a hypothetical mineral surface.

In addition to monodentate mononuclear surfaces species bidentate (mono and binuclear) and multidentate (mono, bi, and trinuclear) species can form at the mineral interface (McBride, 1994; Sposito, 1989; Stumm, 1992a). The formation of inner sphere complexes on (oxy)hydroxide mineral surfaces is strongly dependent upon the pH of the system, which influences the protonation of the adsorbent and adsorbate (Stumm, 1992b).

Surface Complexation Models

Surface complexation models (SCM) describe the adsorption of aqueous ions onto mineral surfaces utilizing a thermodynamic approach where surface reactions are described through a series of mass law and material balances (Westall and Hohl, 1980; Westall, 1986). All SCM's share two common attributes: i) the Gibbs Free energy for surface chemical reactions is separated into chemical and electrostatic components and ii) the electric double layer (EDL) adjacent to the surface contains adsorbed ions placed in one or more specified electrostatic planes in which the potential and charge of the plane are related by an electrostatic model (Tadanier and Eick, 2002; Westall and Hohl, 1980; Westall, 1980). The difference between SCMs lies within the description of the EDL and the distribution of ions to mean planes of adsorption. Although the description of the solid-solution interface varies between models, all

SCMs contain an adsorption model which defines the type(s) and reactivity of surface adsorption sites, and an electrostatic model that specifies the location of charge for the adsorbed species in electrostatic planes that define the mathematical relationships between charge and electric potential for each electrostatic plane.

Adsorption Energetics

Ion adsorption onto a charged surface, as previously stated, involves both chemical and electrostatic changes in the Gibbs Free energy of the system. The relative contribution of each can be determined by separating the total free energy of adsorption into its component parts,

$$\Delta G^0_{tot} = \Delta G^0_{\text{int}} + \Delta G^0_{coul} \quad \textbf{(8)}$$

where

ΔG^0_{tot} = total Gibbs free energy (J mol^{-1})

ΔG^0_{int} = intrinsic Gibbs free energy (chemical free energy) (J mol^{-1})

ΔG^0_{coul} = columbic Gibbs free energy (electrostatic) (J mol^{-1})

Sposito (1984) and Westall (1986) have both reported that the electrostatic term can be theoretically derived from considering the work needed to move an ion of formal charge Z through the interfacial potential gradient. This is expressed mathematically as

$$\Delta G^0_{coul} = \Delta Z F \Psi \quad \textbf{(9)}$$

where

ΔZ = change in the surface charge

F = Faraday's constant (96,485 C mol^{-1})

Ψ = surface potential (V).

In classical thermodynamics, the intrinsic Gibbs Free Energy at standard state is equal to the negative product of the gas constant and temperature multiplied by the natural log of the equilibrium constant of the reaction

$$\Delta G_{\text{int}}^{0} = -RT \ln K^{\text{int}} \quad \textbf{(10)}$$

where

R = gas constant (8.314 J K^{-1} mol^{-1})

T = absolute temperature (K)

K^{int} = thermodynamic equilibrium constant at standard state.

Based on Eq. 9 and 10, Eq. 8 can be rewritten as

$$K^{app} = K^{\text{int}} e^{-\Delta ZF\Psi / RT} \quad \textbf{(11)}$$

where

K^{app} = apparent equilibrium constant

K^{int} = intrinsic equilibrium constant

The difference between the two equilibrium constants arises from the fact that the intrinsic value only considers chemical free energy, while the apparent constant includes both electrostatic and chemical free energy. The exponential term in Eq. 11 represents the Boltzman factor, which has been used to mathematically describe the influence of surface potential on ion adsorption on charged surfaces. In order to apply Eq. 11 to a particular adsorption problem an adsorption model and an electrostatic model are needed to calculate K^{app} and $e^{(-\Delta ZF\Psi / RT)}$, respectively. The adsorption model defines the reactivity and type(s) surface sites, while the electrostatic model specifies the location of the adsorbed species within the EDL and relates the charge associated with an adsorption plane to the electrostatic potential at that plane.

Electric Double Layer Models

Electric double layer models describe the placement of ions into discrete electrostatic planes that define the EDL, and mathematical relationships between charge and potential at the mineral-water interface. Current models of the EDL are based on the work of Gouy (1910) and Chapman (1913) who first quantitatively described the behavior of the EDL and Stern (1924) who proposed the idea of specific adsorption at the solid-solution interface.

Gouy (1910) and Chapman (1913) were among the first to conclude that the distance between charge on a colloid surface and the charge balancing solution counterions exceeded molecular dimensions. Furthermore, they concluded that the counter (opposite charge) and coions (same charge), because they are free to move to some extent, form a diffuse cloud at the mineral-water interface that they referred to as the diffuse double layer (Zelazny et al., 1996). They proposed that within the EDL, colloidal surface charge is balanced by adsorption of counterions and negative adsorption (exclusion) of coions with the bulk of the counter ions occurring near the surface and becoming exponentially more dilute with increasing distance away from the surface (Fig. 1.4) (Parks, 1990).

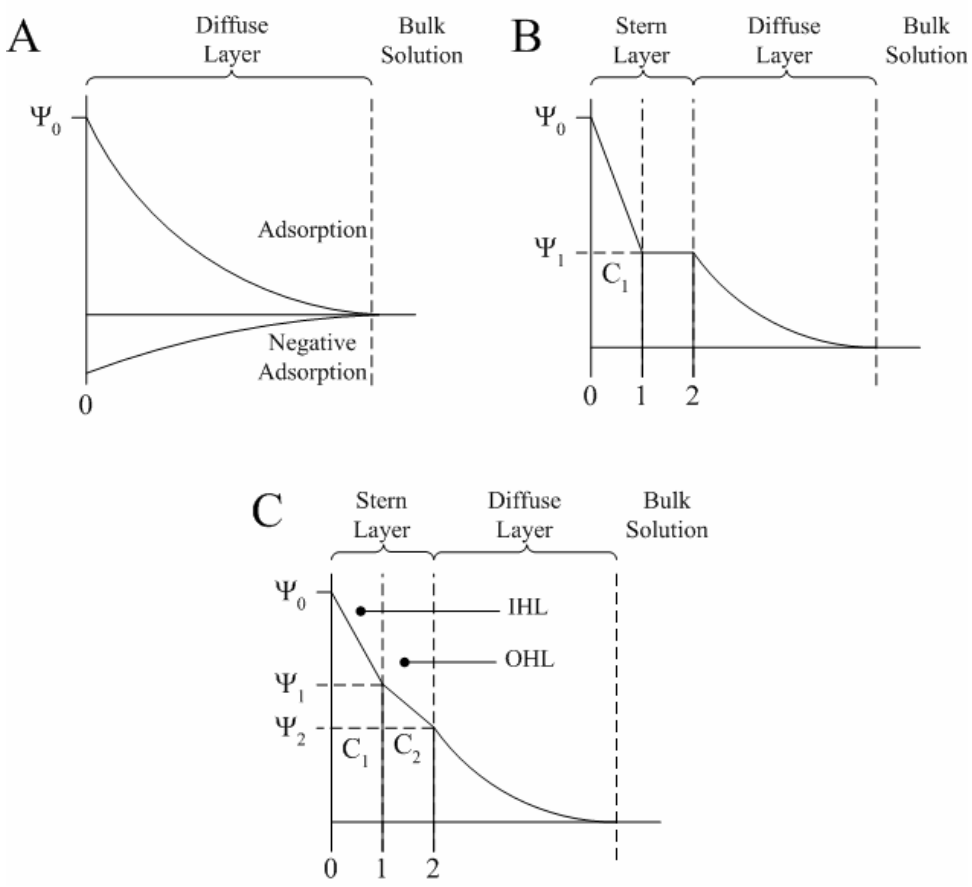

Figure 1.4. Idealized schematic drawing of the electrostatic models illustrating the electric potential decay as a function of distance from the surface and the location of the electrostatic adsorption planes. Diagram assumes conditions typical of a hydroxide surface. A. Gouy Chapman Diffuse Double Layer Model B. Basic Stern Model C. Extended Stern Model

Gouy (1910) and Chapman (1913) were able to model the behavior of electrolyte ions within the EDL by describing the relationship between electrical potential and charge with a one dimensional application of the Poisson-Boltzman Equation

$$\frac{\delta^2\Psi}{\delta x^2} = -\frac{\rho}{\varepsilon\varepsilon_0} \qquad \textbf{(12)}$$

where

Ψ = potential (V)

x = distance from the surface (cm)

ρ = space charge density (C cm^{-3})

ε = dielectric constant (78.5 for water at 298.15 K)

ε_0 = permittivity of free space ($8.854*10^{-14}$ C V^{-1} cm^{-1})

The general form of the Gouy Chapman Diffuse Double Layer model provides an explanation for the behavior of electrolyte ions in regards to ion distribution, counter ion condensation, and electrical potential as a function of distance (x) from the surface

$$\frac{d^2\Psi}{dx^2} = \frac{\kappa^2 \sinh(zF\Psi / RT)}{2F / RT} \quad \textbf{(13)}$$

where

Ψ = potential (V)

x = distance from the surface (cm)

κ = reciprocal thickness of the double layer (cm^{-1})

z = electrolyte ion charge

F = Faraday's constant (96,485 C mol^{-1})

R = gas constant (8.314 J K^{-1} mol^{-1})

T = absolute temperature (K).

Equation 13 can be solved for the diffuse layer charge yielding the following equation (Stumm, 1992a)

$$\sigma_D = -(8RT\varepsilon\varepsilon_0 c \times 10^3)^{1/2} \sinh\left(\frac{zF\Psi_2}{2RT}\right) \quad \textbf{(14)}$$

where

σ_D =diffuse layer charge (C)

ε = dielectric constant (78.5 for water at 298.15 K)

ε_0 = permittivity of free space ($8.854*10^{-14}$ C V^{-1} cm^{-1})

c = electrolyte concentration (M)

Ψ_D = potential at the 2-plane (V)

z = ion valence.

Invoking electroneutrality for the particle double layer system the surface charge is:

$$\sigma_0 = -\sigma_D \quad \textbf{(15)}$$

The Gouy-Champan EDL model was the first model to quantitatively describe the relationship between surface charge (σ_0) and surface potential (Ψ_0) in the EDL and accurately predict the behavior of electrolyte ions at a charged surface. However, two limiting factors prevent its universal application in surface complexation models. First, the model assumes that ions in solution can approach the surface without limit and only electrostatic interactions occur. This limitation poses a problem particularly for variable charge minerals at large surface potential values, moderate to high ionic strengths, and ionic species that are known to coordinate with a mineral surface. Secondly, the model assumes ions to be point charges without volume. This poses a problem at moderate to high ionic strengths when the number of ions predicted to occur in the EDL exceeds the molecular dimensions of the EDL (Gast, 1977).

The problems associated with the Gouy Chapman Diffuse Double Layer model of the EDL were addressed by Stern when he proposed the existence of specifically adsorbed layer ions at the solid-solution interface (Stern, 1924). Stern hypothesized that specifically adsorbed ions occurred at the surface in a region he called the Stern layer. Furthermore, Stern proposed that the Stern layer resembled a parallel plate capacitor, in that electric potential linearly decreased across the Stern layer (capacitor) as a modification to the Gouy-Chapman model (Fig. 1.4). By proposing the existence of an adsorbed layer of ions at the solid-solution interface, followed by a

diffuse double layer as proposed by Gouy and Chapman, Stern was able to refine the limitation imposed on the electrical capacity of the EDL by the finite size of ions (Stern, 1924).

Stern (1924) divided the adsorbed layer into two regions, the Inner and Outer Helmholtz Layers and three adsorption planes, the 0-, 1-, and 2-plane, respectively (Fig. 1.4). Stern specified that the Inner Helmholtz Layer (IHL) contained specifically adsorbed ions with the ion charge residing at either the 0- or 1-plane depending on the ion. The Outer Helmholtz Layer (OHL) was then comprised of fully solvated ions non-specifically adsorbed to the mineral surface with the ion charge residing at the 2-plane (Stumm and Morgan, 1996; Westall, 1986). As a result of accounting for specific and non-specific adsorption in the IHL and OHL, the concentration of and the potential associated with ions located in the diffuse layer is greatly reduced, thus decreasing the inherent error of assuming ions to be point charges (Gast, 1977). The reduction in potential, from the mineral surface to the outer edge of the Stern layer, is a result of treating the adsorbed ions as having specific electrostatic and chemical attractions with the surface (Gast, 1977; Westall and Hohl, 1980). Stern (1924) hypothesized that the IHL and OHL acted as molecular capacitors, arranged in series with specific capacitance factors of C_1 and C_2, respectively (Fig. 1.4). Through the application of electrostatic theory of a molecular capacitor the charge-potential relationship for the IHL is

$$\sigma_0 = C_1(\Psi_0 - \Psi_1) \quad \textbf{(16)}$$

where

Ψ_0 = potential at the mineral surface (V)

Ψ_1 = potential at the 1-plane (V)

σ_0 = surface charge (C)

C_1 = capacitance of the IHP (Farads m^{-2}).

The capacitance factor in Eq. 16 is defined from the theory electrostatics as

$$C = \frac{\varepsilon\varepsilon_0}{d} \quad \textbf{(17)}$$

where

ε = dielectric constant (78.5 for water at 298.15 K)

ε_0 = permittivity of free space ($8.854*10^{-14}$ C V^{-1} cm^{-1})

d = distance between the charged planes (cm).

Similarly, charge-potential relationship for the OHL is mathematically expressed as

$$\sigma_2 = C_2(\Psi_2 - \Psi_1) \quad \textbf{(18)}$$

From the principal of electroneutrality the charge at the 1-plane is equal to

$$\sigma_1 = -(\sigma_0 + \sigma_2) \quad \textbf{(19)}$$

and the resulting charge potential relationship for the 1-plane would then be

$$\sigma_1 = C_1(\Psi_1 - \Psi_0) + C_2(\Psi_1 - \Psi_2) \quad \textbf{(20)}$$

The net charge of ions in the diffuse layer is calculated from the Gouy-Chapman relationship

$$\sigma_2 = -(8RT\varepsilon\varepsilon_0 c \times 10^3)^{1/2} \sinh\left(\frac{zF\Psi_2}{2RT}\right) \quad \textbf{(21)}$$

where

σ_2 = the charge in the diffuse double layer

Ψ_2 = the electrostatic potential at plane 2.

Because Stern viewed the IHL and OHL as two parallel plate capacitors arranged in series, it is possible to calculate the total capacitance across the Stern Layer from the equation

$$\frac{1}{C_T} = \frac{1}{C_1} + \frac{1}{C_2} \quad \textbf{(22)}$$

where

C_T = the total capacitance across the Stern Layer

C_1 = the capacitance of the IHL

C_2 = the capacitance across the OHL

While Stern recognized that the capacitance factor between the 1- and 2-plane should be included in the model of the EDL, he concluded that the error introduced from excluding the 2-plane in the electrical properties would be small, and excluded it from his calculations. The simplified model, containing one capacitance factor is commonly referred to as the Stern Model, while the model of the EDL that includes the second capacitance factor is commonly referred to as the Extended Stern Model (Westall, 1986) or more simply, as the Three Plane Model (Hiemstra et al., 1989a and Hiemstra and Van Reinsdijk, 1996).

Within the constraints of the Stern model, the charge of ions closely associated with the mineral surface are placed in the 0 plane located at the mineral surface and contribute to the surface charge (σ_0) and surface potential (Ψ_0). However, for oxide surfaces this usually only includes H^+ and OH^- ions (Westall, 1986). The charge at the 0-plane can then be calculated from the net adsorption of H^+ and OH^-

$$\sigma_0 = (n_{H^+} + n_{OH^-})eN_A S_D^{-1} A \quad \textbf{(23)}$$

where

σ_0 = surface charge (C m^{-2})

n_{H^+} = net H^+ adsorption (M)

n_{OH^-} = net OH^- adsorption (M)

e = charge of and electron ($1.602*10^{-19}$)

N_A = Avogadro's number ($6.023*10^{23}$)

S_D = suspension density (g L^{-1})

A = specific surface area (g m^{-2}).

Located at the outer edge of the IHL and OHL are the 1- and 2-planes respectively. The 1-plane is comprised of a layer of non-solvated ions that are attracted to the surface by specific chemical interactions with a charge of σ_1 and an electric potential of Ψ_1. The 2-plane is comprised of fully solvated ions non-specifically adsorbed to the surface by electrostatic interactions with a charge of σ_2 and an electric potential of Ψ_2. Charge balance equations for the 1- and 2-plane are postulated in the same manner as for the 0-plane

$$\sigma_1 = (n_{SAC} + n_{SAA})eN_A S_D A \quad \textbf{(24)}$$

where

n_{SAC} = specifically adsorbed cations (M)

n_{SAA} = specifically adsorbed anions (M)

$$\sigma_2 = (n_{NSAC} + n_{NSAA})eN_A S_D A \quad \textbf{(25)}$$

where

n_{NSAC} = non-specifically adsorbed cations (M)

n_{NSAA} = non-specifically adsorbed anions (M)

The introduction of the Inner-Helmholtz and Outer-Helmholtz adsorption layer provides greater reliability in predicting adsorption on high surface potential minerals and in high ionic strength solutions and increased reliability in predicting the concentration and behavior of ions in the diffuse layer (Gast, 1977; Stumm, 1992a; Westall, 1980; Zelazny et al., 1996).

Adsorption Models

Surface Complexation Models rely upon an adsorption model to define the type(s) and reactivities of functional groups present at the mineral surface. Currently, two different and relatively simple models have been proposed to describe surface acidity. Both models consider the mineral surface to be comprised of a homogeneous array of hydroxyl functional groups that behave as weak monoprotic or diprotic acids in solution (Westall, 1986). Both models are thermodynamically consistent and easily described by mass-action and mass-balance equations containing a fixed number of unknown variables and adjustable parameters (Westall, 1986).

The weak diprotic acid model ($2pK_a$) assumes that surface hydroxyl groups behave as weak diprotic acid groups that undergo a two-step protonation reaction as represented in the following equations:

$$\equiv XO^- + H^+ \overset{K_{a1}}{\leftrightarrow} \equiv XOH^0 \quad \textbf{(26)}$$

$$\equiv XOH^0 + H^+ \overset{K_{a2}}{\leftrightarrow} \equiv XOH_2^+ \quad \textbf{(27)}$$

Representing the surface functional groups as diprotic acids incorporates a modest amount of complexity (two dissociation constants) and allows for easy representation of the zero charge state. The mass-action expressions for the $2pK_a$ model are derived in the following manner

$$K_{a1} = \frac{(\equiv XOH^0)}{(\equiv XO^-)(H^+)} e^{-\Delta ZF\Psi_0 / RT} \quad \textbf{(28)}$$

$$K_{a2} = \frac{(\equiv XOH_2^+)}{(\equiv XOH^0)(H^+)} e^{-\Delta ZF\Psi_0 / RT} \quad \textbf{(29)}$$

where

( ) = activity

$e^{-\Delta ZF\Psi_0/RT}$ = the electrostatic energy required to bring an ion against the potential difference from the bulk solution to the surface.

The mass-balance equation for the $2pK_a$ model is expressed in the following manner

$$N_S = n_{\equiv XOH_2^+} + n_{\equiv XOH^0} + n_{\equiv XO^-} \quad \textbf{(30)}$$

where

N_S = the total surface site density (sites m^{-2})

n = the surface site density of each species (sites m^{-2}).

The weak monoprotic acid ($1pK_a$) model, as proposed by Bolt and Van Riemsdjik (1982), considers surface functional groups to be comprised of weak monoprotic acids with the ability to represent both positive and negative charge. The surface protonation reaction, as presented in the following equation does not contain an inherent neutral species; instead the condition of zero charge occurs only when pH equals the pK_a.

$$\equiv XO^{0.5-} + H^+ \overset{K_a}{\leftrightarrow} \equiv XOH^{0.5+} \quad \textbf{(31)}$$

The mass-action and mass-balance equations associated with the $1pK_a$, model are of the same form as the equations described for the $2pK_a$ model and are presented in the following two equations respectively.

$$K_a = \frac{(\equiv XOH^{0.5+})}{(\equiv XO^{0.5-})(H^+)} e^{-\Delta ZF\Psi_0/RT} \quad \textbf{(32)}$$

$$N_S = n_{\equiv XO^{0.5-}} + n_{\equiv XOH^{0.5+}} \quad \textbf{(33)}$$

Using only one chemical reaction to describe the surface charging phenomenon simplifies model calculations and further constrains the outcome by providing one less parameter. It should also be noted that Westall and Hohl (1980) concluded that the $2pK_a$ model reduces to the $1pK_a$ model

when $K_{a1} << K_{a2}$ or when $K_{a1} = K_{a2}$ due to the fact the neutral $\equiv XOH^0$ species becomes insignificant in the mass-balance expressions.

Both the $1pK_a$ and $2pK_a$ adsorption models are equally suited for predicting adsorption behavior of protons onto mineral surfaces (Westall, 1986), however recent research has suggested that the $1pK_a$ model is better suited for describing protonation and deprotonation behavior of (oxy)hydroxide minerals (Geelhoed et al., 1997; Geelhoed et al., 1998; Hiemstra et al., 1989b; Hiemstra et al., 1996; Hiemstra and Van Reinsdijk, 1996; Hiemstra and Van Riemsdijk, 1999; Hiemstra and Van Reimsdijk, 2000; Reitra et al., 1999; Rietra et al., 1999; Rietra et al., 2000; Tadanier and Eick, 2002; Weerasooriya et al., 2002). Additionally, when the actual mineral surface is considered, accounting for different crystal faces, edges, and lattice defects, it becomes obvious that both adsorption models contain a significant number of assumptions (Westall, 1986).

In addition to protonation and deprotonation reactions, the $1pK_a$ and 2 pK_a weak acid models can be used to describe the adsorption of specifically and non-specifically adsorbed ions. The same approach used to describe proton adsorption reactions is applied to the adsorption of other aqueous species, and the appropriate mass-action and mass-balance equations are developed (Westall, 1986).

In the previous discussion of the 1 and $2pK_a$ adsorption models, all molecular interactions are assumed to occur at the mineral's surface. This would indicate one plane of adsorption regardless of the type of molecular interaction (electrostatic, covalent, or ionic bonding) residing

at the mineral's surface. However, most models of the EDL include multiple adsorption planes (such as the Stern Model and Three Plane Model) where the charge of the adsorbate is assigned to a specific adsorption plane, depending on the type of molecular interaction associated with the surface. The same approach previously presented can be used to develop mass-action, mass-balance equations for each electrostatic plane given for a particular model of the EDL.

Mechanistic surface complexation models have become an attractive tool in environmental chemistry based on their ability to estimate the distribution of ions between adsorbed and solution phases and predict the ionic speciation of each phase. Throughout the past 20 years several SCMs have been proposed including the Diffuse Double Layer, Constant Capacitance, Stern, Triple Layer models, and more recently the CD-MUSIC model (Davis and B., 1990; Goldberg, 1992; Hiemstra and Van Reinsdijk, 1996). Numerous articles, book chapters, and text books have documented the extent to which these SCMs can predict ion adsorption under specific conditions. Westall (1986), in a review of the Diffuse Double Layer, Constant Capacitance, Stern, and Extended Stern SCMs, indicated that the Extended Stern was the most fundamentally complete of the four models reviewed. However, Hiemstra et al. (1989a) and Hiemstra and Van Reinsdijk (1996) proposed a SCM that expanded the concept of the three plane model of the EDL by accounting for different coordination environments associated with surface functional group, and for the distribution of charge associated with adsorbing ions between the 0- and 1-electrostatic planes.

The CD Music Model

Hiemstra et al. (1989a) originally proposed the muliti-site ionic composition (MUSIC) model to describe differences in proton affinity for various oxy and hydroxo surface functional groups (singly, doubly, and triply). The model was later refined by Hiemstra and Van Reinsdijk (1996) to include a charge distribution function for the adsorption of specifically adsorbing ions, and the model was renamed the charge distribution multi-site ionic composition (CD-MUSIC) model. The CD-MUSIC model utilizes crystallographic parameters to constrain the type, number, reactivity, and site density of surface functional groups used in the adsorption model. Additionally the CD-MUSIC model uses Pauling's bond valence principal (Pauling, 1929) to describe the local charging environment (Hiemstra et al., 1989b; Hiemstra et al., 1989a; Hiemstra and Van Reinsdijk, 1996). The EDL model most often used in the CD-MUSIC model is the Extended Stern Layer model, which uses three planes to distribute charge across the interface (Fig. 2) (Felmy and Rustad, 1998; Geelhoed et al., 1997; Geelhoed et al., 1998; Hiemstra and Van Reinsdijk, 1996; Hiemstra and Van Riemsdijk, 1999; Reitra et al., 1999; Tadanier and Eick, 2002).

The previous acidity models discussed ($1pK_a$ and $2pK_a$ models) rely on an ambiguous description of surface protonation in regards to the type of functional group present. Additionally, no attempt was made to provide any information about the actual distribution of charge between neighboring functional groups (Westall, 1986). The adsorption model developed by Hiemstra et al. (1989a) and refined by Hiemstra and Van Reinsdijk (1996) is able to overcome these weaknesses through the application of Pauling's valence principal and now more formally known as Brown's valence principal (Brown, 1978; Brown, 1981). Using goethite as

an example, the oxygen or hydroxide ligand may be coordinated to one, two, or three Fe atoms in the goethite structure (i.e. singly, doubly, or triply coordinated surface groups) (Fig. 1.1). According to the valence principal, in a stable coordination structure, the total strength of the valency bonds (ν) that reach an anion from all neighboring cations is equal to the charge of the anion divided by the number of anions coordinated to it:

$$\nu = \frac{Z}{CN} \tag{34}$$

where

ν = valency unit—the contribution of charge from the cation to the anion

Z = charge of the ion

CN = the coordination number of the cation.

Applying this principal to the goethite structure, Fe^{3+} in octahedral coordination with three oxygen and three hydroxyl ligands, the valency unit associated with each ligand from Fe^{3+} is 1/2 (e.g. 3/6). This would indicate that surface charge would occur in non-integer intervals of 0.5 for singly and triply coordinated oxygens and 1.0 for doubly coordinated oxygens.

$$\equiv FeO^{1.5-} + H^+ \overset{pK_{a1}}{\rightarrow} \equiv FeOH^{0.5-} + H^+ \overset{pK_{a2}}{\rightarrow} \equiv FeOH_2^{0.5+} \tag{35}$$

$$\equiv Fe_2O^{1-} + H^+ \overset{pK_{a1}}{\rightarrow} \equiv Fe_2OH^0 = H^+ \overset{pK_{a2}}{\rightarrow} \equiv Fe_2OH_2^{1+} \tag{36}$$

$$\equiv Fe_3O^{0.5-} + H^+ \overset{pK_{a1}}{\rightarrow} \equiv Fe_3OH^{0.5+} \tag{37}$$

Only one protonation reaction is considered for the triply coordinated oxygen due to the fact that only one unbonded electron orbital is present. By formatting the surface acidity reactions in this manner, the CD-MUSIC model is able to provide detailed information about the distribution of charge between neighboring functional groups (Hiemstra et al., 1989a). In addition to providing information about the local charging environment, the CD-MUSIC model is also able to account

for relative affinity of the surface functional groups to undergo protonation or ion coordination reactions due to the influence of the relative charge contribution from the mineral cation (Hiemstra et al., 1989a; Hiemstra and Van Reinsdijk, 1996). This leads to a better estimation of which oxygen and hydroxyl groups are able to participate in coordination reactions at varying environmental conditions (Hiemstra et al., 1989a; Hiemstra et al., 1996; Hiemstra and Van Reinsdijk, 1996; Hiemstra and Van Riemsdijk, 1999). The ability to include a nonzero reference state, as with goethite is also a unique to the CD-MUSIC SCMl (Hiemstra et al., 1989a; Hiemstra and Van Reinsdijk, 1996).

The CD-MUSIC model places charge derived from coordination reactions, weak electrolyte-surface ion pair formation, and diffuse layer counterion adsorption into one of three electrostatic planes. Proton adsorption involves the coordination of hydrogen ions onto surface oxygen and hydroxyl groups. Charge developed from these retractions is placed in the 0-plane since the ion is covalently bonded to the terminating hydroxyl or oxygen group and is indistinguishable from the bulk surface (Hiemstra et al., 1989b; Hiemstra and Van Reinsdijk, 1996). Recent research has shown that surface coordinated oxyanions and metals do not occur in a two dimensional plane at the mineral surface, but instead occupy a three dimensional space with specific geometries (Fendorf and Sparks, 1996). The CD-MUSIC model differs from other conventional SCMs by allowing charge, due to inner-sphere complex formation, to be distributed between the 0- and 1-electrostatic planes (Hiemstra and Van Reinsdijk, 1996). Through the application of Pauling's bond valence principal to inner-sphere complexed metals and oxyanions, charge neutralization requires that a portion (f) of the charge be neutralized by the surface oriented ligands in the 0-plane, and the remaining charge (1- f) by solution oriented ligands in the 1-plane

(Hiemstra and Van Reinsdijk, 1996). If the cation charge is assumed to be symmetrically neutralized by the surrounding ligands, the charge distribution (CD) factor (f) is equal to the fraction of charge neutralized by the surrounding ligands located in the 0-plane, or the number of covalent bonds extended to the mineral surface (Tadanier and Eick, 2002). Using silicic acid (H_4SiO_4) and arsenite (H_3AsO_3) as examples, the CD factors for monodentate surface complexes are 1/4 or 0.25 for silicic acid and 1/3 or 0.33 for arsenite, and for a bindentate complexes the CD factors are 0.5 and 0.66 for silicic acid and arsenite, respectively (Fig. 1.5).

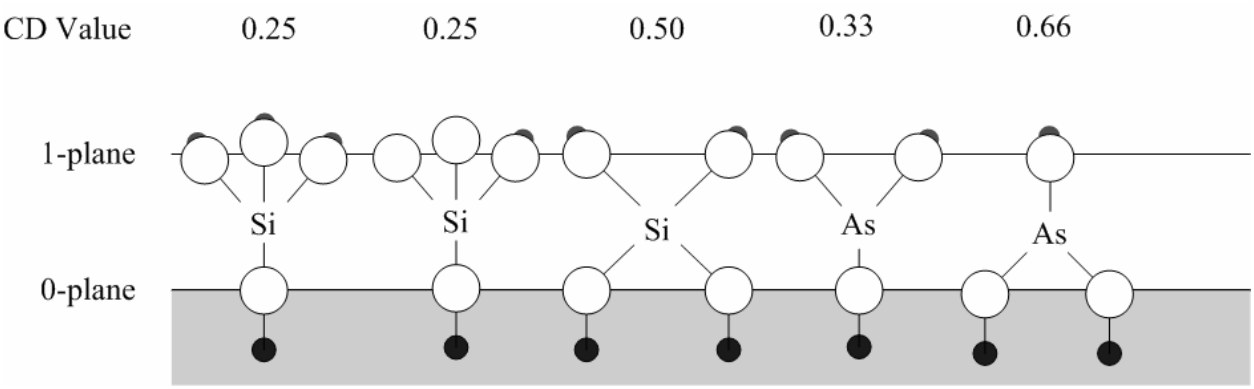

Figure 1.5. Charge distribution (CD) factors for inner-sphere complexes of silicic acid and arsenite on goethite assuming a symmetrical distribution of central cation charge to the surrounding ligands. The CD factor represents the proportion of charge neutralization associated with the surface.

As previously mentioned the CD MUSIC model distributes the charge of coordinated ions between the 0- and 1-plane. In order to accomplish this, the change in the charge (Δz) for the 0- and 1-planes must be calculated. Hiemstra and Van Reinsdijk (1996) defined this phenomenon for the 0- (Δz_0) and 1-plane (Δz_1) in the following equations

$$\Delta z_0 = \Delta n_H z_H + f z_{Me} \quad \textbf{(38)}$$

$$\Delta z_1 = (1 - f) z_{Me} + \sum m_i z_i \quad \textbf{(39)}$$

where

Δn_H = the net change in protons at the 0-plane

z_H = charge on the proton

z_{Me} = charge of the central atom in the coordinated complex

m_i = number of ligands in the 1 plane

z_i = charge on the ligands in the 1-plane

Using silicic acid as an example, and considering the formation of a mondentate singly deprotonated surface complex, Δz_0 and Δz_1 for the reaction

$$\equiv FeOH^{-0.5} + H_3SiO_4^{-1} \rightarrow \equiv FeOSiO(OH)_2^{1.5-} + H_2O \quad \textbf{(40)}$$

would be

$$\Delta z_0 = (-1 \times 1) + 0.25 \times 4 = 0 \quad \textbf{(41)}$$

and

$$\Delta z_1 = (1 - 0.25) \times 4 + \{(1 \times -1) + (1 \times -1) + (1 \times -2)\} = -1 \quad \textbf{(42)}$$

The site density of the reactive surface sites in the CD-MUSIC model is derived from the crystallographic parameters of the mineral lattice and refers to the number of times a specific functional group occurs per unit area (Hiemstra et al., 1989b; Hiemstra et al., 1989a; Hiemstra and Van Reinsdijk, 1996; Schwertmann and Cornell, 1996; Tadanier and Eick, 2002). Using the crystal lattice to define the number of functional groups present is not a unique feature to the CD-MUSIC model (Hiemstra et al., 1989b; Hiemstra et al., 1989a). The technique was first proposed by the creators of the MUSIC model for the purposes of relating the volume of base needed to neutralize surface acidity of minerals with more than one type of surface functional group present, to that predicted by model calculations (e.g. goethite) (Hiemstra et al., 1989b; Hiemstra et al., 1989a). Schwertmann and Cornell (1996) indicate that synthetic and natural goethite crystals exhibit a characteristic euhedral shape that is elongated in the c-axis with the

{021} and {110} faces as the predominant terminal planes. Due to the elongated nature of the crystal form, the relative contributions of the two predominant crystal faces to the total surface area differ greatly. The {110} planes account for approximately 90% of the goethite surface, while the remaining 10% is due to the {021} plane (Schwertmann and Cornell, 1996). Numerous methods have been proposed for determining the actual number of singly, doubly, and triply coordinated oxygens on the goethite surface including molecular calculations, deuterium adsorption, ion adsorption, and acid base titrations (Schwertmann and Cornell, 1996). Barrón and Torrent (1996) using a refined goethite structure, calculated the surface site density for singly, doubly, and triply coordinated oxygen and hydroxyl surface sites on the {110} faces to be 3.0, 9.1, and 3.0 sites nm^{-2} respectively, and 2.7 sites nm^{-2} for the {021} face for singly and doubly coordinated hydroxyl groups, respectively. Using a weighted average, the average site density for singly and triply coordinated oxygen and hydroxyl groups on goethite would be 3.52 sites nm^{-2} for singly and doubly, and 8.19 sites nm^{-2} for triply coordinated sites.

Since its inception, the CD-MUSIC model has been used successfully in describing proton and specific ion adsorption of oxyanions and metals on (oxy)hydroxide surfaces (Geelhoed et al., 1997; Geelhoed et al., 1998; Hiemstra et al., 1989b; Hiemstra et al., 1989a; Hiemstra et al., 1996; Hiemstra and Van Reinsdijk, 1996; Hiemstra and Van Riemsdijk, 1999; Hiemstra and Van Reimsdijk, 2000; Reitra et al., 1999; Rietra et al., 1999; Rietra et al., 2000; Tadanier and Eick, 2002; Weerasooriya et al., 2002). The ability of the CD-MUSIC model to consider the spatial distribution of specifically adsorbing ions allows incorporation of spectroscopic data, related to bond distances and complex orientation into the model (Geelhoed et al., 1997; Geelhoed et al., 1998; Hiemstra and Van Riemsdijk, 1999; Reitra et al., 1999; Rietra et al., 1999; Tadanier and

Eick, 2002). However, because of its lack of incorporation into commonly available computer codes it has been primarily used by its developers to describe oxyanion adsorption onto charge surfaces (Geelhoed et al., 1997; Geelhoed et al., 1998; Hiemstra et al., 1989b; Hiemstra et al., 1989a; Hiemstra et al., 1996; Hiemstra and Van Reinsdijk, 1996; Hiemstra and Van Riemsdijk, 1999; Hiemstra and Van Reimsdijk, 2000; Reitra et al., 1999; Rietra et al., 1999; Rietra et al., 2000). Recently, Tadanier and Eick (2002) developed a method of for formulating the CD-MUSIC model in the common computer complexation modeling program FITEQL. The CD-MUSIC model has been successfully used in the FITEQL using the Triple Layer Model template and adding a correction term to the 0-plane in the mass-balance expressions (B-matrix) to account for the non-zero charge of the reference state. Tadanier and Eick (2002) also provide a detailed description of the technique used to implement the model in FITEQL using Cu^{2+} and PO_4^{3-} as examples.

Comparison of the CD-MUSIC and Triple Layer Surface Complexation Models

Prior to the inception of the MUSIC and CD-MUSIC models, the Triple Layer Model (TLM) as described by Davis and Leckie (1978) was thought to be the most fundamentally complete SCM (Westall, 1986). The TLM is comprised of a $2pK_a$ adsorption model and an Extended Stern model of the EDL. Charge developed from protonation/deprotonation reactions and specific adsorption is placed in the 0-plane and ions that form outer-sphere complexes are palced in the 1-plane. Both the TLM and the CD-MUSIC model were used to describe the adsorption of silicic acid ($Si(OH)_4$) (1.00 mM) on goethite (1 g L^{-1}) in a $NaNO_3$ electrolyte solution (0.010 M) to assess the ability of each model to describe the equilibrium state. The total silicic acid adsorbed

($\mu mol\ m^{-2}$) and the predicted zeta potential data (mV) were compared to adsorption data and zeta potential measurements respectively to evaluate the modeling results. The surface complexation program FITEQL 4.0 was used to calculate the adsorption equilibrium constants, adsorbate speciation data, and the zeta potential data for both the TLM and CD-MUSIC model. The CD-MUSIC model was implemented in FITEQL using the procedure outlined by Tadanier and Eick (2002).

The TLM does not specify a method for determining the number of reactive surface sites, so for comparison purposes surface site density was set equal to the concentration of singly and triply coordinated oxygen and hydroxyl concentrations used in the CD-MUSIC model. The values of the surface acidity constants for goethite, utilizing the 2pKa model, were taken from the literature and the surface acidity constant for the 1pKa model was determined by zeta potential measurements (Goldberg, 1985). The stability constants for the formation of specifically adsorbed $Si(OH)_4$ and non-specifically adsorbed Na^+ and NO_3^- were allowed to optimize for the best fit of the data. A CD factor of 0.25 and 0.5 was used for the formation of silicic acid mono- and bidentate surface complexes respectively. All of the parameters used in both models as well as the chemical reactions considered are listed in Tables 1.1 and 1.2.

Table 1.1. CD Music and TLM model mineral surface parameters for the single ion adsorption modeling

Parameter/Reaction	Value	
	CD-MUSIC	**TLM**
Model Parameters		
Specific Surface Area ($m^2\ g^{-1}$) †	72.75	72.75
Site Density (sites nm^{-2}) (1-13)		
≡FeOH	3.45	6.15
≡Fe_3OH	2.7	
Capacitance factors(F m^{-2})		
C_1	1.5	1.5
C_2	5.0	5.0
CD Factor‡		
Monodentate Complex	0.25	
Bidentate Complex	0.50	

†BET N2 Adsorption isotherm
‡Based on Pauling's Rules

Table 1.2. CD-MUSIC and Triple Layer model surface complexation equilibrium reactions silicic acid adsorption modeling

Chemical Reactions	Log K	
	CD-MUSIC	TLM
Surface Acidity Reactions		
$\equiv FeOH^{-0.5} + H^+ \leftrightarrow \equiv FeOH_2^{+0.5}$	9.56[1-5†]	
$\equiv Fe_3O^{-0.5} + H^+ \leftrightarrow \equiv Fe_3H^{+0.5}$	9.56[1-5†]	
$\equiv FeOH + OH^- \leftrightarrow \equiv FeO^{-1}$		8.13[7]
$\equiv FeOH + H^+ \leftrightarrow \equiv FeOH_2^+$		7.18[7]
Electrolyte-Surface Ion Pair Formation[(4,5)]		
$\equiv FeOH^{-0.5} + Na^+ \leftrightarrow \equiv FeOH\text{-}Na^{+0.5}$	-1	
$\equiv FeOH^{-0.5} + H^+ + NO_3^- \leftrightarrow \equiv FeOH_2\text{-}NO_3^{-0.5}$	8.2	
$\equiv Fe_3O^{-0.5} + Na^+ \leftrightarrow \equiv Fe_3O\text{-}Na^{+0.5}$	-1	
$\equiv Fe_3O^{-0.5} + H^+ + NO_3^- \leftrightarrow \equiv Fe_3OH\text{-}NO_3^{-0.5}$	8.2	
$\equiv FeOH + OH^- + Na+ \leftrightarrow \equiv FeO^-\text{-}Na^+ + H_2O$		8.43[§]
$\equiv FeOH + H^+ + NO_3^- \leftrightarrow \equiv FeOH_2^+\text{-}NO_3^-$		18.85[§]
Aqueous Solution Reactions[6]		
Silicic Acid		
$SiO_2(OH)_2^{-2} + H^+ \leftrightarrow SiO(OH)_3^{-1}$	13.1	
$SiO_2(OH)_2^{-2} + H^+ \leftrightarrow Si(OH)_4^0$	22.96	
Surface Coordination Reactions[‡]		
Silicic Acid		
Monodentate		
$\equiv FeOH^{-0.5} + H^+ + SiO_2(OH)_2^{-2} \leftrightarrow \equiv FeOSiO(OH)_2^{-1.5} + H_2O$	17.66[‡]	21.07[§]
$FeOH^{-0.5} + 2H^+ + SiO_2(OH)_2^{-2} \leftrightarrow \equiv FeOSi(OH)_3^{-0.5} + H_2O$	26.78[‡]	31.95[§]
Bidentate		
$2\equiv FeOH^{-0.5} + H^+ SiO_2(OH)_2^{-2} \leftrightarrow (\equiv FeO)_2SiO(OH)^{-2} + 2H_2O$	22.67[‡]	30.80[§]
$2\equiv FeOH^{-0.5} + 2H^+ + SiO_2(OH)_2^{-2} \leftrightarrow (\equiv FeO)_2Si(OH)_2^{-1} + 2H_2O$	31.69[‡]	41.00[§]

† IEP measurements
‡ CD optimized values
§ TLM optimized values
1. Hiemstra et al. (1996), 2. Hiemstra and Van Reinsdijk (1996), 3. Rietra et al. (2000), 4. Tadanier and Eick (2002), 5. Rietra et al. (2000), 6. Smith (1992), and 7. Goldberg (1985)

The CD-MUSIC and the TLM both adequately described $Si(OH)_4$ adsorption on goethite for the pH range (3-11) and the initial adsorbate solution concentration (1.00 mM) investigated (Fig. 1.6 and 1.7).

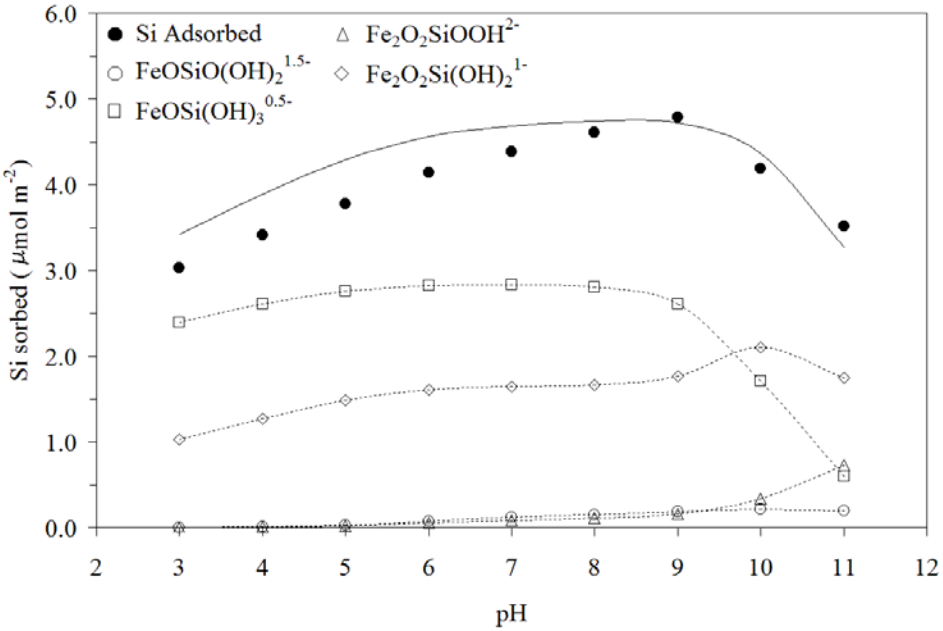

Figure 1.6. Silicic acid adsorption on goethite utilizing the CD-Music model. Si_T = 1.00mM. Closed symbols represent experimental data. Open symbols with dotted lines represent adsorbed Si species based on optimized CD-MUSIC fit to experimental data. Solid line represents cumulative total adsorbed Si species as predicted by the CD-Music model.

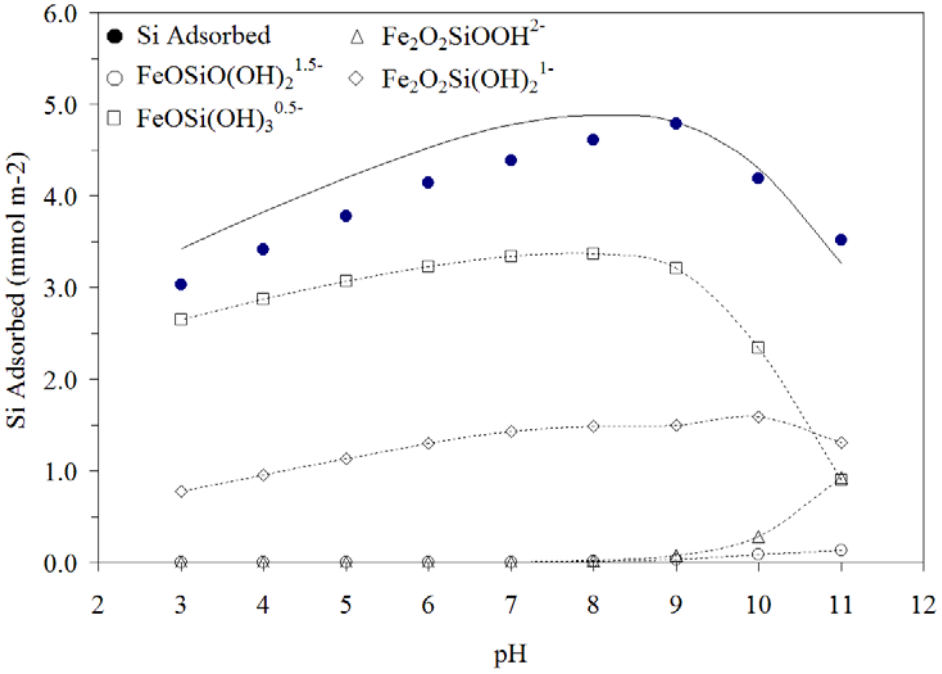

Figure 1.7. Silicic acid adsorption on goethite utilizing the Triple Layer Model. Si_T = 1.00mM. Closed symbols represent experimental data. Open symbols with dotted lines represent adsorbed Si species based on optimized TLM fit to experimental data. Solid line represents cumulative total adsorbed Si species as predicted by the TLM.

Each model was able to predict the pH dependency of silicic acid adsorption over the entire pH range investigated. Additionally, both models slightly over-predicted the amount of silicic acid adsorbed at pH values less than the first dissociation constant for silicic acid ($pK_{aSi} = 9.98$). Both the TLM and CD-MUSIC model predicted very similar speciation data for adsorbed silica, with fully protonated mono- and bidentate complexes being the dominant species at the surface. The only difference between the speciation data for each model was the relative percentage of each species at the surface.

The FITEQL program provides an error term, similar to an r^2 value, which evaluates the ability of the material balance equations, used in model calculations, to describe the adsorption data. Error terms with a value less than 25 are considered to adequately describe adsorption data, generally the lower the value the better the fit. The error terms for both the CD-MUSIC and TLM were 13.1 and 9.2 respectively, well below the prescribed cutoff point. Based solely on upon the adsorption data and the associated error term, neither model appears to provide a better description of the equilibrium state.

In addition to calculating the speciation data, FITEQL also provides electrical potential (Ψ) and charging (σ) data for each of the electrostatic adsorption planes. These results can be compared to experimental data to further evaluate model predictions. Zeta potential data for the adsorption of 1.0 mM silicic acid on goethite is provided in Figure 1.8 in addition to the values predicted by the CD-MUSIC and TLM models . Upon examination of Figure 1.8, it is immediately apparent that the CD-MUSIC model (solid line) provides a more reasonable description of the experimental data than the TLM (dashed line). Additionally, the TLM model predicts the point

of zero charge to occur at approximately pH 9 nearly 2 pH units above the experimentally determined value, 7.2. While the CD-MUSIC model overestimates zeta potential at moderate pH values (4-8) it provides a reasonably good description of the experimental data over the entire pH range.

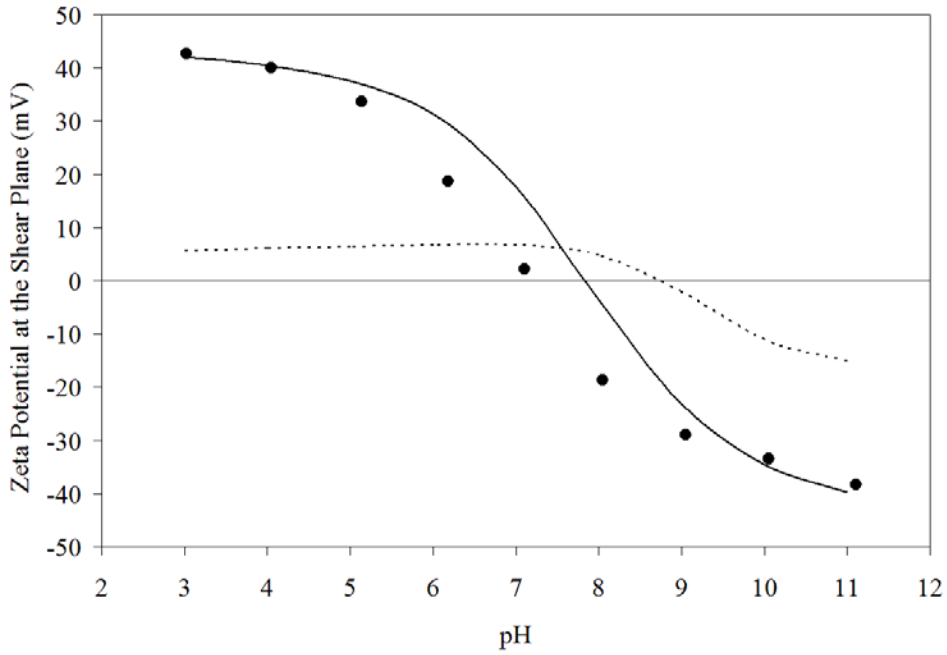

Figure 1.8. Zeta potential data for the adsorption of 1.0 mM silicic acid on goethite for the pH range of 3-11. The solid circles represent experimentally determined zeta potential data. The solid line represents the predicted zeta potential data for the CD-Music Model. The dashed line represents the predicted zeta potential data for the TLM.

While both SCMs were able to adequately describe silicic acid adsorption on goethite, only the CD-MUSIC model was able to provide reasonable predictions for electric potential data at equilibrium. The results of the model comparisons do not indicate that the CD-MUSIC model is any more fundamentally correct than the TLM, since only one adsorbate at a single initial solution concentration has been considered. However, the ability of the CD-MUSIC model to

consider a non-zero reference state ($\equiv FeOH^{0.5-}$) and the distribution of charge between two electrostatic planes may allow for a more realistic interpretation of the solid/solution interface.

Conclusions

The evolution of charge at the mineral surface is one of the most important factors controlling the sorption and retention of aqueous ions at the solid-solution interface (Gast, 1977). The surface charge, and the corresponding electric potential, of (hydr)oxide minerals is controlled primarily by three solution properties: pH, ionic strength, and the presence of surface coordinating ions, and three mineral surface properties: specific surface area, surface functional group density, and the coordination environments of surface functional groups (Gast, 1977; McBride, 1994; Sposito, 1984; Stumm, 1978; Zelazny et al., 1996). The ability to accurately predict the influence of these parameters upon surface charge would allow for accurate prediction of the distribution of ions between the solid-solution interface. The recently developed CD-MUSIC model is currently the only surface complexation model able to more fully account for the major solution and mineral surface properties previously mentioned (Hiemstra et al., 1989b; Hiemstra et al., 1989a; Hiemstra et al., 1996; Hiemstra and Van Reinsdijk, 1996; Hiemstra and Van Riemsdijk, 1999; Rietra et al., 2000)

References

Barrón, V., and J. Torrent. 1996. Surface hydroxyl Configuration of various Crystal Faces of Hematite and Goethite. Journal of Colloid and Interface Science 177:407-410.

Bolt, G.H., and W.H. Van Riemsdjik. 1982. Ion adsorption on inorganic variable charge constituents, p. 459-504, *In* G. H. Bolt, ed. Soil Chemistry: B. Physico-chemical models. Elsevier Scientific Publishing Co., Amsterdam, The Netherlands.

Brown, I.D. 1978. Bond valences--A simple structural model for inorganic chemistry. Chem. Soc. Rev. 7:359-367.

Brown, I.D. 1981. The bond valence method: An empirical approach to chemical structure and bonding, p. 1-30, *In* M. a. N. O'Keefe, A., ed. Structure and bonding in crystals II. Academic Press, New York.

Chapman, D.L. 1913. A contribution to the theory of electrocapollarity. Philosophical Magazine and Journal of Science
25:475-481.

Davis, J.A., and J.O. Leckie. 1978. Surface ionization and complexation at the oxide/water interface. I. Computation of the electrical double layer properties in simple electrolytes. Journal of Colloid and Interface Science 63: 32-43.

Davis, J.A., and D.B. Kent. 1990. Surface complexation modeling in aqueous geochemistry *In* M. F. J. a. W. Hochella, A. F., ed. Mineral-Water Interface Geochemistry, Vol. 23. Minerological Sosiety of America, Washington D. C.

Dzombak, D.A., and F.M. Morel. 1990. Surface Complexation Modeling Hydrous Ferric Oxide John Wily and Sons, New York.

Felmy, A.R., and J.R. Rustad. 1998. Molecular static's calculations of proton binding to goethite

surfaces: Thermodynamic modeling of the surface charging and protonation of goethite in aqueous solution. Geochimica et Cosmochimica acta 62:25-31.

Fendorf, S.E., and D.L. Sparks. 1996. X-Ray Absorption Fine Structure Spectroscopy, p. 377-416, *In* D. L. Sparks, ed. Methods of Soil Analysis Part 3 Chemical Methods. Soil Science Society of America Inc., Madison, Wisconsin.

Gast, R. 1977. Surface and Colloid Chemistry Soil Science Society of America, Madison WI.

Geelhoed, J.S., T. Hiemstra, and W.H. Van Riemsdijk. 1997. Phosphate and sulfate adsorption of goethite: Single anion ands competitive adsorption. Geochimica et Cosmochimica Acta 61:2389-2396.

Geelhoed, J.S., T. Hiemstra, and W.H. Van Riemsdijk. 1998. Competitive interaction between phosphate and citrate on goethite. Environmental Science and technology 32:1219-1223.

Goldberg, S. 1985. Chemical modeling of anion competition on goethite using the constant capacitance model. Soil Science Society of America Journal 49:851-856.

Goldberg, S. 1992. Use of surface complexation models in soil chemical systems, p. 233-329, *In* D. L. Sparks, ed. Advances in Agronomy, Vol. 47. Academic Press, Inc., San Diego.

Gouy, G. 1910. Sur la constitution de la charge electrique a la surface d' un eletolute. J Phys. Radium 9:457-468.

Hiemstra, T., W.H. Van Riemsdijk, and G.H. Bolt. 1989a. Multisite proton adsorption modeling at the solid/solution interface of (hydr)oxides: A new approach

I. Model description and evaluation of intrinsic reaction constants. Journal of Colloid and Interface Science 133:91-104.

Hiemstra, T., J.M.C. De Wit, and W.H. Van Riemsdijk. 1989b. Multisite proton adsorption modeling at the solid/solution interface of (hydr)oxides: a new approach

II. Application to various important (hydr)oxides. Journal of Surface and Interface Science 133:105-115.

Hiemstra, T., P. Venema, and W.H. Van Riemsdijk. 1996. Intrinic proton affinity of reactive surface groups of metal (hydr)oxides: the bond valence principal. Journal of Colloid and Interface Science 184:680-692.

Hiemstra, T., and W.H. Van Reinsdijk. 1996. A surface structural approach to ion adsorption: the charge distribution (CD) model. Journal of Colloid and Interface Science 179:488-508.

Hiemstra, T., and W.H. Van Riemsdijk. 1999. Surface structural ion adsorption modeling of competitive binding of oxyanions by metal (hydr)oxides. Journal of Colloid and Interface Science 210:182-193.

Hiemstra, T., and W.H. Van Reimsdijk. 2000. Flouride adsorption on goethite in relation to different types of surface sites. Journal of Colloid and Interface Science 225:94-104.

McBride, M.B. 1994. Environmental Chemistry of Soils Oxford Press, New York.

Parks, G.A. 1990. Surface energy and adsorption at mineral water interfaces: an introduction, p. 133-169, *In* M. F. J. a. W. Hochella, A. F., ed. Mineral-Water Interface Geochemistry, Vol. 23. Minerological Sosiety of America, Washington D. C.

Pauling, L. 1929. The principals determining the structure of complex ionic crystals. Journal of the American Chemical Society 51:1010-1026.

Reitra, R.P.J.J., T. Hiemstra, and W.H. Van Riemsdijk. 1999. The relationship between molecular structure and ion adsorption on variable charge minerals. Geochimica et Cosmochimica Acta 63:3009-3015.

Rietra, R.P.J.J., T. Hiemstra, and W. Reimsdijk. 1999. Sulfate Adsorption on Goethite. Journal of Colloid and Interface Science 218:511-521.

Rietra, R.P.J.J., T. Hiemstra, and W.H. Van Riemsdijk. 2000. Electrolyte anion affinity and its effect on oxyanion adsorption on goethite. Journal of Colloid and Interface Science 229:199-206.

Schwertmann, U., and R.M. Cornell. 1996. The iron oxides: structures, properties, reactions, occurrence and uses VCH, Weinheim, FR of Germany.

Smith, R.M.and A.E. Martel. 1992. Critical Stability Constants Plenum Press, New York.

Sparks, D.L. 1999. Soil Physical Chemistry CRC Press, Boca Raton.

Sposito, G. 1984. The surface chemistry of soils Oxford University Press, New York.

Sposito, G. 1989. The Chemistry of Soils Oxford University Press, New York.

Stern, O. 1924. Zur Theorie der eiecktrolytischen doppelschict. Z. Electrochem. 30:508-516.

Stumm, W. 1992a. Chemistry of the solid water interface John Wiley and Sons, New York.

Stumm, W. 1992b. The inner-sphere surface complex, p. 1-32, *In* C. P. Huang, Omelia, C. R., and Morgan, J. J., ed. Aquatic chemistry interfacial and interspecies processes. American Chemical Society, Washington D.C.

Stumm, W. and J.J. Morgan. 1996. Aquatic Chemistry Chemical Equilibria and Rates in Natural Waters. 3rd ed. John Wiley & Sons Inc., New York.

Tadanier, C.J. and M.J. Eick. 2002. Formulating the charge-distribution multisite surface complexation model using FITEQL. Soil Science Society of America 66:1505-1517.

Weerasooriya, R., H.K.D.K. Wijesekara, and A. Bandara. 2002. Surface complexation modeling of cadmium adsorption on gibbsite. Colloids and Surfaces 207:13-24.

Westall, J., and H. Hohl. 1980. A comparison of elkectrostatic models for the oxide/solution interface. Advances in Colloid and Interface Science 12:265-294.

Westall, J. 1980. Chemical equilibrium including adsorption on charged surfaces, p. 33-44, *In* M. C. a. L. Kavanaugh, J. O., ed. Particulates in water, Vol. 189. American Chemical Society, Washington D.C.

Westall, J.C. 1986. Chemical and electrostatic models for reactions at the oxide-solution interface, p. 54-78, *In* J. A. Davis and K. F. Hayes, eds. Geochemical processes at mineral surfaces, Vol. ACS Symposium Series, 323. American Chemical Society, Washington D.C.

Zelazny, L.W., L. He, and A. Vawormhoudt. 1996. Charge Analysis of Soils and Anion Exchange, p. 1231-1253. *In* D. L. Sparks, ed. Methods of Soil Analysis Part 3 Chemical Methods. Soil Science Society of America Inc., Madison, Wisconsin.

2. Competitive Adsorption of Silicic Acid and Arsenite on Goethite: Equilibrium Studies and Surface Complexation Modeling

Abstract—The adsorption behavior of silicic acid and arsenite alone and competitively on goethite over a broad pH range (3-11) at environmentally relevant concentrations was investigated utilizing pH adsorption data and zeta potential measurements. Both addition scenarios (Si before As(III) and As(III) before Si) were examined. The results of the adsorption experiments and zeta potential measurements were then used to model the single ion and competitive ion adsorption on goethite with the CD-MUSIC model implemented in the FITEQL 4.0 computer program. Silicic acid adsorption was reduced by the presence of arsenite for all but one of the adsorption scenarios examined, while in contrast silicic acid had little effect upon arsenite adsorption. However, the presence of silicic acid, regardless of the addition scenario, dramatically increased the arsenite equilibrium solution concentration over the entire pH range investigated. The CD-MUSIC model was able to predict the single ion adsorption behavior of silicic acid and arsenite on goethite. The modeled zeta potential data provided further evidence of the CD-MUSIC model's ability to describe the single anion adsorption on goethite. Our model was also able to collectively describe adsorption and zeta potential data for the low Si-arsenite adsorption scenario quite well however, our model under-predicted silicic acid adsorption for the high Si-arsenite competitive scenario.

Introduction

Silicate minerals are ubiquitous constituents of terrestrial environments and through chemical weathering provide a continual supply of dissolved silica (Iller, 1979). The concentration of dissolved silica varies considerably depending on the type of silicate mineralogy present and climatological factors. In a review of soluble silica in nature, Iller (1979) reported that the average concentration of silica ranged from 0.17 to 1.24 mM (5-35 mg L^{-1}) in natural waters and soils with a few exceeding 2.7 mM (75 mg L^{-1}). McKeague and Cline (1963a) investigated the water soluble silica concentrations in five soil orders, and found that the water soluble silica

concentration varied from 0.35 to 1.3 mM (10-35 mg L^{-1}), and silica concentrations were highly dependent upon the type of mineralogy present.

In dilute solutions, less than 1.10 mM (31 mg L^{-1}), dissolved silica is believed to only exist as the very weak monomeric silicic acid ($Si(OH)_4$, $pK_{a1} = 9.98$) (Alverez and Sparks, 1985; Applin, 1987; Iller, 1979; Smith and Martel, 1992; Swedlund and Webster, 1999). At concentrations exceeding 1.10 mM, silicic acid has been shown to form silica di- and trimeric species in solution (Alverez and Sparks, 1985; Applin, 1987). Additionally, the presence of Fe and Al has been shown to contribute to the formation of silicic acid polymers at concentrations below 1.10 mM (31 mg L^{-1}) (Iller, 1979). The speciation of dissolved monomeric and polymeric silica species in the presence of amorphous silica have been documented in the literature, but very little thermodynamic data exists for dissolved silica in the absence of amorphous silica (Dove and Rimstidt, 1994; Elegawahary and Lindsay, 1972; Iller, 1979; Sillén and Martell, 1964). Alverez and Sparks (1985), utilizing laser Ramen spectroscopy, confirmed the presence of polymeric silica species at silica concentrations of 1.07 mM, and Applin (1987) calculated the stability constant of dimeric silica ($Si_2O(OH)_6$) to be 330 (log K = 2.52) for silica solution concentrations of 0.17 to 2.8 mM (5-80 mg L^{-1}) at pH 5.5 and 298 K.

Silicic acid, like many other oxyanions, binds covalently through ligand exchange at hydrous oxide surfaces forming an inner-sphere surface complex (Sigg and Stumm, 1981). Previous research has shown that silicic acid has a high affinity for Fe and Al (hydr)oxide surfaces and its adsorption is highly pH dependent with maximum adsorption occurring near the first dissociation constant for silicic acid (Gustafsson, 2001; Hingsten et al., 1972; McKeague and Cline, 1963a;

Meng et al., 2000; Obihara and Russell, 1972; Sigg and Stumm, 1981; Swedlund and Webster, 1999; Vempati et al., 1990). The mechanism by which silicic acid binds with (hydr)oxides surfaces is not well understood. Several research investigations have concluded that silicic acid forms an inner-sphere complex, but the type of complex (mono- vs. bidentate or mono-, vs. bi, vs. trinuclear) formed at varying Si concentrations and pH is unclear (Hansen et al., 1994a; Hansen et al., 1994b; Obihara and Russell, 1972; Sigg and Stumm, 1981; Waltham and Eick, 2002). Previous efforts to model silicic acid adsorption on ferrihydrite, goethite, and gibbsite have only considered the formation of one type of surface complex, monodentate mononuclear or bidentate mononuclear (Goldberg, 1985; Gustafsson, 2001; Hansen et al., 1994a; Hansen et al., 1994b; Meng et al., 2000; Swedlund and Webster, 1999). Given that no clear spectroscopic evidence exists to suggest what silicic acid species may be present at the solid-solution interface, modeling silicic acid adsorption using surface complexation models presents a challenge. Few studies have examined the adsorption or formation of polymeric silica species on Fe (hydr)oxide surfaces. Vempati et al. (1990) confirmed the existence of Si polymers on ferrihydrite when Si solution concentration equaled or exceeded 3.5 mM, while Hansen et al. (1994a) reported the formation of Si-O-Si bonds for silicic acid adsorbed on ferrihydrite at initial Si solution concentrations of 0.97 mM. Unfortunately, neither study provided any information on the stability of the adsorbed species. Swedlund and Webster (1999), relying upon Hansen et al. (1994a) and Vempati et al. (1990) results, modeled silicic acid adsorption on ferrihydrite considering two different types of dimeric Si species, and determined that neither one dramatically improved the model fit.

Iron (hydr)oxides minerals display a high affinity for numerous oxyanions present in terrestrial ecosystems (Schwertmann and Cornell, 1996). Since silicic acid is present at relatively high concentrations, compared with anthropogenically introduced oxyanions, it may compete for adsorption sites on Fe (hydr)oxides. Understanding these competitive interactions is critical in assessing the potential bioavailability of contaminants in soils and sediments. Few studies have investigated the influence of silicic acid on oxyanion adsorption on Fe (hrydr)oxides (Gustafsson, 2001; Hetzl and McColl, 1997; Meng et al., 2000; Obihara and Russell, 1972; Swedlund and Webster, 1999; Waltham and Eick, 2002). However, these studies suggest that silicic acid does not adversely effect oxyanion adsorption when the difference between the pK_{a1} values for silicic acid and the competing oxyanion are large (e.g. phosphate, arsenate, and oxalic acid), but can be significant when the differences are small (e.g. arsenite) (Gustafsson, 2001; Hetzl and McColl, 1997; Meng et al., 2000; Obihara and Russell, 1972; Swedlund and Webster, 1999; Waltham and Eick, 2002).

Arsenic is a highly toxic trace element and a known carcinogen that is widely dispersed in the environment due to anthropogenic and natural sources (Sadiq, 1997). Ingestion of minute amounts of arsenic (65 mg) at one time, or through reoccurring exposure, can trigger adverse health conditions in humans (Chappell et al., 1997). Due to the increasing amounts of arsenic in the environment and the small exposure level required for potential adverse health conditions the EPA lowered the drinking water standards from 50 to 10 $\mu g\ L^{-1}$ in October 2001. High concentrations of arsenic have been introduced into the environment through application of arsenical pesticides, dust particulate matter from metal smeltering operations, and degradation of pressure treated lumber. The two most commonly occurring forms of inorganic arsenic in soils

and sediments are arsenate [AsO_4^{3-}, As(V)] and the weak acid arsenite [AsO_3^{3-}, As(III)]. In a review of the environmental chemistry of arsenic, Tamaki and Frankenbeger (1992) concluded that arsenite was the more mobile and toxic form of the two species. The mechanism by which arsenite binds with Fe and Al (hydr)oxides has been examined using surface spectroscopies and different results have been obtained depending upon surface coverage and spectroscopic technique. Sun and Doner (1996) and Manning et al. (1998) examined arsenite adsorption on goethite at elevated concentrations (7.5 to 60 mM and 133 or 266 mM). Both researchers concluded that arsenite formed bidentate binuclear bridging complexes on goethite. In contrast, Goldberg and Johnston (2001) concluded that at low concentrations (0.01 or 1.00 mM) arsenite formed both inner- and outer-sphere surface complexes on goethite. Recently, Arai et al. (2001), using low angle x-ray absorption spectroscopy, concluded that arsenite at low concentrations (0.7 mM) formed both inner and outer sphere surface complexes with γ-Al_2O_3 and identified monodentate mononuclear and bindentate mononuclear surface complexes.

Several studies have examined the competitive adsorption of silicic acid and arsenite on ferrihydrite from an equilibrium standpoint, and have attempted to model the competitive interaction using the Triple Layer and the Diffuse Double Layer model (Meng et al., 2000; Swedlund and Webster, 1999). Swedlund and Webster (1999) concluded that silicic acid did not influence arsenite adsorption in the pH range 4-12 and were able to accurately predict silicic acid and arsenite adsorption using the Diffuse Double Layer model when Si concentrations were less than 0.17 mM Si. At concentration above 0.17 mM Swedlund and Webster (1999) found that the diffuse double layer model under-predicted silicic acid adsorption. Meng et al. (2000) reported a 30% reduction in arsenite adsorption in the presence of silicic acid when Si solution

concentrations exceeded 10 mg L^{-1}. These conflicting results could,in part, be due to differences between the preparations of ferrihydrite samples utilized. Ferrihydrite is a poorly-ordered Fe hydroxide, and two samples synthesized from different methods could have extremely different sorption properties (Schwertmann and Cornell, 1996). The use of a crystalline Fe hydroxide mineral surface, where the type and number of surface sites present is known, may help to clarify these conflicting results.

Accordingly, the objectives of this study were: i) determine the adsorption behavior of silicic acid and arsenite alone and competitively on goethite at several environmentally relevant concentrations, ii) model silicic acid and arsenite adsorption on goethite using the CD-MUSIC model, and iii) use the equilibrium constants derived from the single anion adsorption modeling to predict effects of the competitive interaction and compare the modeling results to the adsorption data.

Materials and Methods

Oxide Synthesis and Characterization

Goethite used in the adsorption experiments was synthesized by oxidation of ferric nitrate ($Fe(NO_3)_3$) using a method described by Schwertmann and Cornell (1991). The procedure was altered slightly by slowly adding 4 M NaOH, during titration to pH 12, to achieve a higher specific surface area. Excess salts from the hydrolysis reaction were removed by dialysis until conductivity of the wash solution was near that of distilled doubly-deionized water exposed to the atmosphere. All solutions were prepared with distilled doubly-deionized water, reagent grade chemicals, and contact with glass surfaces was avoided to prevent silica contamination.

The goethite was washed with 0.40 M HNO_3 for 1 h to remove short ordered phases, centrifuged to separate colloidal goethite crystals, resuspended, and redialized. The clean goethite was freeze-dried for storage prior to adsorption experiments. The identity and purity of the goethite sample was confirmed by x-ray diffraction (XRD), differential scanning calorimetry (DSC), thermogravimetric analysis (TGA), field emission scanning electron microscopy (FESEM), and ammonium oxalate in the dark (Fe_O) to total iron ratio total iron-Fe_T (total iron determined by citrate-bicarbonate-dithionite method) (Loeppert and Inskeep, 1996; Schwertmann and Cornell, 1991). X-ray diffraction, TGA, and DSC patterns were consistent with those presented in Schwertmann and Cornell (1991) and a goethite standard from Bayer®. Scanning electron microscopy images indicated that synthetic goethite colloids were of uniform shape and size, and that the crystals were similar to those found in natural environments (Schwertmann and Cornell, 1996). Colloids were euhedral acicular crystals approximately 200 nm meters in length and 25 nm in diameter. The ammonium oxalate in the dark to total iron ratio (0.28 %) indicated minimal amounts of amorphous or short-ordered crystals. Specific surface area was 72.75 $m^2\ g^{-1}$ as determined by a five point N_2 Brunauer-Emmett-Teller (BET) gas adsorption isotherm. The point of zero charge as determined by the isoelectric point (IEP) was 9.56.

Single Ion Adsorption

Adsorption studies were conducted to determine the effect of pH on arsenite (AsO_3^{3-}) and silicic acid (H_4SiO_4) adsorption onto goethite at two initial solution concentrations for As(III) (0.05 and 0.10 mM) and three initial solution concentrations for silicic acid (0.10, 0.50, 1.00 mM). All adsorption edges were conducted in duplicate over a pH range of 3-11, at constant ionic strength (0.01M $NaNO_3$) and adsorbent concentration (1 g L^{-1}). All adsorption edges were conducted

from pH 3 to 11 to eliminate hysteresis effects. All stock solutions were prepared with reagent grade sodium salts and distilled doubly-deionized water.

Arsenite adsorption studies were conducted in flat bottomed, Teflon lined, water-jacketed reaction vessels. The vessels were covered with a glass lid containing ports for a stirrer, pH electrode, burette tip, sample pipette, and N_2 gas. An appropriate amount of goethite (0.4000 g) was placed in the Teflon container and 375 ml of 0.01 M $NaNO_3$ was added. The suspension was dispersed for ~3 minutes using a sonic dismembrator. The Teflon container was placed in the water-jacketed reaction vessel and stirred at 300 rpm and sparged with N_2 to minimize CO_2 contamination throughout the experiment. The suspension was allowed to hydrate for at least 24 h, and adjusted to the appropriate pH with a Brinkman 716 Stat-Trino pH stat prior to the addition of arsenite. After the pH had stabilized, the suspension was brought to volume (400 mL) less the volume of arsenite to be added. An appropriate amount of arsenite stock solution was added to the suspension and the pH was readjusted. Arsenite was allowed to equilibrate with the goethite surface at pH 3.00 for 2 h prior to taking the first sample. After the prescribed equilibration time, a 7.00 mL sample was removed from the reaction vessel with a 10 mL Rainin® automated digital pipette and immediately filtered through a 0.2 μm Fisherbrand® membrane into a previously acid washed polyethylene test tube. After sampling the pH, the reaction vessel was raised by one pH unit using NaOH and allowed to requilibrate (arsenite 2 h).

Silicic acid adsorption studies were conducted using a batch technique with nine individual 250 mL polycarbonate centrifuge bottles for a pH range of 3-11. The batch technique was chosen over the pH-stat method for silicic acid due to the extended equilibration time of 40 hours

(Waltham and Eick, 2002). An appropriate amount of goethite (0.2000 g) was added to each centrifuge bottle followed by 180 mL of background electrolyte (0.01M $NaNO_3$). The suspension was dispersed for ~3 minutes using a sonic dismebrator. After dispersing, the suspension was sparged with N_2 and the pH was adjusted to the appropriate value using 0.10 M NaOH or HNO_3. After pH adjustment, the sample was sealed and placed in a New Brunswick Scientific Innova 4230 Refrigerated Incubator Shaker and allowed to hydrate for at least 24 h. After the initial hydration period the suspension was sparged with N_2 and brought to volume (200 mL) less the volume of silicic acid to be added. The silicic acid was added from a 0.0287 M sodium silicate stock solution in 0.1 M NaOH to prevent polymerization (Iller, 1979). The pH of the goethite suspension was checked and readjusted to the appropriate value periodically throughout the equilibration time period. After the 40 h equilibration time period, a 7.00 mL sample was removed from the reaction vessel with a 10 mL Rainin® automated digital pipette and immediately filtered through a 0.2 μm Fisherbrand ® membrane into a previously acid washed polyethylene test tube and the pH of the suspension was recorded.

Competitive Ion Adsorption

The competitive adsorption of silicic acid and arsenite on goethite, at two loading concentrations, was investigated over a broad pH range, 3-11. Both addition scenarios, (1) initial equilibration of silicic acid with goethite followed by the addition of arsenite, and (2) initial equilibration of arsenite with goethite followed by silicic acid addition, were examined. All adsorption studies were conducted in duplicate at a constant ionic strength (0.01 M $NaNO_3$), and sorbent suspension density (1 g L^{-1}). Adsorption studies were conducted using the batch technique described for the silicic acid adsorption studies, with the following modifications. The initial oxyanion was added to the goethite suspension to achieve the appropriate solution concentration (0.10 and 1.00 mM

for silicic acid or 0.05 and 0.10 mM for arsenite) and the pH was readjusted and the suspensions were allowed to equilibrate (40 h for silicic acid and 4 h for arsenite). Following equilibration of the initial oxyanion, the second oxyanion was added to the system. Again, the pH was readjusted to the ascribed value and the suspension was sparged with N_2. The suspensions were then allowed to equilibrate over a ~50 h period. Samples were sparged with N_2 for 5 min every 8-10 h. After sparging, the pH of the goethite suspensions was checked and adjusted as necessary. Following the 50 h time period the final pH of the suspensions was recorded, and a 7 mL sample was filtered through a 0.2 μm Fisherbrand® membrane into a previously acid washed polyethylene test tube. Arsenic and silicic acid solution concentrations were measured by inductively coupled plasma atomic emission spectrophotometry (ICP-AES). Adsorbed oxyanion concentrations were calculated from the initial solution concentration minus the final oxyanion concentration.

Zeta Potential Measurements

When a colloidal particle moves in an electric field, or when fluid flows past a particle, an immobile hydrodynamic boundary layer of fluid moves with the particle. If the electric double layer (EDL) is thicker than the boundary layer then the outer most counter ions will be stripped away, resulting in a charge separation at the slipping plane giving rise to what is commonly known as the zeta potential (ζ) (Fig. 2.1) (Parks, 1990).

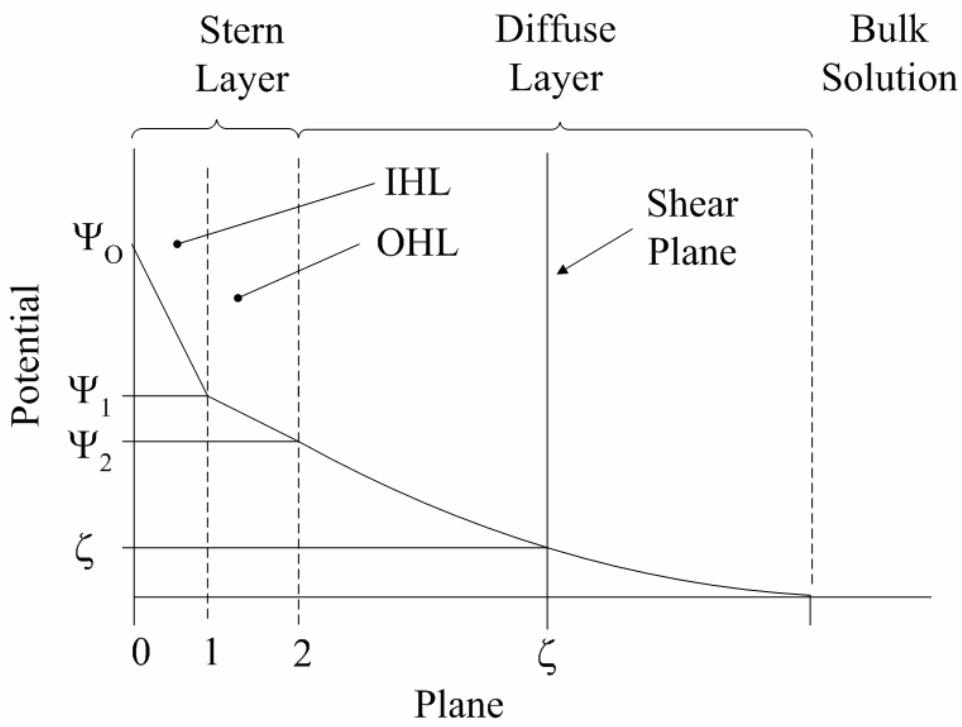

Figure 2.1. Schematic drawing of the slipping plane and the location of the zeta potential (ζ) and the associated charge at the slipping plane (σ_ζ).

The colloidal particle is left with a net charge and a potential gradient is generated in the direction of particle movement in the applied electric field. The electric potential at the boundary layer can be calculated from electrophoretic mobility measurements (i.e. the velocity of the particle in an applied electric field) (Parks, 1990). The equation relating electrophoretic mobility to the electric potential at the slipping plane was originally derived for a spherical particle, however this equation has also been applied to non-spherical particles including clay (disc), goethite (rod), and amorphous mineral and organic materials with reasonable results (Kosmulski, 2001).

Zeta potential measurements of mineral suspensions are dependent upon pH, ionic strength, and the presence of specifically adsorbing ions. Generally, as the pH of the suspension is increased

the zeta potential for minerals will move from positive to negative values. The pH at which the particle does not experience an electric potential in an applied electrical field is known as the isoelectric point (IEP) (Kosmulski, 2001; Parks, 1990). Changes in the ionic strength and non-specific adsorption of ions will not change the pH of the IEP. However, specific adsorption of ions can alter the IEP, and zeta potential measurements can be used to determine adsorption mechanisms (e.g. inner- or outer-sphere complex formation) (Kosmulski, 2001; Parks, 1990). Typically, cation specific adsorption will shift the IEP to a higher pH because the surface becomes more positively charged, while anion adsorption will shift the IEP to a lower pH as the surface becomes more negatively charged. The degree to which the IEP shifts is related to the concentration of the adsorbed ion, the type of surface complex and the degree of protonation of the adsorbed oxyanion. Additionally, the degree to which to an adsorbing ion shifts the IEP is related to the surface complex stability (Parks, 1990). So, a more strongly adsorbed ion will cause a greater shift in the IEP than a more weakly held ion.

In this study, zeta potential data were collected over the entire pH range (3-11) for both arsenite and silicic acid single ion adsorption edges at all concentrations and for selected pH values (3, 5, 7, 9, and 11) and addition scenarios (silicic acid before arsenite) for the competitive ion adsorption edges. The addition scenario of silicic acid before arsenite was chosen for zeta potential measurements based on results from the adsorption studies that demonstrated there was little difference between addition scenarios. The adsorption suspensions for zeta potential measurements for single ion and competitive ion scenarios were prepared using the methods previously described for the adsorption studies. Zeta potentials were determined from microelectrophoresis measurements on a Malvern Zetasizer 3000HSa. Based on preliminary

data and particle size, the voltage applied to the capillary cell was set at 100 V and a Henry function (f(Ka)) of 1.5 was used in calculating the zeta potential. The pH of each 10 mL sample was measured before zeta potential measurement to account for any drift due to adsorption of atmospheric CO_2. The electrophoretic capillary cell was rinsed with 50 ml of 0.001 M $NaNO_3$ prior to each analysis. Five independent zeta potential measurements were collected for each sample to ensure accurate and reproducible data.

Surface Complexation Modeling

The adsorption of silicic acid and arsenite alone and competitively on goethite was modeled using the Charge Distribution Multisite Ionic Composition (CD-MUSIC) model using $SiO_2(OH)_2^{2-}$ and AsO_3^{3-} as the base species. The fundamental theory and development of the combined surface complexation and electrostatic model was presented earlier in the Theoretical Background section and has been extensively described in numerous publications. (Hiemstra et al., 1989a; Hiemstra et al., 1989b; Hiemstra et al., 1996; Rietra et al., 2000; Tadanier and Eick, 2002).

The surface functional groups on goethite differ in the number of Fe atoms (n) bound to them leading to singly (n = 1), doubly (n = 2), and triply coordinated (n = 3) sites. The proton affinities for each of these sites have been calculated using a refined version of the original Music model and the actual bond valences for each site. Hiemstra et al. (1989a) and Hiemstra et al. (1996), reported that the pK values for the protonation or deprotonation of doubly coordinated surface hydroxyl groups lies outside the environmental pH range (2-12) and doubly coordinated oxygens are therefore considered inert. Additionally, Hiemstra et al. (1996) concluded that the

triply coordinated sites were able to under go only one protonation step due to the presence of only one un-bonded oxygen orbital. Hiemstra et al. (1989a) and Hiemstra et al. (1996) further concluded that the log K value for the deprotonation of singly coordinated surface functional groups occurs above pH 11, and does not contribute to the overall charging behavior of goethite within the normal environmental pH range (3-11). Based on these previous conclusions, the surface acidity of goethite is controlled by two reactions (Table 2.1). The log K values for both reactions were set equal to the experimentally determined point of zero charge, as determined by electrophoretic mobility measurements (pH 9.56), which is a common practice when utilizing the CD-MUSIC model (Geelhoed et al., 1997; Geelhoed et al., 1998; Hiemstra et al., 1989b; Hiemstra et al., 1996; Hiemstra and Van Reinsdijk, 1996; Hiemstra and Van Riemsdijk, 1999; Hiemstra and Van Reimsdijk, 2000; Rietra et al., 1999; Rietra et al., 2000; Tadanier and Eick, 2002). Additionally, there is a large body of evidence that indicates the log K value or IEP for synthetic goethite occurs between 9 and 9.5 (Kosmulski, 2001).

Table 2.1. CD-MUSIC model surface complexation equilibrium reactions for the single anion (silicic acid and As(III)) and competitive asnion adsorption modeling

Chemical Reactions	Log K
Surface Acidity Reactions[1-5†]	
$\equiv FeOH^{-0.5} + H^+ \leftrightarrow \equiv FeOH_2^{+0.5}$	9.56
$\equiv Fe_3O^{-0.5} + H^+ \leftrightarrow \equiv Fe_3H^{+0.5}$	9.56
Electrolyte-Surface Ion Pair Formation[(4,5)]	
$\equiv FeOH^{-0.5} + Na^+ \leftrightarrow \equiv FeOH\text{-}Na^{+0.5}$	-1
$\equiv FeOH^{-0.5} + H^+ + NO_3^- \leftrightarrow \equiv FeOH_2\text{-}NO_3^{-0.5}$	8.56
$\equiv Fe_3O^{-0.5} + Na^+ \leftrightarrow \equiv FeO\text{-}Na^{+0.5}$	-1
$\equiv Fe_3O^{-0.5} + H^+ + NO_3^- \leftrightarrow \equiv FeOH\text{-}NO_3^{-0.5}$	8.56
Aqueous Solution Reactions[5]	
Silicic Acid	
$SiO_2(OH)_2^{-2} + H^+ \leftrightarrow SiO(OH)_3^{-1}$	13.1
$SiO_2(OH)_2^{-2} + 2H^+ \leftrightarrow Si(OH)_4^0$	22.96
As(III)	
$AsO_3^{-3} + H^+ \leftrightarrow AsO_2OH^{-2}$	13.4
$AsO_3^{-3} + 2H^+ \leftrightarrow AsO(OH)_2^{-1}$	25.53
$AsO_3^{-3} + 3H^+ \leftrightarrow As(OH)_3^0$	34.75
Surface Coordination Reactions[‡]	
Silicic Acid	
Monodentate	
$\equiv FeOH^{-0.5} + H^+ + SiO_2(OH)_2^{-2} \leftrightarrow \equiv FeOSiO(OH)_2^{-1.5} + H_2O$	17.66
$\equiv FeOH^{-0.5} + 2H^+ + SiO_2(OH)_2^{-2} \leftrightarrow \equiv FeOSi(OH)_3^{-0.5} + H_2O$	26.78
Bidentate	
$2\equiv FeOH^{-0.5} + H^+ + SiO_2(OH)_2^{-2} \leftrightarrow (\equiv FeO)_2SiO(OH)^{-2} + 2H_2O$	22.67
$2\equiv FeOH^{-0.5} + 2H^+ + SiO_2(OH)_2^{-2} \leftrightarrow (\equiv FeO)_2Si(OH)_2^{-1} + 2H_2O$	31.69
As(III)	
Monodentate	
$\equiv FeOH^{-0.5} + AsO_3^{-3} + H^+ \leftrightarrow \equiv FeOAsO_2^{-2.5} + H_2O$	23.22
$\equiv FeOH^{-0.5} + AsO_3^{-3} + 2H^+ \leftrightarrow \equiv FeOAsO(OH)^{-1.5} + H_2O$	33.90
$\equiv FeOH^{-0.5} + AsO_3^{-3} + 3H^+ \leftrightarrow \equiv FeOAs(OH)_2^{-0.5} + H_2O$	39.99
Bidentate	
$2\equiv FeOH^{-0.5} + AsO_3^{-3} + 3H^+ \leftrightarrow (\equiv FeO)_2As(OH)^{-1} + 2H_2O$	46.67

†IEP measurements
‡CD optimized values
1. Hiemstra et al. (1996), 2. Hiemstra and Van Reinsdijk (1996), 3. Rietra et al. (2000), 4. Tadanier and Eick (2002), and 5. (Smith and Martel, 1992)

Surface site density for singly and triply coordinated surface functional groups for goethite was taken from Barrón and Torrent (1996). Using a refined goethite structure, Barrón and Torrent

(1996) calculated the surface density for singly, doubly, and triply coordinated oxygen and hydroxyl surface sites on the {110} faces to be 3.0, 9.1, and 3.0 sites nm^{-2} respectively, and 8.2 sites nm^{-2} on the {021} face for singly and doubly coordinated hydroxyl groups, respectively. Using a weighted average, the average site density for singly, doubly, and triply coordinated oxygen and hydroxyl surface groups on goethite would be 3.52 sites nm^{-2} for singly and doubly, and 8.19 sites nm^{-2} for triply coordinated sites. Hiemstra and Van Reinsdijk (1996) proposed that along the {110} plane the triply coordinated functional groups have different positions in the surface structure and hence different proton affinities. Furthermore, they proposed that two-thirds of the triply coordinated oxygens undergo hydrogen bonding with singly coordinated groups and remain effectively uncharged over the entire pH range. This would allow only one-thrird of the triply coordinated sites to undergo proton adsorption, and changes the surface site density of triply coordinated groups from 8.19 to 2.7 sites nm^{-2}, 1/3 the original value. The surface site densities for singly and triply coordinated sites determined from the Barrón and Torrent (1996) study and applying Hiemstra and Van Riemsdijk (1996) description of the triply coordinated sites, the reactive surface site density for goethite is 3.52 and 2.7 sites nm^{-2} for singly and triply coordinated sites, respectively. Additionally, these values are similar to those listed in the literature for application of the CD-MUSIC model to the goethite surface (Geelhoed et al., 1997; Geelhoed et al., 1998; Hiemstra et al., 1996; Hiemstra and Van Reinsdijk, 1996; Hiemstra and Van Riemsdijk, 1999; Hiemstra and Van Reimsdijk, 2000; Reitra et al., 1999; Rietra et al., 1999; Rietra et al., 2000; Tadanier and Eick, 2002).

Ions of the electrolyte solution are assumed to form ion pairs (Table 2.2) whose charges are present at the head of the diffuse layer (2-plane) and are assumed to be point charges (Chapter 1

Fig. 4). The log K values for the formation of the electrolyte ion pairs have been previously determined by Rietra et al. (2000) and have been set equal to the literature values of -1 for Na^+ and PZC-1 for NO_3^-.

Specifically adsorbed ions approach the surface more closely than ion pairs since the adsorbate and the surface share one or more ligands. The CD-MUSIC model allows the charge of specifically adsorbing ions to be distributed between the 0- and 1-electrostaic planes in an effort to more realistically depict the solid-solution interface. The CD factor (f) represents the portion of the adsorbing central cation charge that is neutralized by surface ligands located at the 0-plane. While (1- f) represents the portion of the adsorbing cation charge neutralized by solution oriented ligands in the 1-plane (Hiemstra and Van Reinsdijk, 1996). If the charge of the adsorbing cation is assumed to symmetrically neutralized by all surrounding ligands then f equals the number of surface oriented ligands (L_S) divided by the total number of ligands coordinated to the central cation (L_T), as presented in the following equation and shown in Figure 1.5 in Chapter 1.

$$f = \frac{L_s}{L_T} \qquad \textbf{(43)}$$

Application of Equation 1 to mono- and bidentate silicic acid surface complexes yields a CD factor (f) of 0.25 and 0.50, respectively. In the case of arsenite, mono- and bidentate surface complexes Equation 1 yields CD factors of 0.33 and 0.66, respectively.

The computer program FITEQL 4.0 was used to calculate the equilibrium constants for silicic acid and arsenite adsorption on goethite. While the CD-MUSIC model is not explicitly listed as

one of the surface complexation models (SCM) available for use in FITEQL 4.0, Tadanier and Eick (2002) recently developed a method of implementing it into the existing computer code. The CD-MUSIC model was implemented through the existing Triple Layer Model within FITEQL. The electrostatic components in the 0-plane mass balance matrix are adjusted to reflect the actual charge (± 0.5) of the reactive goethite adsorption sites (Tadanier and Eick, 2002). Model parameters and chemical reactions used in the CD-MUSIC model are in Tables 2.1 and 2.2.

Table 2.2. CD-MUSIC model mineral surface parameters for the single ion and competitive ion adsorption modeling.

Parameter/Reaction	Value
Specific Surface Area ($m^2\ g^{-1}$) †	72.75
Site Density (sites nm^{-2}) (1-13)	
≡FeOH	3.45
≡Fe_3OH	2.7
Capacitance factors(F m^{-2})	
C_1	1.5
C_2	5.5

†BET N2 Adsorption isotherm

Results and Discussion

Adsorption Edges

Silicic acid adsorption on goethite was examined at three initial Si solution concentrations of 0.10, 0.50, and 1.00 mM. The low concentration (0.10 mM) is representative of dissolved silica concentrations in fresh waters, while the high concentration (1.00 mM) more closely resembles dissolved silica concentrations in soils (Iller, 1979; McKeague and Cline, 1963b). Adsorption of silicic acid on goethite for the three initial solution concentrations is presented in Figure 2.2. Adsorption was highly pH dependent, giving rise to the formation of an adsorption envelope with maximum adsorption occurring near pH 9 (Fig. 2.2 and Table 2.3). Additionally, the pH

dependency of silicic acid adsorption increases with increasing Si_T concentration. The increased pH dependency of silicic acid adsorption with increasing concentration is due to the unfavorable thermodynamics of the initial deprotonation of silicic acid prior to the ligand exchange reaction. Similar results have been reported in the literature for silicic acid adsorption on other Fe (hydr)oxides and soils (Hansen et al., 1994b; McKeague and Cline, 1963a; Meng et al., 2000; Obihara and Russell, 1972; Swedlund and Webster, 1999; Waltham and Eick, 2002).

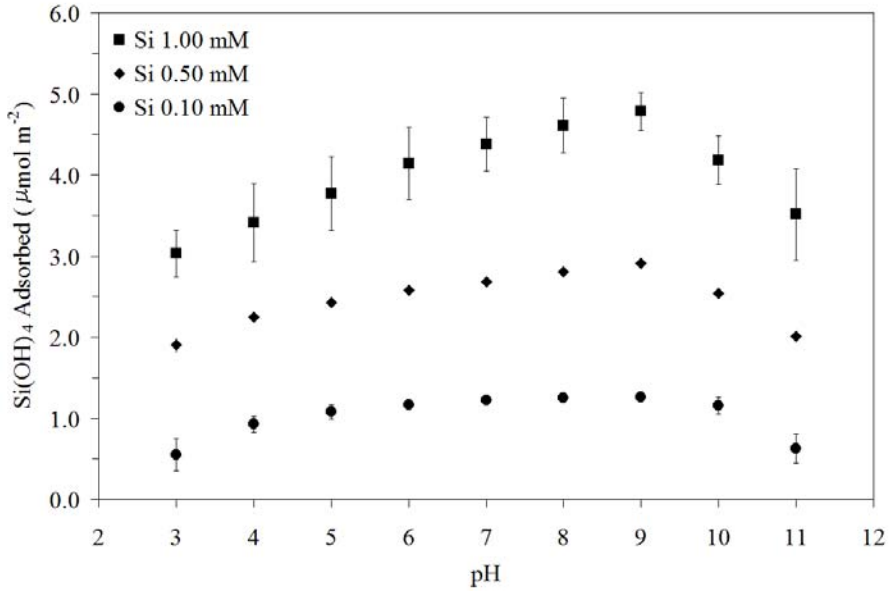

Figure 2.2. Silicic acid pH adsorption edges on goehite Si_T = 0.10, 0.50, and 1.00 mM. Suspension density = 1 g L^{-1}, background electrolyte 0.01 M $NaNO_3$

Table 2.3. Percentage of Silicic acid adsorbed for the three initial Si solution concentrations

	Percent Silicic acid adsorbed		
pH	**0.10 mM**	**0.50 mM**	**1.00 mM**
11	43.2	16.6	18.4
10	81.7	24.8	23.4
9	89.9	30.4	27.9
8	89.1	28.9	26.6
7	86.9	27.0	24.8
6	82.5	25.4	22.9
5	76.0	23.0	20.3
4	64.9	20.3	17.6
3	37.5	15.0	14.7

Silicic acid adsorption at 1.00 mM concentration displayed more variation than at lower concentrations, as indicated by the error bars in Fig. 2.2. Error bars in all figures presented represent the range of observations. The increased variability of silicic acid adsorption at the 1.0 mM initial solution concentration may be due to of Si polymer formation in solution or at the goethite surface.

Evidence of silica polymerization on goethite is suggested by examination of the adsorption isotherm in Figure 2.3. Typically, as mineral surface sites become saturated by an adsorbate, the adsorption isotherm begins to plateau and eventually levels off. (McBride, 1994; Sposito, 1989) However, even at pH 9 when 70% of the singly coordinated functional groups are participating in surface complexation reactions, adsorption continues to increase, indicating that the surface is not saturated or close to saturation. Previous studies have demonstrated the formation of Si polymers on ferrihydrite and in solution at similar silicic acid concentrations (Alverez and Sparks, 1985; Applin, 1987; Hansen et al., 1994b; Vempati et al., 1990). Small solution polymers expected at these Si solution concentrations are to small to be removed by filtration; therefore this must be a surface phenomenon.

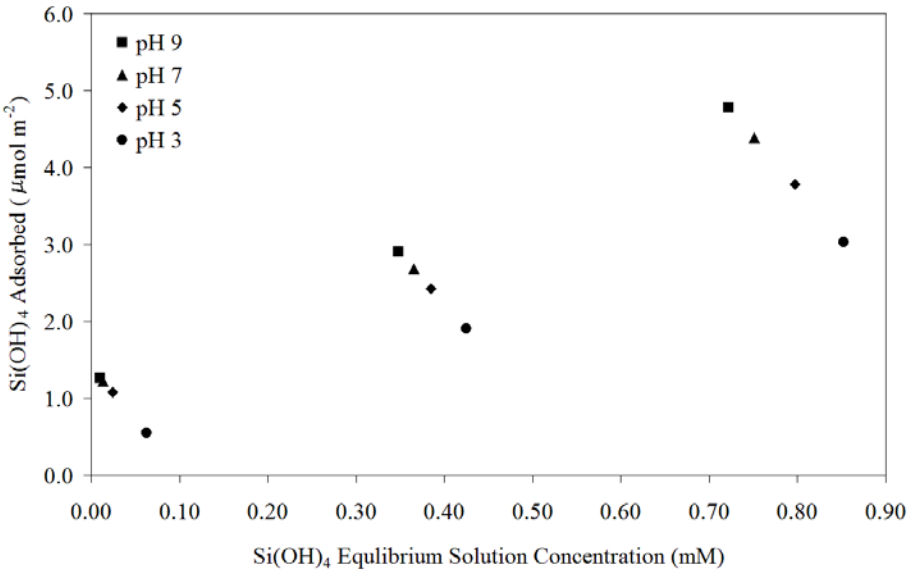

Figure 2.3. Adsorption isotherm of silicic acid on goethite. Suspension density = 1 g L^{-1}, background electrolyte 0.01 M $NaNO_3$

Arsenite adsorption on goethite was investigated at initial solution concentrations of 0.05 and 0.10 mM. Although these concentrations exceed EPA's current drinking water standards of 10 ppb, they were chosen to represent point-source emission or a worst-case scenario. Results of the arsenite adsorption on goethite are presented in Figure 2.4. Arsenite adsorption on goethite displayed very little pH dependency for the concentrations investigated. Additionally, the percentage of arsenite adsorbed was greater than 98% over the entire pH range investigated (Table 2.4). Similar results for arsenite adsorption by Fe hydroxides has also been documented in the literature (Arai et al., 2001; Goldberg and Johnston, 2001; Manning et al., 1998; Meng et al., 2000; Sun and Doner, 1996;Swedlund and Webster, 1999; Waltham and Eick, 2002).

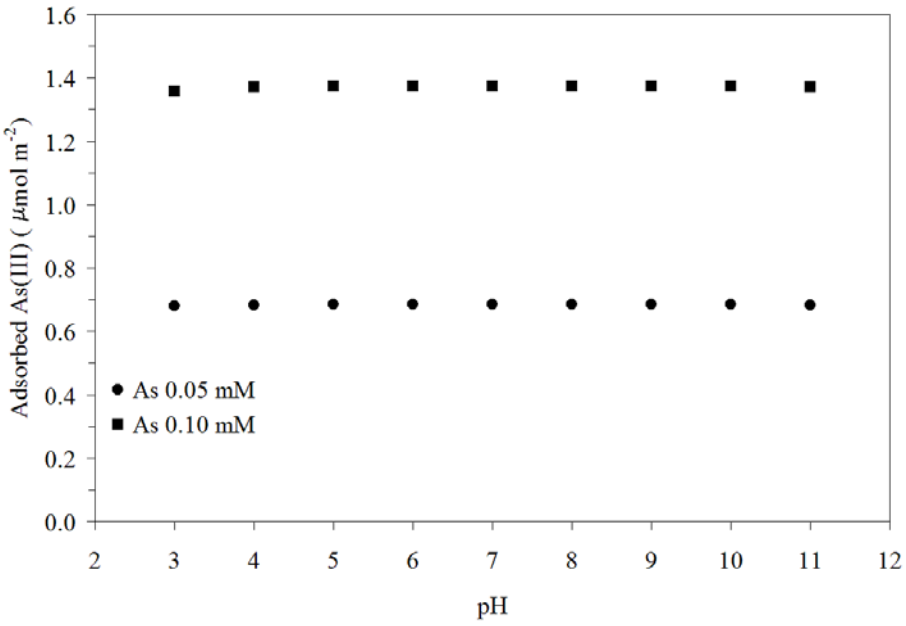

Figure 2.4. Arsenite pH adsorption edge for initial solution concentrations of 0.05 and 0.10 mM. Suspension density = 1 g L^{-1}, background electrolyte 0.01 M $NaNO_3$

Table 2.4. Percentage of arsenite adsorbed for the two initial As(III) solution concentrations.

	Percent As (III) adsorbed	
pH	**0.05 mM**	**0.10 mM**
11	99.30	98.45
10	99.74	99.87
9	99.74	99.93
8	99.74	99.93
7	99.74	99.93
6	99.57	99.93
5	99.69	99.93
4	99.44	99.77
3	98.83	98.84

The results of the competitive adsorption studies are presented in Figures 5-8. The competitive studies were conducted for both concentrations of arsenite (0.05 and 0.1 mM) and the high and low concentrations of silicic acid (0.10 and 1.00 mM). All of the possible combinations of initial solution concentrations and the effect of order of adsorbate addition were investigated. Based on the initial concentration of silicic acid the competitive adsorption studies can be separated into

two categories: i) the influence of 0.10 mM silicic acid on arsenite adsorption (low Si) and ii) the influence of 1.00 mM silicic acid on arsenite adsorption (high Si).

The results from the competitive adsorption for low Si and arsenite are presented in Figures 5 and 6. Silicic acid did not influence arsenite adsorption at either of the investigated concentrations. Additionally, the adsorbate addition order did not influence arsenite adsorption. However, arsenite reduced silicic acid adsorption at both concentrations and under both addition scenarios (Fig. 5 and 6). There is also a greater reduction in silicic acid adsorption at the higher initial arsenite solution concentration (0.10 mM). The results for low Si demonstrate that arsenite is able to out-compete silicic acid for adsorption sites on goethite. Furthermore, this would indicate arsenite may somehow change the adsorption environment at the solid-solution interface, because even at equimolar oxyanion concentrations, the goethite surface is well below saturation. The previously discussed results are in close agreement with those presented by Swedlund and Webster (1999) who also witnessed a reduction in silicic acid adsorption (0.10 mM) on ferrihydrite in the presence of arsenite (0.053 μM).

Results from the competitive adsorption of high Si and arsenite are presented in Figures 2.7 and 2.8. In contrast to the low Si scenario, silicic acid reduced arsenite adsorption at pH 8 and above for the low arsenite concentration (Fig. 2.7), and over the entire pH range for the high arsenite concentration (Fig. 2.8). These reductions in arsenite adsorption could be due to saturation of the available adsorption sites on the goethite surface. As with the low Si scenario, there was a greater reduction in silicic acid adsorption than arsenite adsorption, again indicating that arsenite is the more stable surface complex. Arsenite reduced silicic acid adsorption for all but one of the

competitive adsorption scenarios—high Si and high arsenite when silicic acid is added before arsenite (Fig. 2.8). This result is unexpected and not consistent with the results presented. Additionally, nothing has been presented in the literature to offer a possible explanation to the observed results. Two possible explanations are: i) experimental error and ii) the system had not fully equilibrated. Because the adsorption edges were conducted in duplicate from nine individual batch experiments, it seems highly unlikely that the increased silicic acid adsorption was due to experimental error. It seems more likely that the increased arsenite concentration and possible presence of Si polymers reduced the kinetics at which the system reaches equilibrium, resulting in a longer equilibration period.

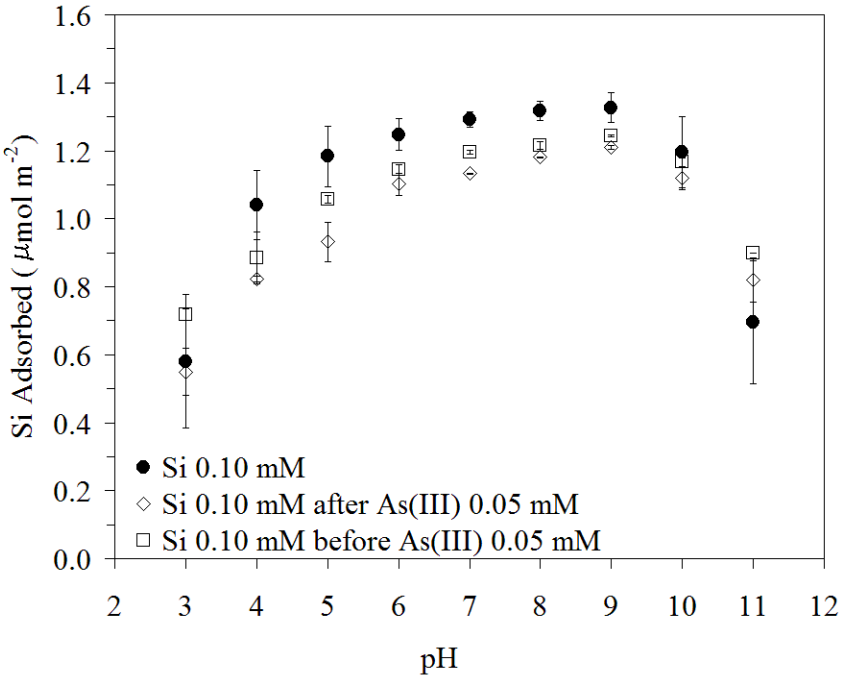

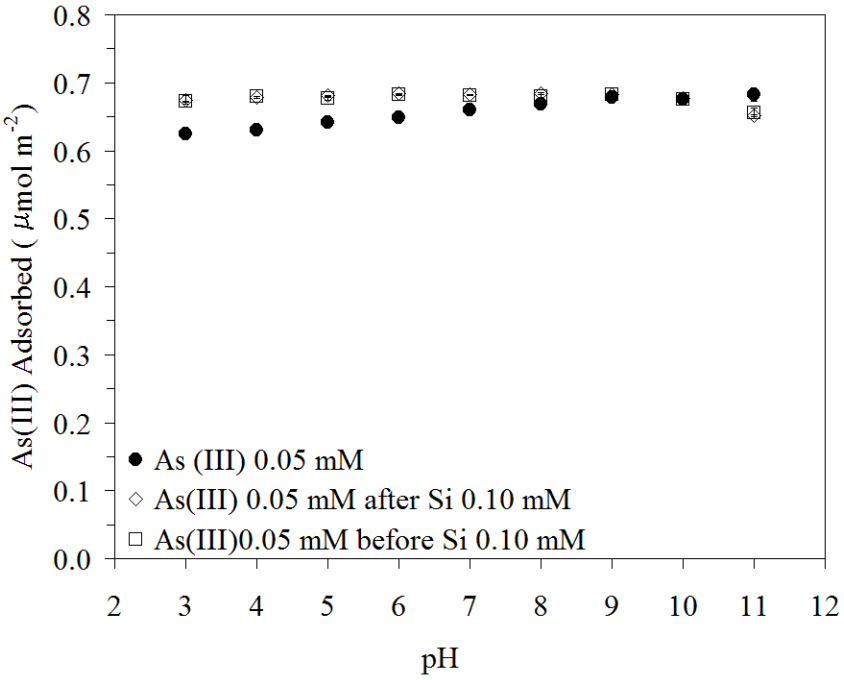

Figure 2.5. Competitive adsorption of 0.10 mM silicic acid and 0.05 mM arsenite on goethite. Suspension density = 1 g L^{-1}, background electrolyte 0.01 M $NaNO_3$

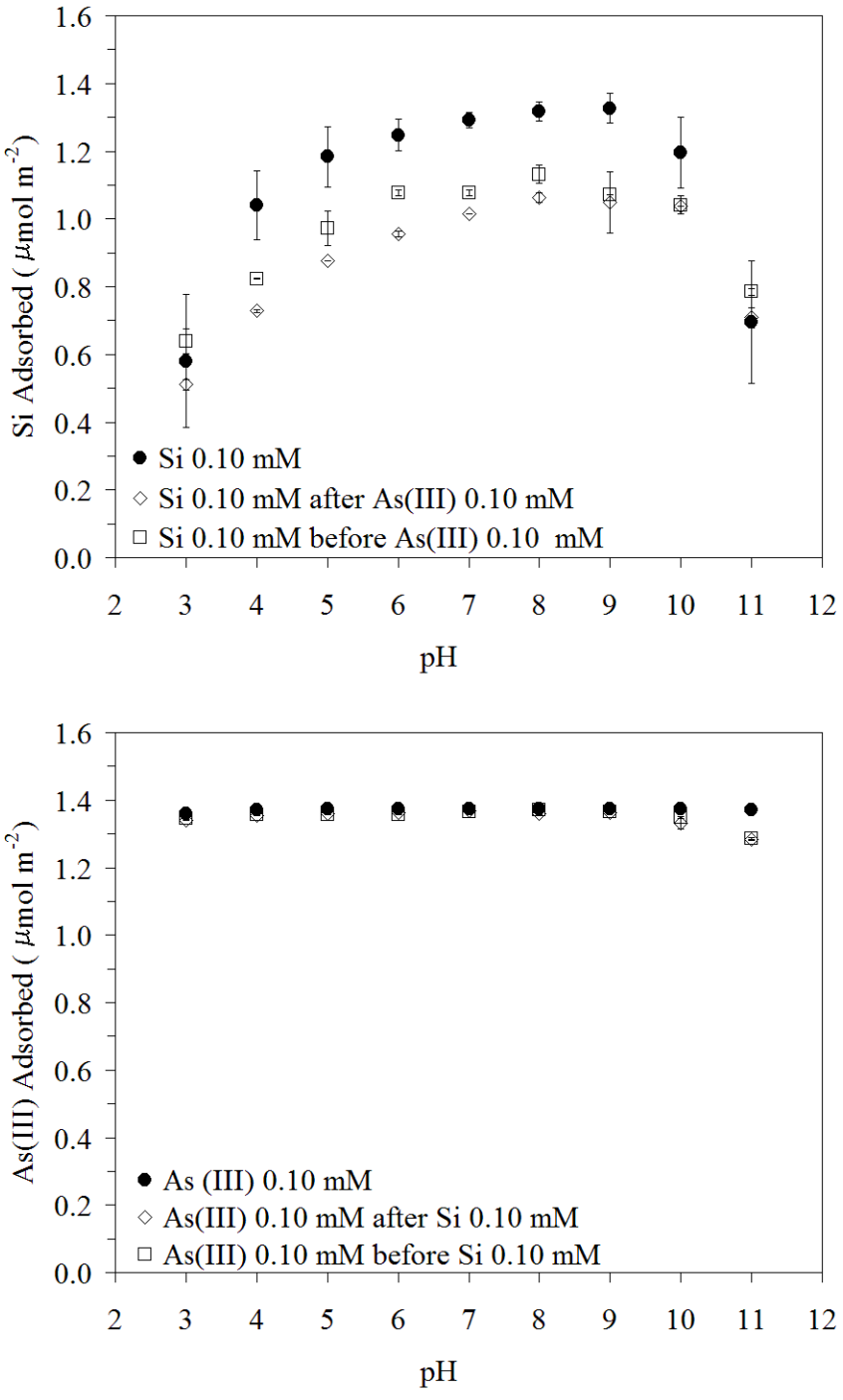

Figure 2.6. Competitive adsorption of 0.10 mM Silicic acid and 0.10 mM arsenite on goethite. Suspension density = 1 g L^{-1}, background electrolyte 0.01 M $NaNO_3$

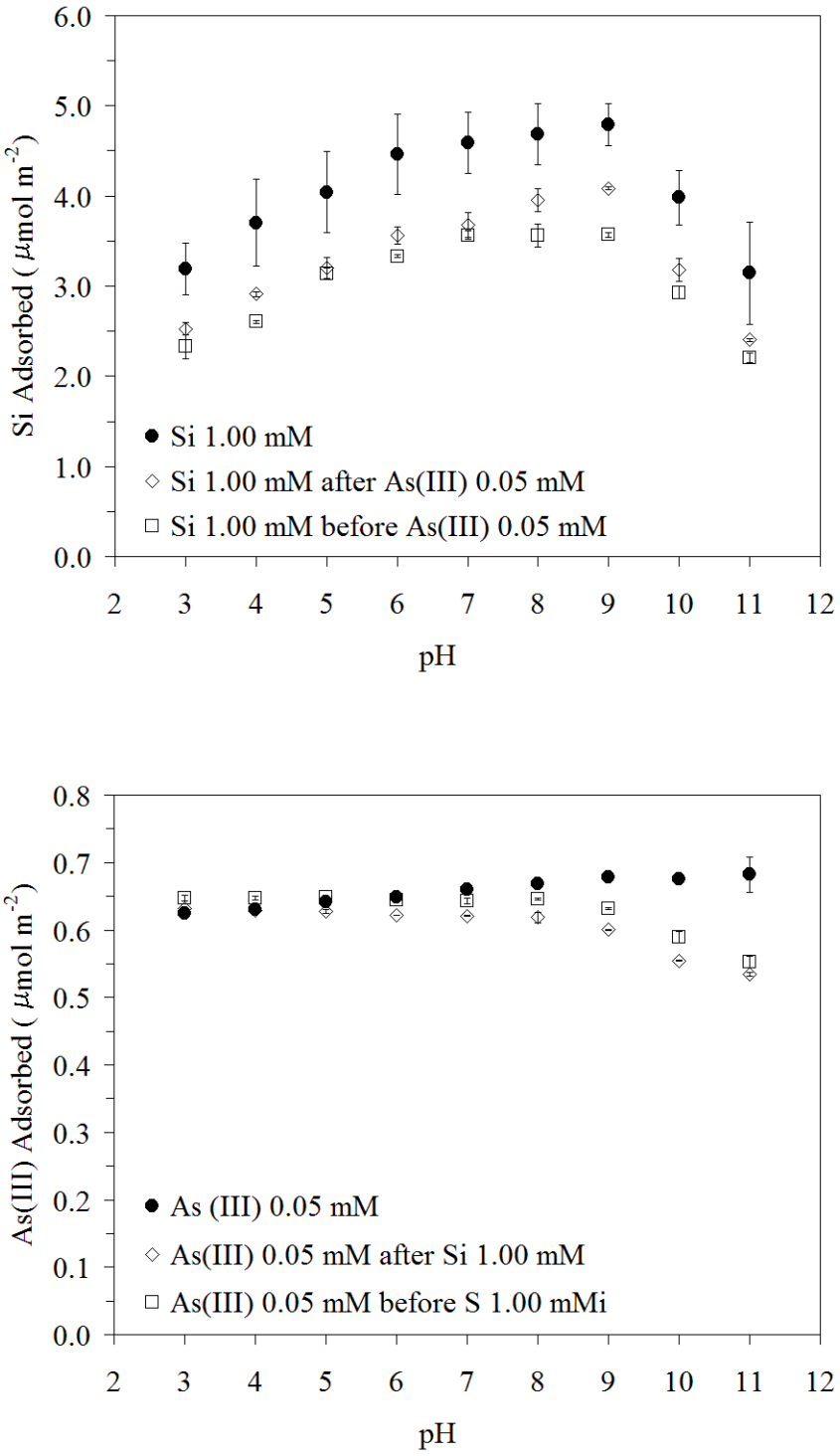

Figure 2.7. Competitive adsorption of 1.00 mM Silicic acid and 0.05 mM arsenite on goethite. Suspension density = 1 g L^{-1}, background electrolyte 0.01 M $NaNO_3$

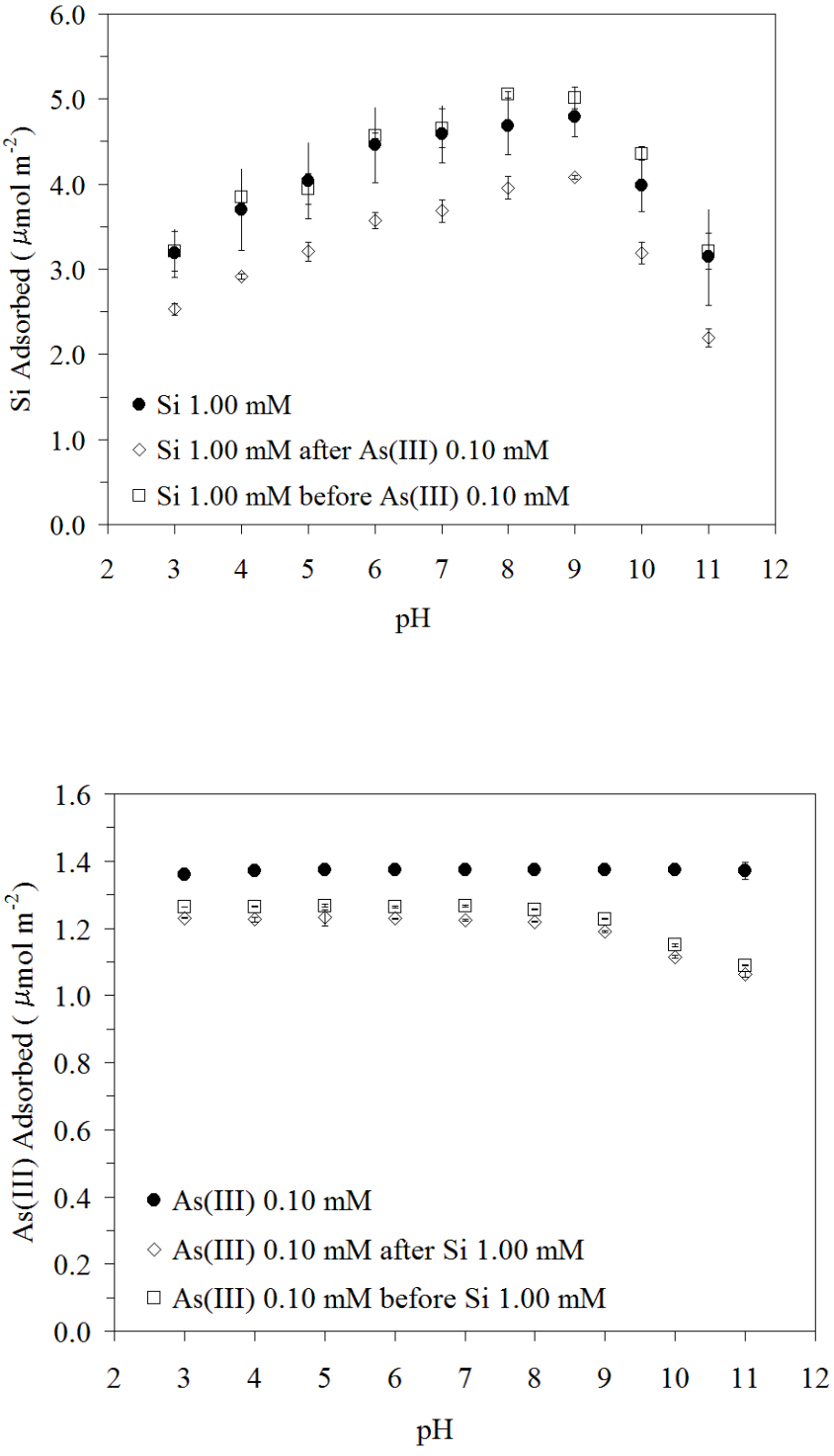

Figure 2.8. Competitive adsorption of 1.00 mM silicic acid and 0.10 mM arsenite on goethite. Suspension density = 1 g L^{-1}, background electrolyte 0.01 M $NaNO_3$

Although silicic acid only had a modest influence on arsenite adsorption at high loadings, it dramatically influences arsenite equilibrium solution concentrations (Fig. 2.9). The effect of silicic acid is greatest at the 1.00 mM concentration where arsenite solution concentrations are 100 times greater than when arsenite is present alone (Table 2.5). This would indicate that competition of silicic acid for surface adsorption sites dramatically increases the amount of potentially bioavailable and mobile arsenite in soils and sediments. Similar results have also been reported for arsenite adsorption in the presence of dissolved organic carbon (Grafe et al., 2001; Grafe et al., 2002). Results of this study, and those of Grafe et al. (2001 and 2002), would indicate that the increased mobility of arsenite maybe due to the adsorption of naturally occurring organic and inorganic ligands on Fe (hydr)oxide minerals.

Table 2.5. Increase in arsenite equilibrium solution concentration in the presence of silicic acid

pH	Arsenite 0.10 mM				
	As(III) equilibrium solution concentration (mg L^{-1})				
	Alone	Si 0.10 mM		Si 1.00 mM	
		Added before Si	Added after Si	Added before Si	Added after Si
11	0.018	0.485	0.520	1.733	1.707
10	0.005	0.150	0.161	1.417	1.427
9	0.005	0.056	0.063	0.993	0.991
8	0.005	0.057	0.052	0.839	0.843
7	0.005	0.060	0.054	0.793	0.802
6	0.005	0.080	0.057	0.810	0.783
5	0.016	0.081	0.071	0.785	0.766
4	0.005	0.112	0.105	0.795	0.800
3	0.010	0.183	0.169	0.795	0.792
pH	Arsenite 0.05 mM				
	As(III) equilibrium solution concetration (mg L^{-1})				
	Alone	Si 0.10 mM		Si 1.00 mM	
		Added before Si	Added after Si	Added before Si	Added after Si
11	0.021	0.196	0.520	0.881	0.925
10	0.012	0.059	0.161	0.839	0.817
9	0.016	0.024	0.063	0.582	0.565
8	0.005	0.016	0.052	0.495	0.471
7	0.010	0.031	0.054	0.457	0.456
6	0.011	0.021	0.057	0.454	0.452
5	0.016	0.031	0.071	0.433	0.421
4	0.026	0.050	0.105	0.450	0.419
3	0.010	0.071	0.169	0.410	0.406

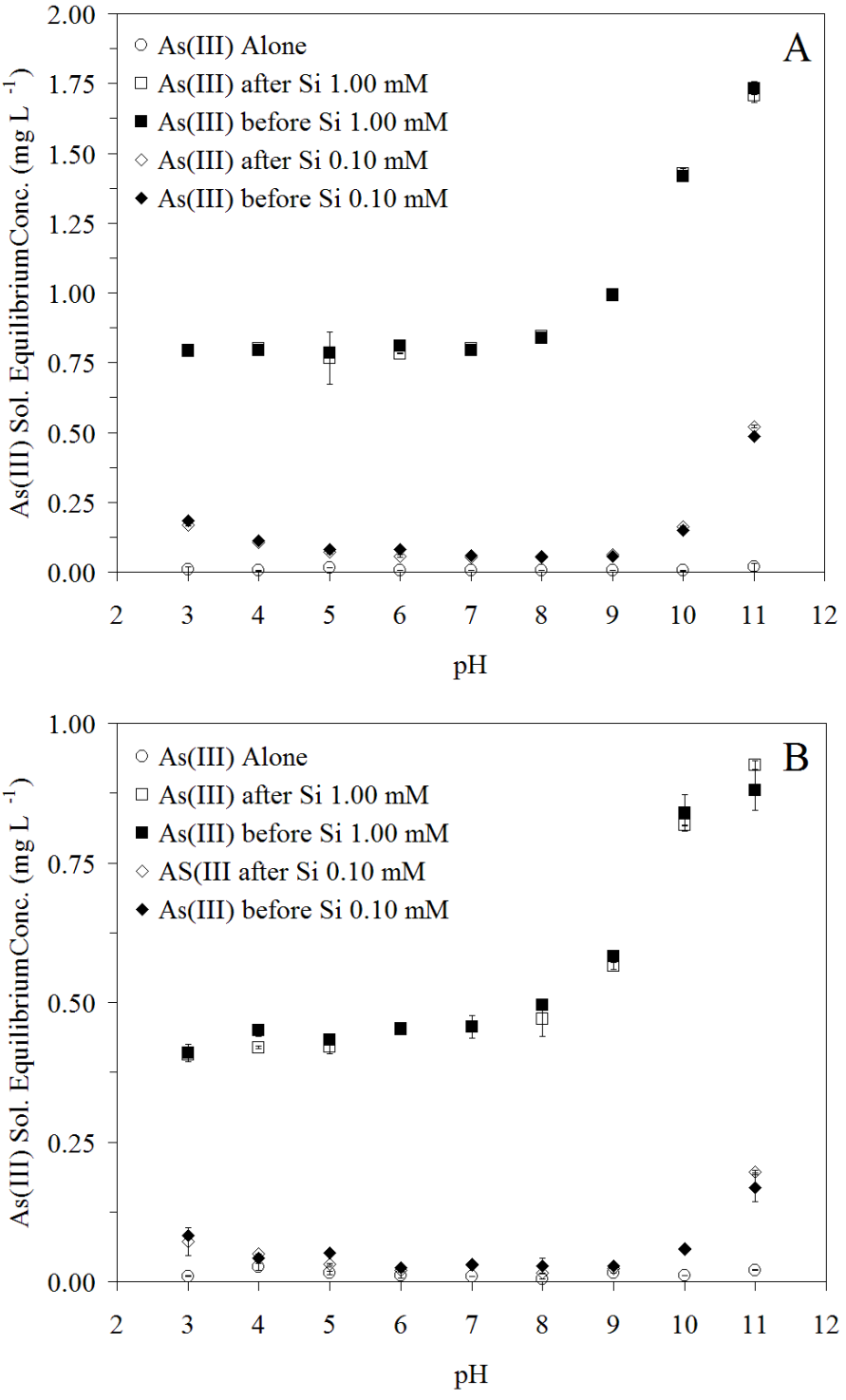

Figure 2.9. Arsenite equilibrium solution concentration in the presence of silicic acid. A) $As(III)_T$ = 0.10 mM and B) $As(III)_T$ = 0.05 mM. Suspension density = 1 g L^{-1}, background electrolyte 0.01 M $NaNO_3$

Zeta Potential Measurements

Zeta potential measurements were conducted on all of the single ion pH adsorption isotherms over the entire pH range studied, and for selected competitive adsorption scenarios and pH values. The results of the single ion adsorption zeta potential measurements are presented in Figure 10 and the IEP for each pH adsorption edge is presented in Table 2.6.

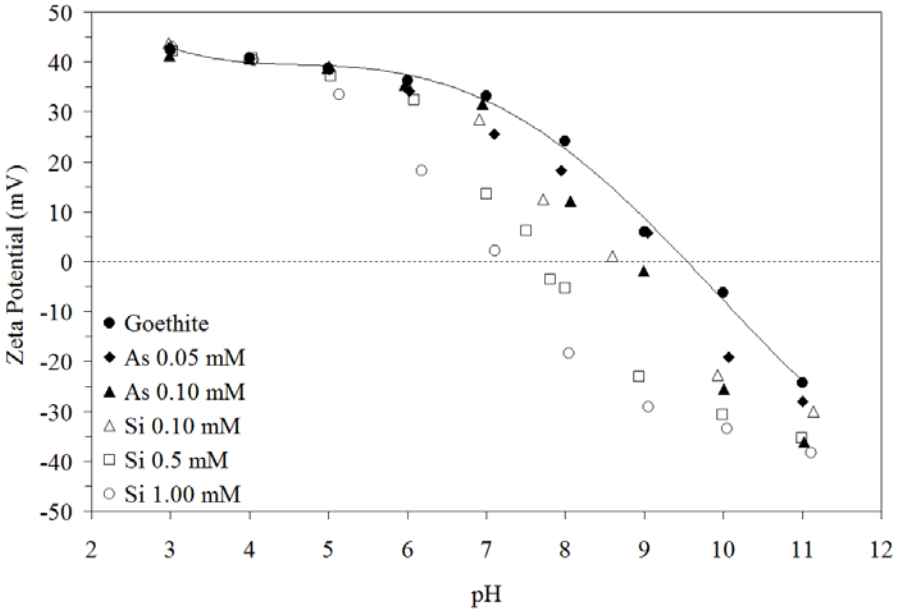

Figure 2.10. Zeta potential measurements for the single ion pH adsorption edges. The solid line represents the zeta potential edge for the goethite surface in the absence of silicic acid and arsenite as fit by a fourth order polynomial equation. Suspension density = 1 g L^{-1}, background electrolyte 0.01 M $NaNO_3$

Table 2.6. IEP values from the zeta potential measurements for the single ion pH adsorption edges.

Oxyanion	Concentration (mM)	IEP
None	0.00	9.6
$Si(OH)_4$	0.10	8.8
$Si(OH)_4$	0.50	7.8
$Si(OH)_4$	1.00	7.1
$As(OH)_3$	0.05	9.1
$As(OH)_3$	0.10	8.9

The solid line in Figure 2.9 has been fitted to the zeta potential data for goethite in the absence of silicic acid and arsenite. Isoelectric point calculations were determined by fitting a fourth ordered polynomial equation to the zeta potential edge, and then solving for the condition of zero potential. The IEP shifted to lower pH values for each of the single ion pH adsorption isotherms, indicating that both arsenite and silicic acid form an inner-sphere surface complex with goethite. Additionally, the IEP reduction increased with increasing oxyanion concentration, which is to be expected with inner-sphere surface complex formation (Kosmulski, 2001). The competitive pH adsorption data from the previous section indicated that arsenite was the more stable surface complex in each scenario investigated. However, the difference between the IEP shift for equi-molar concentrations of silicic acid and arsenite (0.10 mM) were nearly identical (Table 2.6). This would indicate that both oxyanions have a similar affinity for the goethite surface and should experience equal reductions in adsorption at equal concentrations. One potential reason for observed differences in the competitive adsorption edges would be that the displaced arsenite forms an outer-sphere complex with goethite. This would explain why there was no reduction in arsenite adsorption for the low Si solution (Fig. 2.5 and 2.6), and minimal reduction for the high Si concentration (Fig 2.7 and 2.8).

The results of the selected competitive adsorption edges are presented in Figure 2.11 and the shift in the IEP of goethite is presented Table 2.7. The solid line represents goethite in the absence of silicic acid and arsenite, and the dashed line represent the zeta potential data for silicic acid alone at the high and low Si concentrations. Zeta potential data and shifts in the IEP for both the high and low Si concentration showed very little dependence upon the initial concentration of arsenite present (Fig. 2.11 and Table 2.7).

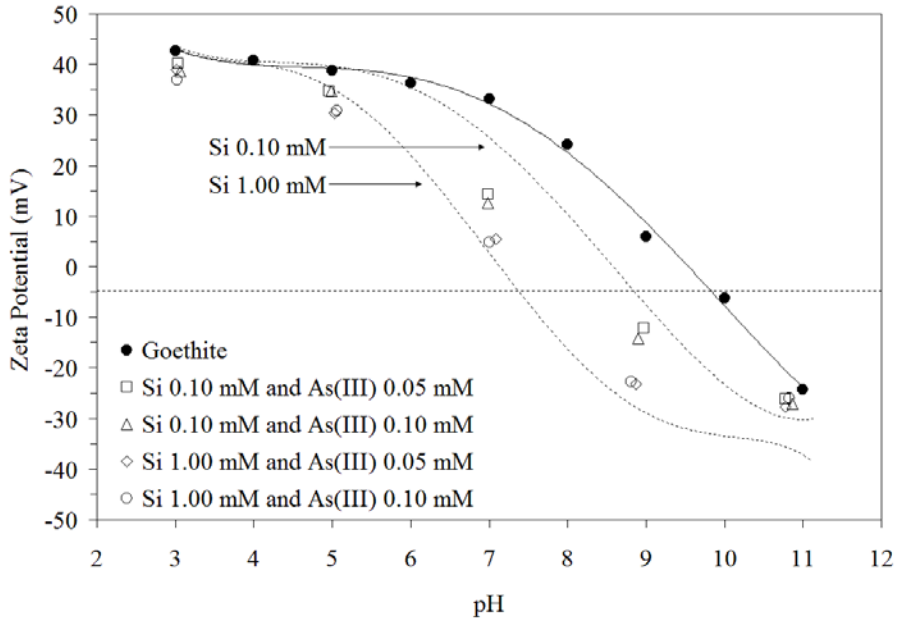

Figure 2.11. Zeta potential measurements for the competitive ion pH adsorption edges. The solid represents the zeta potential edge for the goethite surface in the absence of silicic acid and As(III). Dashed lines represent the zeta potential edges for silicic acid alone at the 0.10 and 1.00 mM initial solution concentrations.

Table 2.7. Calculated IEP values from the zeta potential measurements for the competitive ion pH adsorption edges.

Oxyanion	Concentration (mM)	IEP
$Si(OH)_4$	0.10	8
$As(OH)_3$	0.05	
$Si(OH)_4$	0.10	7.9
$As(OH)_3$	0.10	
$Si(OH)_4$	1.00	7.2
$As(OH)_3$	0.05	
$Si(OH)_4$	1.00	7.2
$As(OH)_3$	0.10	

The IEP of the low Si concentration in the presence of arsenite is approximately one pH unit less than silicic acid alone (Tables 2.6 and 2.7). These results would indicate that both arsenite and silicic acid specifically adsorb to the goethite surface. However, there is a very slight increase in the IEP for high Si concentration. In the presence of arsenite, similar IEP values for silicic acid

adsorption alone or in the presence of arsenite indicates the possibility that arsenite forms an outer-sphere surface complex with goethite in the presence of silicic acid.

Adsorption Surface Complexation Modeling

The adsorption of silicic acid and arsenite alone, and an in competition on goethite, was modeled using the CD-MUSIC surface complexation model developed by (Hiemstra and Van Reinsdijk, 1996), and implemented in FITEQL 4.0 using the method outlined by Tadanier and Eick (2002). The surface chemical reactions considered, and the modeling parameters used for both silicic acid and arsenite adsorption are located in Tables 2.1 and 2.2.

Zeta potential measurements were used to evaluate CD-MUSIC model parameters and calculated equilibrium constants for single and competitive ion adsorption. In order to use zeta potential data the location of the plane of shear must be known. However, the location is dependent upon numerous environmental conditions (pH, ionic strength, temperature, and presence of specifically adsorbing ions) and is difficult to determine (Kosmulski, 2001). The location of the plane of shear was estimated as the position in the diffuse double layer at which the electrical potential calculated from Gouy Chapman theory $\Psi(x)$ was equal to the experimentally measured zeta potential (Fig. 1). The electrical potential as a function of position in the diffuse layer was calculated from Gouy Chapman theory according to

$$\tanh\left(\frac{ze\Psi_x}{4kT}\right) = \tanh\left(\frac{ze\Psi_2}{4kT}\right)e^{-\mathrm{K}x} \qquad \textbf{(44)}$$

where

z = bulk ion charge (+1 or 1- for Na^+ and NO_3^-)

e = charge of a electron ($1.62*10^{-19}$ C)

Ψ_x = electric potential at a distance x from the 2-plane (V)

k = Boltzmann constant ($1.38*10^{23}$ J K^{-1})

T = temperature (K)

Ψ_2 = electric potential at the 2-plane (V)

κ = double layer thickness (cm^{-1})

x = distance from the 2-plane (cm).

The electric potential at the 2-plane was determined for each oxyanion adsorption scenario from CD-MUSIC model output. Comparison of calculated $\Psi(x)$ values over the range of 0.1 to 2.8 nm from the 2-plane (into the diffuse layer) with experimentally measured zeta potential data indicated that the shear plane was located at a distance of approximately 2.5 nm from the 2-plane.

The electric potential in the diffuse layer was calculated for distances of 0.1 to 2.8 nm away form the 2-plane and results were compared to zeta potential data for each of the single ion zeta potential edges to identify the approximate location of the plane of shear. Comparison of modeling results and zeta potential data indicated that the plain of shear was located approximately 2.5 nm away from the 2-plane. Zeta potential measurements were then employed to evaluate the parameters used and equilibrium constants calculated by the CD-MUSIC model by comparing the fit of the model calculated zeta potential, assuming the plane of shear is 2.5 nm from the 2-plane, to the experimental zeta potential data.

Single Anion Adsorption

Arsenite adsorption data was modeled using a single set of adsorption equilibrium constants generated by FITEQL for both arsenite concentrations. The adsorption modeling results for both arsenite concentrations are presented in Figure 2.12. Five possible surface complexes were used to model arsenite adsorption on goethite and are listed in Table 2.8 along with their CD-MUSIC optimized intrinsic equilibrium constants. The surface complex species used to model arsenite adsorption were taken from the literature based on spectroscopic investigations utilizing attenuated total reflectance Fourier transformed infrared spectroscopy (ATR-FTIR), X-ray adsorption spectroscopy (XAS), and Raman spectroscopy (Arai et al., 2001; Manning et al., 1998; Sun and Doner, 1996).

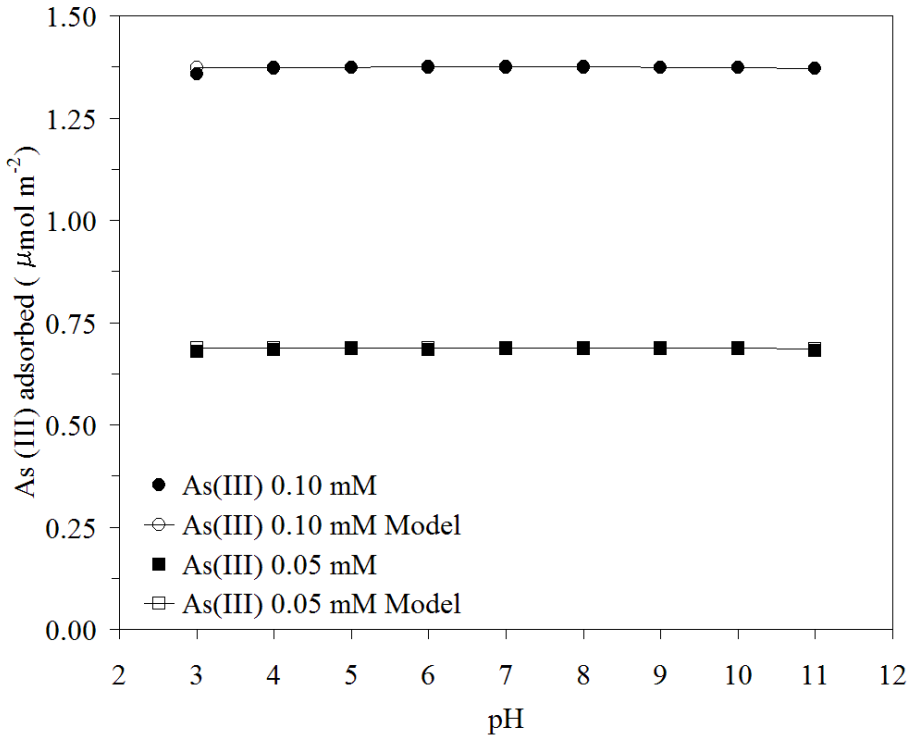

Figure 2.12. Arsenite adsorption on goethite utilizing the CD-MUSIC model at two arsenite concentrations, 0.05 and 0.10 mM. Solid symbols represent adsorption data. Solid lines represent predicted model concentrations. Suspension density = 1 g L^{-1}, background electrolyte 0.01 M $NaNO_3$

Table 2.8. Arsenite surface species and CD-MUSIC optimized equilibrium constants.

Surface Complex	Surface Complex Abbreviation	Log K
$\equiv FeOAsO_2^{2.5-}$	$Fe\text{-}As^{2.5-}$	23.92
$\equiv FeOAsOOH^{1.5-}$	$Fe\text{-}As^{1.5-}$	33.14
$\equiv FeOAs(OH)_2^{0.5-}$	$Fe\text{-}As^{0.5-}$	47.73
$\equiv Fe_2O_2AsO^{2-}$	$Fe\text{-}As^{2-}$	37.55
$\equiv Fe_2O_2As(OH)_2^{1-}$	$Fe\text{-}As^{1-}$	46.77

The CD-MUSIC model was able to accurately predict arsenite adsorption for the two concentrations investigated with a goodness of fit parameter of less than 0.10 for both concentrations.

The modeled surface speciation and zeta potentials for arsenite adsorption are presented in Figures 2.18 and 2.19, respectively. The two most predominant species predicted for both arsenite concentrations are the $Fe\text{-}As^{-0.5}$ and $Fe\text{-}As^{1-}$ species with the bidentate species more predominant at the 0.05 mM concentration and the monodentate species at the 0.10 mM concentration. Additionally the CD-MUSIC model was also able to accurately predict the zeta potential data over the entire pH range investigated as well as the IEP for both arsenite concentrations (Table 2.9 and Fig. 2.19). The surface speciation predicted by the CD-MUSIC model does conflict somewhat with current research as to what types of arsenite complexes are present at the goethite surface. The presence of bidentate surface complexes for arsenite adsorbed onto the goethite have been identified by XAS and FTIR, however, both studies found insufficient evidence to report the formation of a monodentate complex (Manning et al., 1998; Sun and Doner, 1996). However, the formation of monodentate and outer-sphere surface complexes has been reported for arsenite adsorption on γAl_2O_3 and Fe and Al amorphous oxides (Arai et al., 2001; Goldberg and Johnston, 2001).

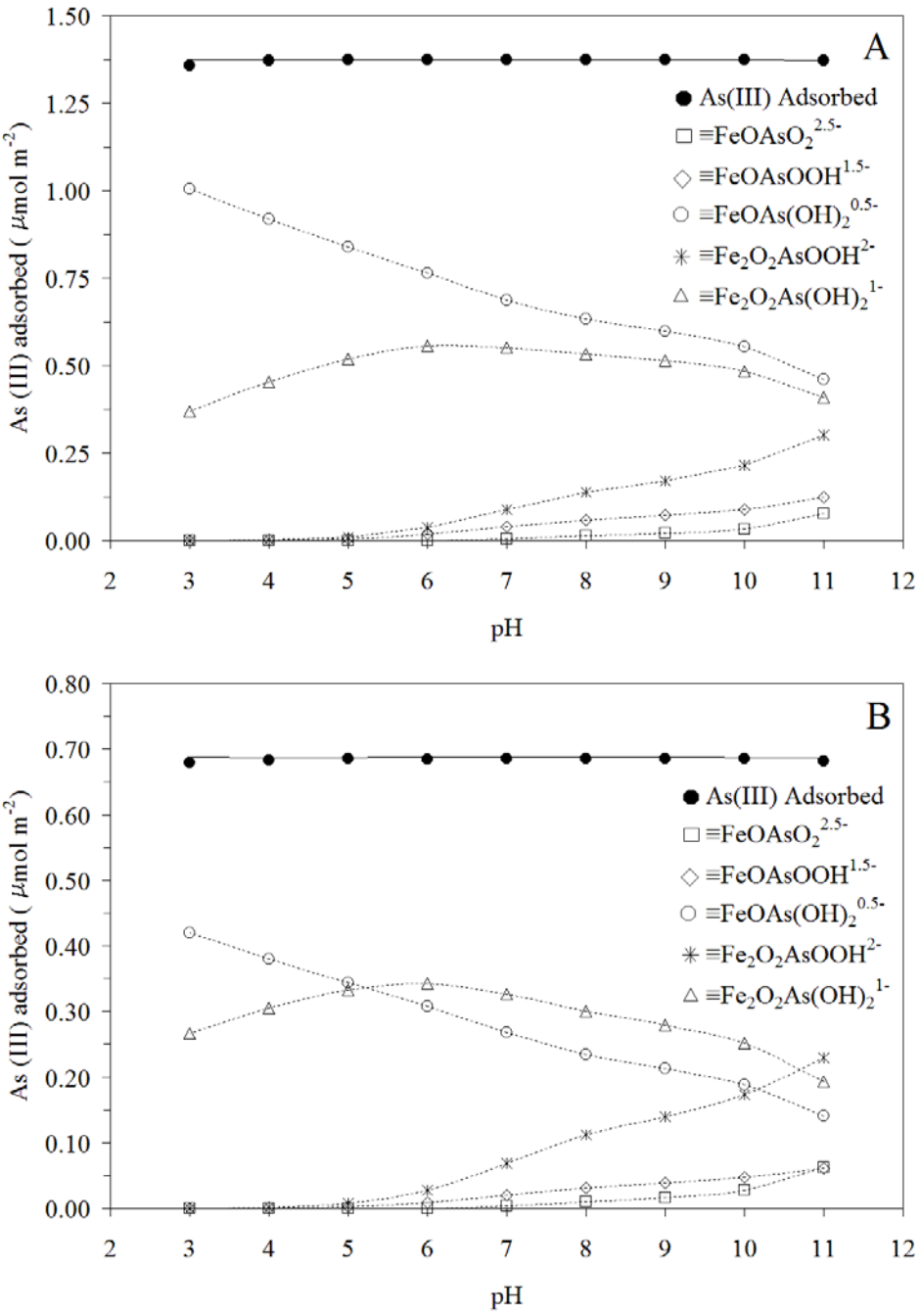

Figure 2.13. Arsenite adsorption on goethite utilizing the CD-MUSIC model. A) $As(III)_T$ = 0.10 mM and B) $As(III)_T$ = 0.05 mM. Closed symbols represent experimental data. Open symbols and dashed lines represent adsorbed arsenite species based on optimized CD-MUSIC model fit to experimental data. Solid line represents cumulative total of adsorbed arsenite as predicted by the CD-MUSIC model. Suspension density = 1 g L^{-1}, background electrolyte 0.01 M $NaNO_3$

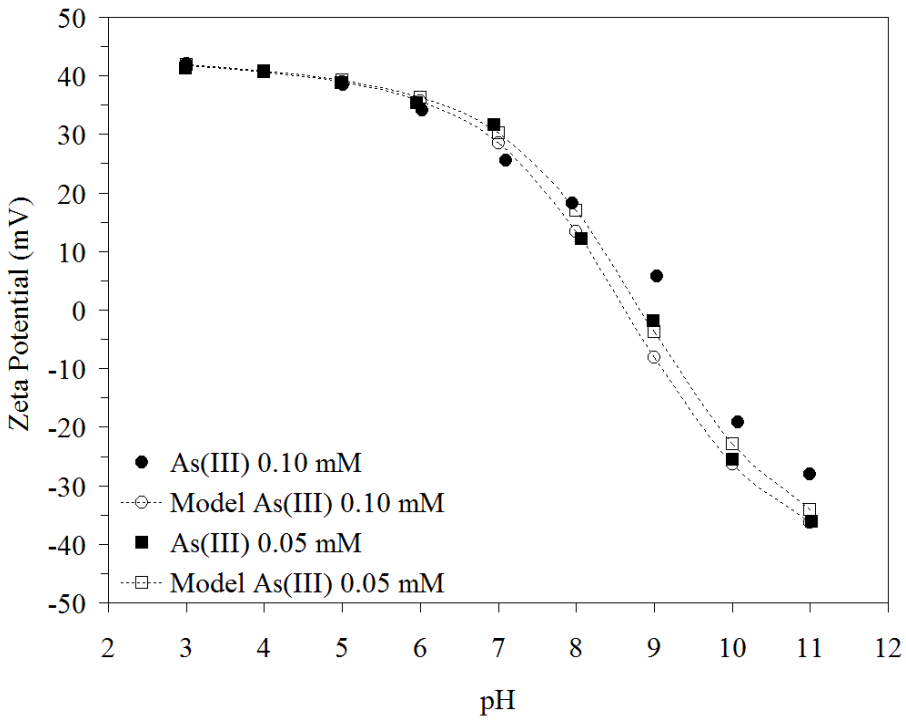

Figure 2.14. Predicted zeta potentials utilizing the CD-MUSIC model. Closed symbols represent experimental zeta potential data. Solid line represents zeta potential data for goethite in the absence of silicic acid and arsenite. Dashed lines represent model predicted zeta potentials assuming the plane of shear is located 2.5 nm from the 2-plane. Suspension density = 1 g L^{-1}, background electrolyte 0.01 M $NaNO_3$

As a first attempt at modeling arsenite adsorption, only bidentate species were considered, in accordance with spectroscopic evidence presented by Manning et al. (1998) and Sun and Doner (1996). While the CD-MUSIC model was able to describe arsenite adsorption using only bidentate species, it was unable to accurately predict the zeta potential data. Several model parameters were varied to try to improve the prediction of the zeta potential measurements; however the only way to accurately model the data was to allow for the formation of a monodentate surface complex.

Silicic acid adsorption on goethite was modeled using one set of equilibrium constants for all three concentrations. The modeling results for all three initial solution concentrations are

presented in Figure 2.15. Four possible surface complexes were used to model silicic acid adsorption on goethite and are listed in Table 2.8 along with their CD-MUSIC optimized intrinsic equilibrium constants. Potential silicic acid surface species were chosen based on solution species present in the pH range investigated (Fig. 2.16) (Applin, 1987; Smith and Martel, 1992)

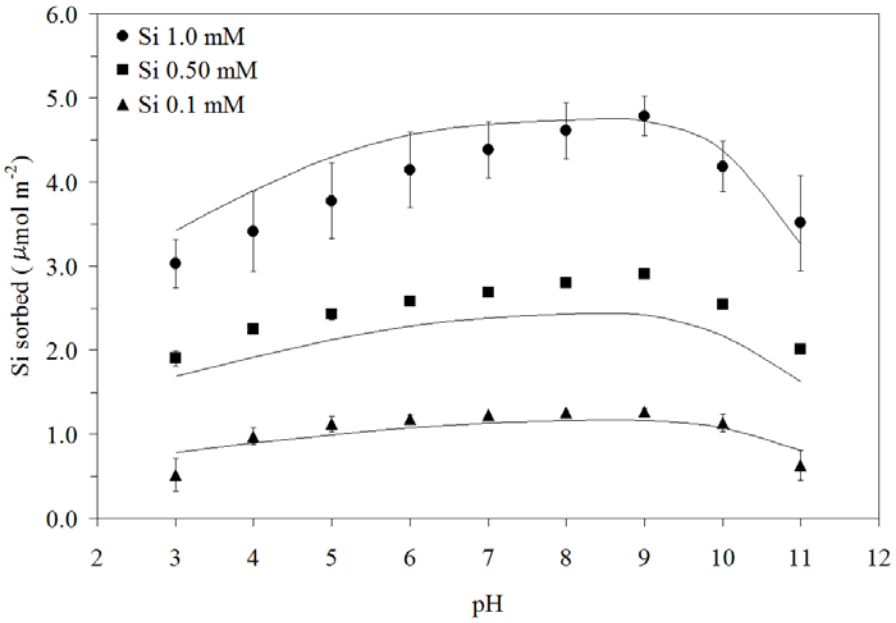

Figure 2.15. Silicic acid adsorption on goethite utilizing the CD-MUSIC model at three Si concentrations, 0.10, 0.50, and 1.00 mM. Solid symbols represent adsorption data. Solid lines represent predicted model concentrations Suspension density = 1 g L^{-1}, background electrolyte 0.01 M $NaNO_3$.

Table 2.9. Silicic acid surface species and CD-MUSIC optimized equilibrium constants.

Surface Complex	Surface Complex Abbreviation	Log K
$\equiv FeOSiO(OH)_2^{1.5-}$	$Fe\text{-}Si^{0.5-}$	17.66
$\equiv FeOSi(OH)_3^{0.5-}$	$Fe\text{-}Si^{1.5-}$	26.78
$\equiv Fe_2O_2SiOOH^{2-}$	$Fe\text{-}Si^{1-}$	22.67
$\equiv Fe_2O_2Si(OH)_2^{1-}$	$Fe\text{-}Si^{2-}$	32.19

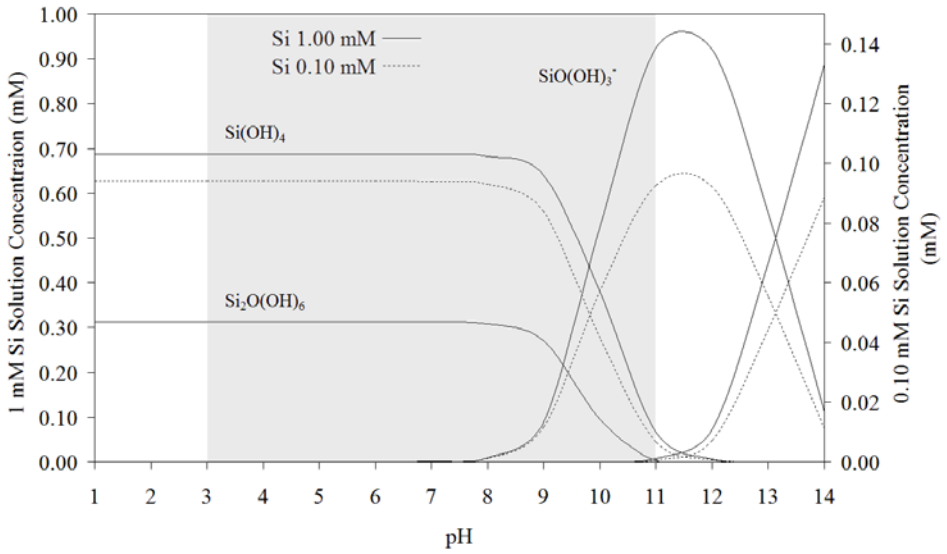

Figure 2.16. Silicic acid solution speciation data. The shaded region represents the pH range investigated in the current study.

The equilibrium constants presented in Table 2.9 were calculated using the 1.00 mM adsorption data and then adjusted to improve the model fit at the two lower Si concentrations. The CD-MUSIC model was able to adequately describe the adsorption behavior of silicic acid for the concentration investigated, as shown in Figure 2.15. The zeta potential predictions (Fig. 2.17) also generally capture the adsorption behavior of silicic acid on goethite, although the predicted values were slightly more positive than experimentally determined values in the circumneutral pH range.

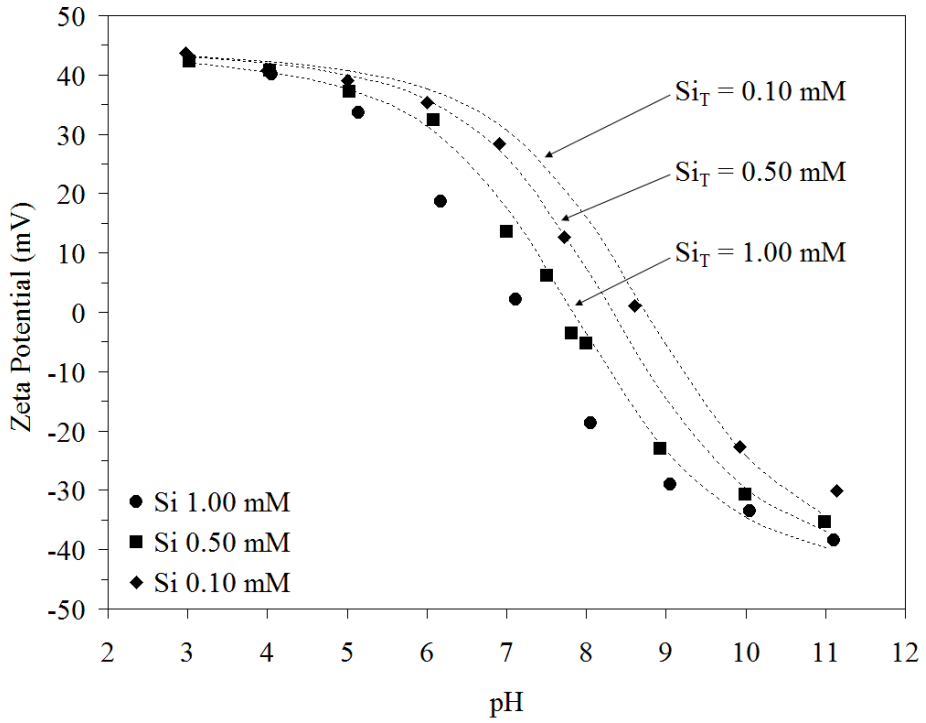

Figure 2.17. Predicted zeta potentials utilizing the CD-MUSIC model. Closed symbols represent experimental zeta potential data. Solid line represents zeta potential data for goethite in the absence of silicic acid and arsenite. Dashed lines represent model predicted zeta potentials assuming the plane of shear is located 2.5 nm from the 2-plane.

The CD-MUSIC model was better able to describe the zeta potential data below pH 6 and above pH 9 where zeta potential values exceeded ±25 mV (where the influence of surface charge is greatest). Additionally, the model was able to more accurately predict zeta potential measurements at lower loading rates as compared to the high loading rate of 1.00 mM. This could be due in part to a change in the location of shear plane, or the charge associated with the modeled Si surface complexes does not accurately describe the species present at the goethite surface. If the location of the plane of shear moves with increasing Si concentration then there should be a general reduction or increase in zeta potential values over the entire pH range (Fig. 2.18), and not in an isolated pH range as is seen in Figure 2.17 with the Si 1.00 mM concentration.

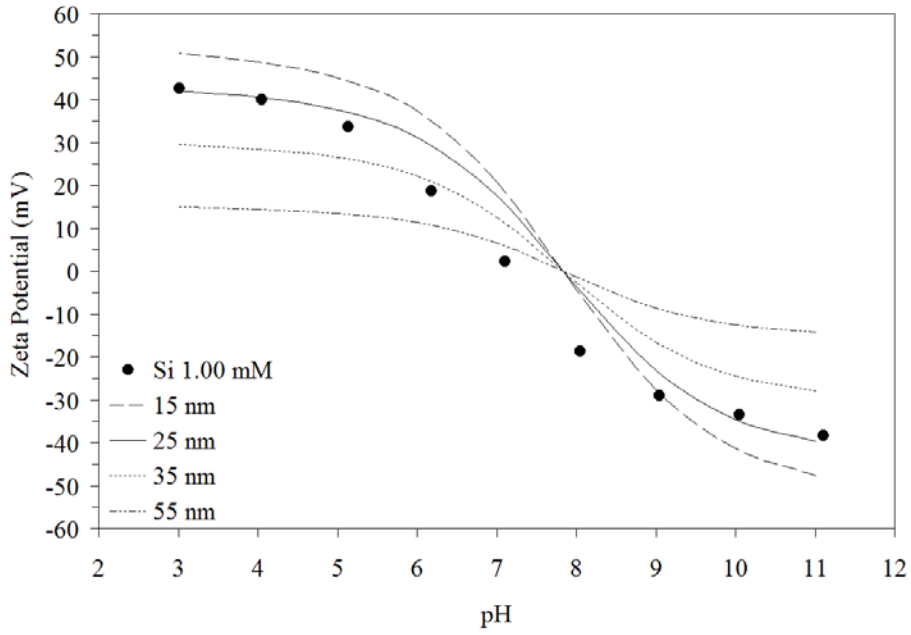

Figure 2.18. The influence of the distance to the plane of shear on zeta potential measurements. Closed symbols represent experimental data. Lines represent the CD-MUSIC predicted zeta potentials for 15 to 55 nm distances from the 2-plane.

The difference between the model predicted and experimental zeta potential values from pH 6-9 are more likely due to an inaccurate representation of the Si surface complex species. Because all of the potential monomer surface complexes have been considered, the use of Si polymers species may provide a better description of the zeta potential data. Additionally, the inclusion of polymeric surface species may also improve the CD-MUSIC model fit to the adsorption data. However, currently no attempt has been made to use the CD-MUSIC model to predict adsorbate polymerization or nucleation on mineral surfaces, and the ability of the CD-MUSIC model to consider the possibility is unclear.

Determining a single set of equilibrium constants that adequately describe silicic acid adsorption on goethite was problematic. Numerous combinations of the four species, adjustment of the charge distribution factor (f), and inclusion of polymeric Si surface species were considered.

However, no one adjustment was able to further improve the model fit to experimental data shown in Figure 2.15. Adjustment of other model parameters such as the CD factor *f* or inclusion of polymeric surface species may improve the model fit to experimental adsorption data. However, indiscriminant variation of model parameters, without experimental justification, defeats the purpose of mechanistic surface complexation modeling and transforms the process into a curve fitting exercise. Due to the lack of direct evidence to confirm the presence of Si polymer formation on the goethite surface, it was not considered in the model presented in Figure 2.15 and the species in Table 2.9.

For all three Si concentrations the two most predominant surface complexes were the $Fe\text{-}Si^{0.5-}$ and $Fe\text{-}Si^{1-}$species, as shown in Figure 2.19. At the low Si concentration the two bidentate complexes ($Fe\text{-}Si^{1-}$; $Fe\text{-}Si^{2-}$) accounted for nearly 85% of the predicted surface species over the entire pH range (Fig. 2.19). However, as silicic acid concentration was increased, the monodentate species $Fe\text{-}Si^{0.5-}$ becomes increasingly more prominent, and accounts for approximately 75% of the surface species when the pH is less than 10. Similar trends in surface speciation for other oxyanions (a shift from bidentate to monodentate speciation with increased surface coverage) have been reported in the literature (Tadanier and Eick, 2003). Figure 2.19 also indicates that $Fe\text{-}Si^{1.5-}$ is not a significant surface species at any of the three silicic acid concentrations.

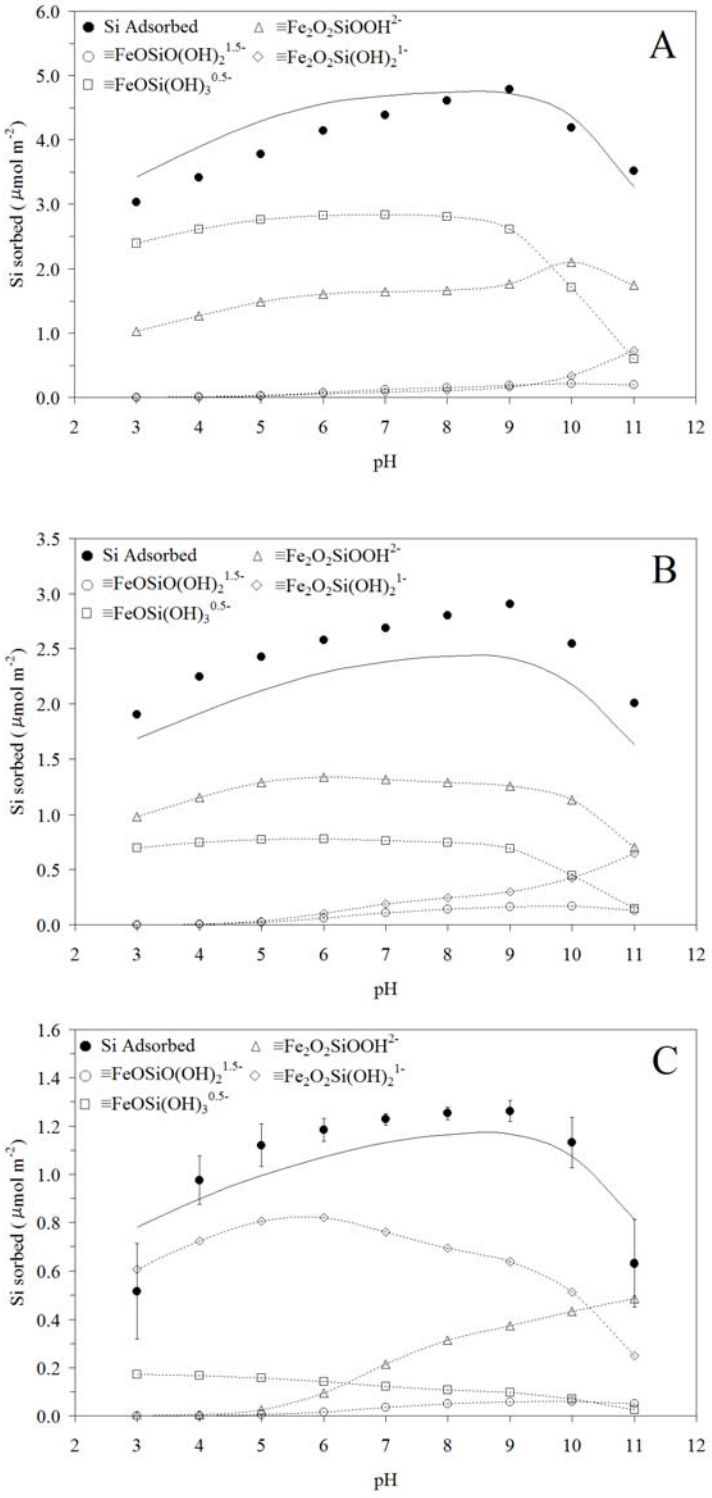

Figure 2.19. Silicic acid adsorption on goethite utilizing the CD-MUSIC model. A) Si_T = 1.00 mM, B) Si_T = 0.50 mM, and C) Si_T = 0.10mM. Closed symbols represent experimental data. Open symbols and dashed lines represent adsorbed Si species based on optimized CD-MUSIC model fit to experimental data. Solid line represents cumulative total of adsorbed Si species as predicted by the CD-MUSIC model. Suspension density = 1 g L^{-1}, background electrolyte 0.01 M $NaNO_3$

Competitive Anion Adsorption

The competitive adsorption of silicic acid and arsenite on goethite was modeled using the CD-MUSIC model optimized equilibrium constants generated for the single anion adsorption modeling (Table 2.10). The results of the low Si concentration modeling are presented in Figure 2.20. The CD-MUSIC model was able to accurately predict arsenite adsorption at both concentrations, but under-predicted silicic acid adsorption at low pH for both arsenite concentrations (Fig. 2.20 A and B solid line). Recently, Arai et al. (2001) reported the presence of outer-sphere adsorption of arsenite on γAl_2O_3. In an effort to improve the predicted silicic acid adsorption, we introduced outer-sphere arsenite that interacted with triply coordinated hydroxyls ($Fe_3OH—AsO(OH)_2^{1-}$). By allowing for the formation of this additional complex, additional singly coordinated hydroxyl sites are available for complexation with silicic acid. The equilibrium constant for the outer sphere arsenite complex was optimized for both arsenic concentrations. The model results that include the arsenite outer sphere complex are also presented in Figure 2.20 (dashed lines), and the equilibrium constant are listed in Table 2.10.

Table 2.10. Silicic acid and arsenite surface species and CD-Music optimized equilibrium constants

Surface Complex	Surface Complex Abbreviation	Log K
$\equiv FeOSiO(OH)_2^{1.5-}$	$Fe\text{-}Si^{0.5-}$	17.66
$\equiv FeOSi(OH)_3^{0.5-}$	$Fe\text{-}Si^{1.5-}$	26.78
$\equiv Fe_2O_2SiOOH^{2-}$	$Fe\text{-}Si^{1-}$	22.67
$\equiv Fe_2O_2Si(OH)_2^{1-}$	$Fe\text{-}Si^{2-}$	32.19
$\equiv FeOAsO_2^{2.5-}$	$Fe\text{-}As^{2.5-}$	23.92
$\equiv FeOAsOOH^{1.5-}$	$Fe\text{-}As^{1.5-}$	33.14
$\equiv FeOAs(OH)_2^{0.5-}$	$Fe\text{-}As^{0.5-}$	47.73
$\equiv Fe_2O_2AsO^{2-}$	$Fe\text{-}As^{2-}$	37.55
$\equiv Fe_2O_2As(OH)_2^{1-}$	$Fe\text{-}As^{1-}$	46.77
$\equiv Fe_3OH—AsO(OH)_2^{1-}$	$Fe_3\text{-}As^{1.5-}$	50.91

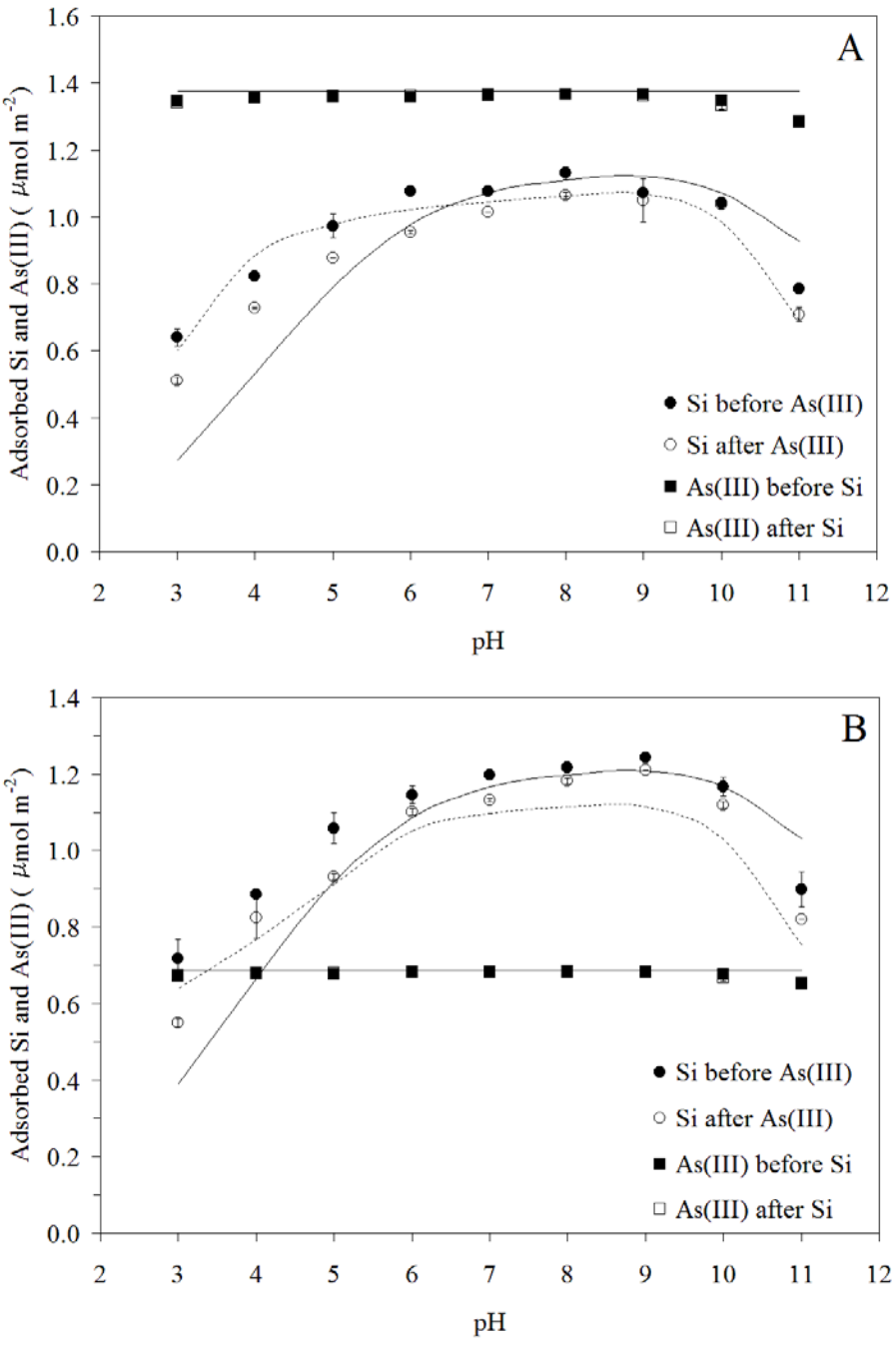

Figure 2.20. Silicic acid and arsenite adsorption on goethite utilizing the CD-MUSIC optimized equilibrium constants generated for the single anion adsorption systems. Symbols represent experimental data. Solid lines represent cumulative arsenite and silicic acid adsorption predicted by the CD-MUSIC model optimized equilibrium constants. Dashed lines represent cumulative arsenite and silicic acid adsorption predicted by the CD-MUSIC model for arsenite bonding by both inner- and outer- sphere mechanisms. A) $As(III)_T$ = 0.10 mM and Si_T = 0.10 mM and B) $As(III)_T$ = 0.05 mM and Si_T = 0.10 mM. Suspension density = 1 g L^{-1}, background electrolyte 0.01 M $NaNO_3$

The introduction of the outer-sphere arsenite complex slightly improved the predicted silicic acid adsorption for low pH at both arsenite concentrations, but degraded the model prediction of silicic acid adsorption above pH 6 for the arsenite 0.10 mM concentration. Improved model predictions may be obtained through optimizing the inner and outer Helmholtz factors. Failure to optimize the capacitance factors poses a particular problem with the OHL, due to the additional negative charge in the layer when the outer-sphere arsenite complex is included in the model.

The results of the modeled zeta potential data for the low Si competitive adsorption scenarios are presented in Figure 2.21. As with the model prediction of adsorption data, the impact of including the outer-sphere arsenite complex in the model fit to zeta potential data was pH dependent. Neither model (arsenite binding by only inner-sphere or inner- and outer-sphere mechanisms) fit the low Si zeta potential data appreciably better over the entire pH range investigated. The model predictions of both adsorption and zeta potential data indicate that further refinement in either surface species or other model parameters may be warranted.

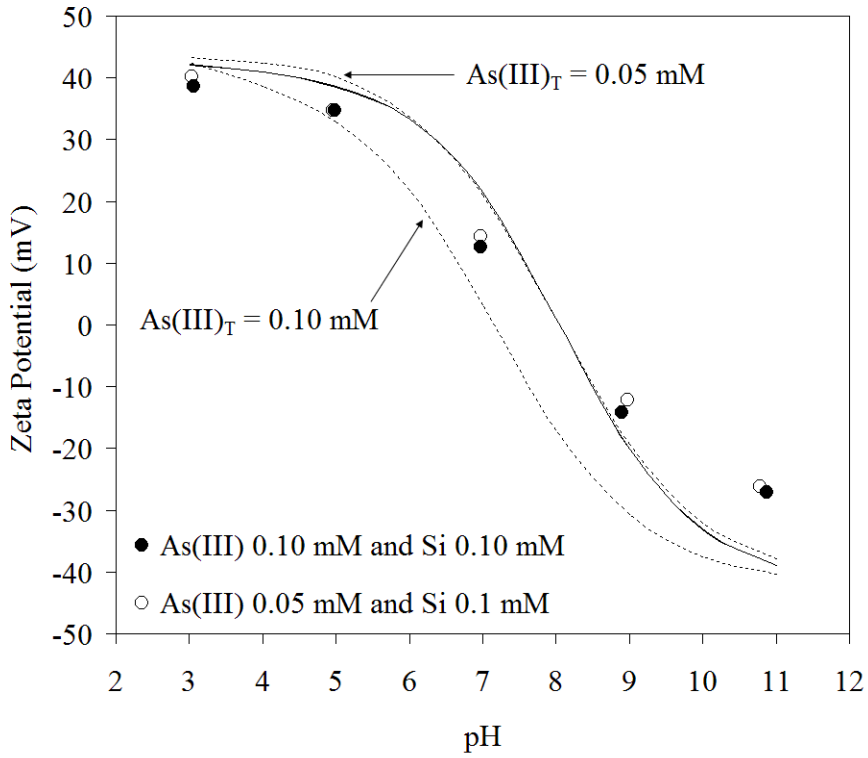

Figure 2.21. Calculated zeta potentials utilizing the CD-MUSIC model for the competitive adsorption of the low Si concentration (0.10 mM) scenarios. Symbols represent experimental data. Solid line represents predicted zeta potentials for arsenite binding by only inner-sphere mechanisms. Dashed line represents predicted zeta potentials for arsenite binding by both inner and outer-sphere mechanisms. Suspension density = 1 g L^{-1}, background electrolyte 0.01 M $NaNO_3$

The CD-MUSIC modeling results for the high Si competitive adsorption are presented in Figure 2.22 and the equilibrium constants used for modeling are presented in Table 2.11. As with the low Si scenarios arsenite adsorption was modeled once considering only inner-sphere binding (solid lines) and considering both inner- and outer-sphere adsorption (dashed lines). Our model significantly under-predicted silicic acid adsorption for both arsenite concentrations regardless of the arsenite binding mechanism. Attempts to further refine the equilibrium constant for the outer-sphere arsenite complex, using the high Si adsorption data, did not significantly improve model prediction of silicic acid adsorption. Therefore, this equilibrium constant was used without further optimization.

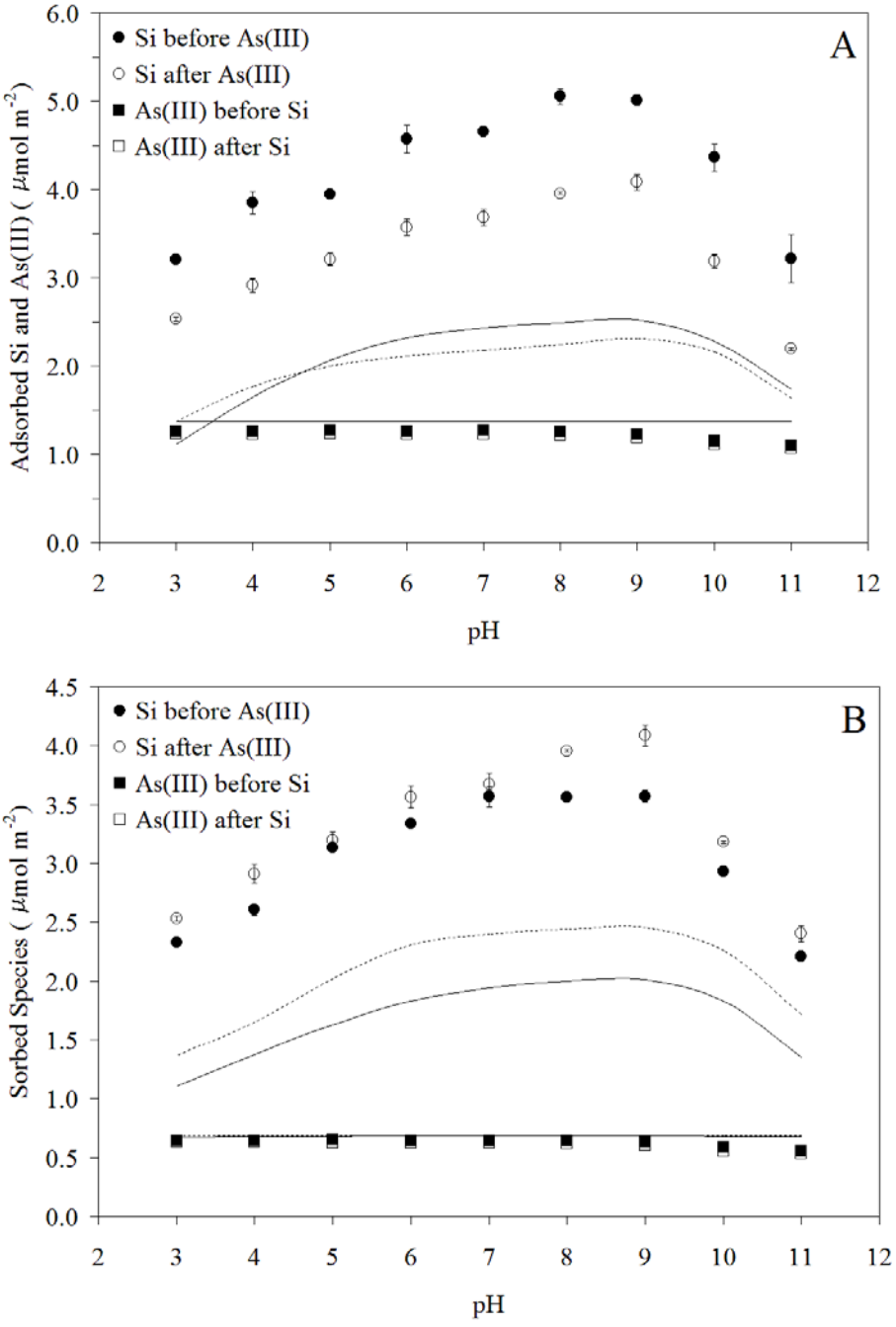

Figure 2.22. Silicic acid and arsenite adsorption on goethite utilizing the CD-MUSIC optimized equilibrium constants generated for the single anion adsorption systems. Symbols represent experimental data. Solid lines represent cumulative arsenite and silicic acid adsorption predicted by the CD-MUSIC model optimized equilibrium constants. Dashed lines represent cumulative arsenite and silicic acid adsorption predicted by the CD-MUSIC model for arsenite bonding by both inner- and outer- sphere mechanisms. A) $As(III)_T$ = 0.10 mM and Si_T = 1.00 mM and B) $As(III)_T$ = 0.05 mM and Si_T = 1.00 mM. Suspension density = 1 g L^{-1}, background electrolyte 0.01 M $NaNO_3$

The zeta potential predictions for the high Si scenario are presented in Figure 2.23. The predicted zeta potentials for the competitive adsorption for the high Si concentration were over- and under-estimated at low and high pH values, respectively.

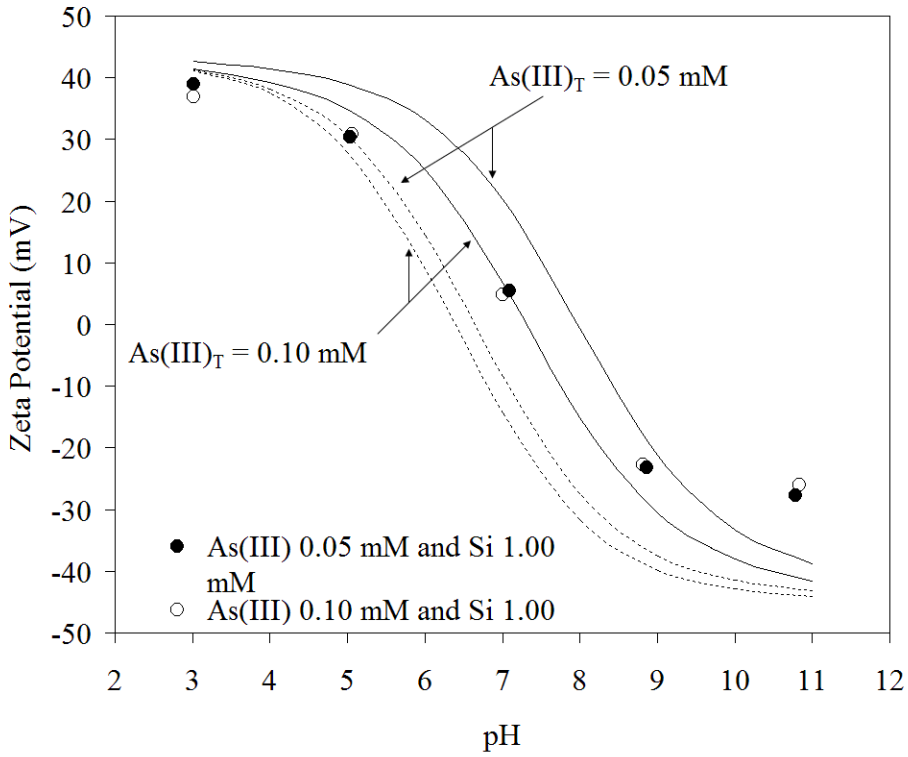

Figure 2.23. Calculated zeta potentials utilizing the CD-MUSIC model for the competitive adsorption of the high Si concentration (1.00 mM) scenarios. Symbols represent experimental data. Solid line represents predicted zeta potentials for arsenite binding by only inner-sphere mechanisms.

The under-predicted adsorption of silicic acid by the CD-MUSIC model is due to the lack of sufficient singly coordinated adsorption sites. If only monodentate species are considered over 80% of the surface sites are occupied by silicic acid or arsenite above pH 4 (based upon the surface site density calculations of Barrón and Torrent (1996)). Additionally at pH 9 and 10 for arsenite at the 0.10 mM concentration, the surface coverage exceeds 90%. In contrast, predicted surface coverage never exceeded 70% using our model, either with or without the formation of arsenite outer-sphere complexes. If Si polymers formed at the goethite surface, the number of

singly coordinated surface sites participating in surface complexes would more than likely decrease enabling singly coordinated hydroxyl groups to participate in charge balancing reactions. Additionally, Si polymer formation would influence the charge constraints used in the model, possibly allowing for improved predictions. The model fit may also be improved by including inner-sphere adsorption at triply coordinated sites; however, there is no precedent in the literature for this practice.

Conclusions

Silicic acid adsorption was reduced by the presence of arsenite for all but one of the competive adsorption scenarios investigated, indicating that arsenite is the more stable surface species. For all of the competitive adsorption scenarios investigated, 95% or more of the arsenite was removed from solution, indicating that silicic acid does not dramatically influence arsenite adsorption on goethite for the conditions investigated. However, silicic acid does increase the arsenite equilibrium solution concentration by three orders of magnitude at the 1.00 mM silicic acid concentration between pH 3 and 9 for both arsenite concentrations examined. These results are of critical importance considering that most soils and sediments contain dissolved silica concentrations close to those used in the current study. Furthermore, silicic acid is not currently considered as a chemical parameter when predicting arsenite mobility and bioavailability in the environment (Chappell et al., 1997; Nickson et al., 2000; Sadiq, 1997; Tamaki and Frankenbeger, 1992). Additionally, the increased arsenite solution concentration provides a possible explanation for the increased mobility of arsenite in the environment as noted by Tamaki and Frankenbeger (1992).

The CD-MUSIC model was able to predict the single ion adsorption behavior of silicic acid and arsenite on goethite. The modeled zeta potential data provided further evidence of the CD-MUSIC model's ability to describe the single anion adsorption on goethite. Our model was also able to collectively describe adsorption and zeta potential data for the low Si-arsenite adsorption scenario quite well, however the model under-predicted silicic acid adsorption for the high Si-arsenite competitive scenario. Additional spectroscopic studies of silicic acid adsorption on goethite may help elucidate the formation of silica polymeric species that could be used in the model.

We observed a decrease in the value of the isoelectric point for silicic acid and arsenite adsorption on goethite, which is consistent with formation of inner-sphere complexes. Although the formation of outer-sphere arsenite surface complexes has been identified in certain arsenite-mineral systems, inclusion of outer-sphere surface-complexes did not appreciably improve the fit of our model to the experimental data. Based on the current results there is insufficient evidence to definitively conclude that outer-sphere arsenite complexes existed for the conditions investigated. However, if present, outer-sphere surface complexes are known to be less stable than those bound by inner-sphere mechanisms, potentially making them more bioavailable and mobile in soils and sediments (McBride, 1994; Sparks, 1999; Sposito, 1984; Stumm, 1992). This offers yet another possible explanation of the increased mobility of arsenite in soils and sediments.

References

Alverez, R., and D.L. Sparks. 1985. Polymerization of silicate anions in solutions at low concentrations. Nature 318:649-651.

Applin, K.R. 1987. The diffusion of dissolved silica in dilute aqueous solution. Geochimica et Cosmochimica 51:2147-2151.

Arai, Y., E.J. Elzinga, and D.L. Sparks. 2001. X-ray absorption spectroscopic investigation of arsenite and arsenate adsorption at the aluminum oxide-water interface. Journal of Colloid and Interface Science 235:80-88.

Barrón, V., and J. Torrent. 1996. Surface hydroxyl Configuration of various Crystal Faces of Hematite and Goethite. Journal of Colloid and Interface Science 177:407-410.

Chappell, W.R., B.D. Beck, K.G. Brown, R. Chaney, C.R. Cothern, K.J. Irgolic, D.W. Norh, and I. Thorton. 1997. Inorganic arsenic: a need and an opportunity to improve risk assessment. Environmental Health Perspectives 105:1060-1066.

Dove, P.M., and J.P. Rimstidt. 1994. Silica-Water Interactions, p. 237-308, *In* P. J. Heaney, et al., eds. Silica physical behavior, geochemistry and material applications, Vol. 29. Mineralogical Society of America, Washington D.C.

Geelhoed, J.S., T. Hiemstra, and W.H. Van Riemsdijk. 1997. Phosphate and sulfate adsorption of goethite: Single anion ands competitive adsorption. Geochimica et Cosmochimica Acta 61:2389-2396.

Geelhoed, J.S., T. Hiemstra, and W.H. Van Riemsdijk. 1998. Competitive interaction between phosphate and citrate on goethite. Environmental Science and technology 32:1219-1223.

Goldberg, S. 1985. Chemical modeling of anion competition on goethite using the constant capacitance model. Soil Science Society of America Journal 49:851-856.

Goldberg, S., and C. Johnston. 2001. Mechanisms of arsenic adsorption on amorphous oxides evaluated using macroscopic measurements, vibrational spectroscopy, and surface complexation modeling. Journal of Colloid and Interface Science 234:204-216.

Grafe, M., M.J. Eick, and P.R. Grossl. 2001. Adsorption of arsenate (V) and arsenite (III) on goethite in the presence and absence of dissolved organic carbon. Soil Science Society of America Journal 65:1680-1687.

Grafe, M., M.J. Eick, P.R. Grossl, and A.M. Saunders. 2002. Adsorption of arsenate and arsenite on ferrihydrite in the presence and absence of dissolved organic carbon. Journal of Environmental Quality 31:1115-1123.

Gustafsson, J.P. 2001. Modeling competitive anion adsorption on oxide minerals and an allophane soiling soil. European Journal of Soil Science 52:639-653.

Hansen, H.C.B., B. Rabenlange, K. Raulundrasmussen, and O.K. Borggaard. 1994a. Monosilicate adsorption by ferrihydrite and goethite at pH 3-6. Soil Science 158:40-46.

Hansen, H.C.B., T.P. Wetche, K. Raulund-Rasmussen, and O.K. Borggaard. 1994b. Stability constants for silicate adsorbed to ferrihydrite. Clay Minerals 29:341-350.

Hetzl, F., and J.G. McColl. 1997. Silicon, aluminum, and oxalic acid interactions in two California forest soils. Communications in Soil Science, Plant Analysis 28:1209-1222.

Hiemstra, T., W.H. Van Riemsdijk, and G.H. Bolt. 1989a. Multisite proton adsorption modeling at the solid/solution interface of (hydr)oxides: A new approach

I. Model description and evaluation of intrinsic reaction constants. Journal of Colloid and Interface Science 133:91-104.

Hiemstra, T., J.M.C. De Wit, and W.H. Van Riemsdijk. 1989b. Multisite proton adsorption

modeling at the solid/solution interface of (hydr)oxides: a new approach II. Application to various important (hydr)oxides. Journal of Surface and Interface Science 133:105-115.

Hiemstra, T., P. Venema, and W.H. Van Riemsdijk. 1996. Intrinsic proton affinity of reactive surface groups of metal (hydr)oxides: the bond valence principal. Journal of Colloid and Interface Science 184:680-692.

Hiemstra, T., and W.H. Van Reinsdijk. 1996. A surface structural approach to ion adsorption: the charge distribution (CD) model. Journal of Colloid and Interface Science 179:488-508.

Hiemstra, T., and W.H. Van Riemsdijk. 1999. Surface structural ion adsorption modeling of competitive binding of oxyanions by metal (hydr)oxides. Journal of Colloid and Interface Science 210:182-193.

Hiemstra, T., and W.H. Van Reimsdijk. 2000. Flouride adsorption on goethite in relation to different types of surface sites. Journal of Colloid and Interface Science 225:94-104.

Hingsten, F.J., A.M. Posner, and J.P. Quirk. 1972. Anion adsorption by goethite and gibbsite I. The role of the proton in determining adsorption envelopes. Journal of Soil Science 23:177-192.

Iller, R.K. 1979. The chemistry of Silica Jon Wiley & Sons, New York.

Kosmulski, M. 2001. Chemical properties of material surfaces Marcel Dekker, Inc., New York.

Loeppert, R.L., and W.P. Inskeep. 1996. Iron, *In* D. L. Sparks, ed. Methods of Soil Analysis, Part 3. SSSA Book Ser. No. 5. SSSA, Madison, WI.

Manning, B.A., S.E. Fendorf, and S. Goldberg. 1998. Surface structures and stability of As(III) on goethite: evidence for inner sphere complexes. Environmental Science and Technology 32:2383-2388.

McBride, M.B. 1994. Environmental Chemistry of Soils Oxford Press, New York.

McKeague, J.A., and M.G. Cline. 1963a. Silica in soil solutions II. The adsorption of monosilicic acid by soil and by other substances. Canadian Journal of Soil Science 43:83-96.

McKeague, J.A., and M.G. Cline. 1963b. Silica in soil solutions I. The form and concentration of dissolved silica in aqueous extracts of some soils. Canadian Journal of Soil Science 43:70-82.

Meng, X.G., S. Bang, and G.P. Korfiatis. 2000. Effects of silicate, sulfate, and carbonate on arsenic removal by ferric chloride. Water Research 34:1255-1261.

Obihara, C.H., and E.W. Russell. 1972. Specific adsorption of silicate and phosphate by soils. Journal of Soil Science 23:105-117.

Parks, G.A. 1990. Surface energy and adsorption at mineral water interfaces: an introduction, p. 133-169, *In* M. F. J. Hochella and A. F. White, eds. Mineral-Water Interface Geochemistry, Vol. 23. Mineralogical Society of America, Washington D. C.

Reitra, R.P.J.J., T. Hiemstra, and W.H. Van Riemsdijk. 1999. The relationship between molecular structure and ion adsorption on variable charge minerals. Geochimica et Cosmochimica Acta 63:3009-3015.

Rietra, R.P.J.J., T. Hiemstra, and W. Reimsdijk. 1999. Sulfate Adsorption on Goethite. Journal of Colloid and Interface Science 218:511-521.

Rietra, R.P.J.J., T. Hiemstra, and W.H. Van Riemsdijk. 2000. Electrolyte anion affinity and its effect on oxyanion adsorption on goethite. Journal of Colloid and Interface Science 229:199-206.

Sadiq, M. 1997. Arsenic Chemistry in soils: an overview of thermodynamic predictions and field observations. Water, Air, and Soil Pollution 93:117-136.

Schwertmann, U., and R.M. Cornell. 1991. Iron oxides in the labratory: preparation and

characterization VCH, Weinheim, FR of Germany.

Schwertmann, U., and R.M. Cornell. 1996. The iron oxides: structures, propoerties, reactions, occurrence and uses VCH, Weinheim, FR of Germany.

Sigg, L., and W. Stumm. 1981. The interaction of anions and weak acids with the hydrous goethite (α-FeOOH)surface. Colloids and Surfaces 2:101-117.

Sillén, L.G., and A.E. Martell. 1964. Stability complexes of metal ion complexes. 2nd edition. The Chemical Society of London.

Smith, R.M., and A.E. Martel. 1992. Critical Stability Constants Plenum Press, New York.

Sposito, G. 1989. The Chemistry of Soils Oxford University Press, New York.

Sun, X., and H.E. Doner. 1996. An investigation of arsenate and arsenite bonding structures on goethite by FTIR. Soil Science 161 12.

Swedlund, P.J., and J.G. Webster. 1999. Adsorption and polymerisation of silicic acid on ferrihydrite, and its effect on arsenic adsorption. Water Research 33:3413-3422.

Tadanier, C.J., and M.J. Eick. 2002. Formulating the charge-distribution multisite surface complexation model using FITEQL. Soil Science Society of America 66:1505-1517.

Tadanier, C.J., and M.J. Eick. 2003. Phosphate adsorption on goethite.

Tamaki, S., and W.T. Frankenbeger. 1992. Environmental chemistry of arsenic, p. 79-110 Reviews of environmental contamination and toxicology, Vol. 124. Springer-Verlag, New York.

Vempati, R.K., R.H. Loeppert, D.C. Dufner, and D.L. Cocke. 1990. X-ray photoelectron spectroscopy as a tool to differentiate silicon-bonding state in amorphous iron oxides. Soil Science Society of America 54:695-698.

Waltham, C., and M.J. Eick. 2002. Kinetics of arsenic adsorption on goethite in the presence of

sorbed silicic acid. Soil Science Society of America 66:818-825.

Curriculum Vitae

Todd Peter Luxton

Current Address
Department of Crop and Soil Environmental Science
VPI&SU
Blacksburg, VA 24061-0404
(540) 231-6539 (office)
(540) 552-2933 (home)
tluxton@vt.edu

Permanent Address
10067 Oakridge Dr
Wexford, PA 15090

Education

Virginia Polytechnical Institute and State University
Blacksburg, VA 24061
M.S. in Crop and Soil Environmental Sciences (Emphasis Environmental Soil Chemistry)—Graduated December 2002
Thesis Topic: The Competitive Adsorption on Mono Silicic Acid and Arsenite on Goethite
Thesis Advisor: Dr. Matthew Eick,
Cumulative GPA 3.44

The Pennsylvania State University
State College, PA
B.S in Environmental Soil Science—Graduated May 2000
Minor in Geosciences
Major and Minor GPA 3.5
Cumulative GPA 3.0

Research/Work Experience

Master's Research, Department of Crop and Soil Environmental Sciences, Virginia Polytechnic Institute and State University (August 2000 through December2002)

- Designed and developed experiments for analyzing the equilibrium competitive adsorption of dissolved silica and arsenite (As III) on goethite a common soil iron hydroxide
- Modeled the surface complexation reactions for the competitive adsorption of dissolved silica and arsenite onto the goethite mineral surface utilizing the CD Music (charge distribution and ionic composition) surface complexation model implemented through FITEQL 4.0 and Visual MINTEQ.
- Conducted electrophoretic mobility experiments with goethite and dissolved silica and arsenite coated goethite surfaces to determine changes in surface potential due adsorbing oxyanions and offer validation to complexation modeling results

- Designed experiments to determine the influence of dissolved silica on the adsorption rate of arsenite, and chromate onto the goethite mineral surface
- Oversaw laboratory equipment and supplies
- Maintained laboratory equipment including pH titration units, Micromeritics Specific Surface Area Analyzer, Malvern Zeta Meter, and Beckman UV-Vis Spectrophotometer
- Preparing two manuscripts for publication

Research Technician for Lee Daniels, Professor of Soil Science, in the Department of Crop and Soil Environmental Science Department, Virginia Polytechnic Institute and State University(May 2002 through Agust2002)

- Conducted Total Characterization Leaching Procedure (TCLP) analysis on Adam's Process treated Department of Energy waste materials
- Designed toxicity tests for estimating heavy metal bioavailability utilizing Eisenia fetida (earthworms)
- Conducted greenhouse experiments assessing the ability of calcium carbonate amended biosolids to neutralize acidity and support vegetative growth on surface exposed sulfide mineral sediments
- Designed denitrification studies for biosolid amended mine spoil soils

Environmental Consultant at Crouse and Company, Pittsburgh, PA (May 2000 through August 2000)

- Participated in Phase 1 and 2 site assessments
- Prepared mass balances for toxic chemical release inventories in accordance with EPCRA Section 313
- Gained experience in planning, designing, and constructing residential onsite waste disposal systems
- Worked closely with project managers in the write-up and presentation of project finding and conclusions.

Undergraduate Research with Jon Chorover Professor of Environmental Soil Chemistry at The Pennsylvania State University (May1999 through May 2000)

- Designed and developed experiments for analyzing the influence of dissolved organic mater, at several concentrations, on the kinetics of lead release from lead contaminated rifle range soils
- Collected stream water and bulk density soil samples for laboratory analysis
- Conducted research in the dynamics of lead release from soil

Laboratory Assistant for Peter Deines Professor of Geochemistry at The Pennsylvania State University (June 1996 through August 1996)

- Prepared crystal samples for laboratory analysis
- Maintained laboratory equipment
- Photographed mineral thin slices under various forms of radiation
- Laboratory Assistant at the USDA Pasture Lab for Bob Byers Professor of Entomology at The Pennsylvania State University (May 1996 through December 1996)
- Maintained clover and alfalfa field plots

- Collected soil, forage, and insect samples at various dairy cattle experiment sites
- Identified forage and insect specimens
- Developed database for data collection and analysis

Instructional Experience

Teaching Assistant at Virginia Polytechnic Institute and State University, Blacksburg, VA (August 2002 through Present)

- Laboratory Instructor for two undergraduate introductory soil science courses: Soils in the Landscape (non-major) and Introductory Soil Science (major)
- Teaching Assistant for Principals of Environmental Science
- Developed practical laboratory exercises to introduce and familiarize undergraduate students with fundamental principals of soil chemistry and bioavailability
- Worked closely with supervising professor to revise and update laboratory text
- Planned weekly lectures introducing concepts, theories, and procedures pertinent to laboratory exercises
- Helped prepare, graded assignments and exams

The Scheyer Institute for Innovation in Learning at The Pennsylvania State University, State College, PA (January 1996 through Amy 1997)

- Helped to develop innovative classroom techniques to facilitate collaborative learning
- Developed and facilitated a quality control circle devoted to evaluating collaborative learning techniques used in the lecture
- Participated in University sponsored workshops on establishing a collaborative learning environment in the college classroom
- Participated as a panel member on a discussion of "The Pitfalls of Collaborative Learning in the College Classroom" at the 1996 Higher Education Conference in Washington, D.C.
- Collected and interpreted data on the effectiveness of collaborative learning techniques

Affiliations

Soil Science Society of America
Virginia Tech Graduate Honor Committee

Honors

Member of the Penn State 2000 first place national soil judging team
College of Agricultural Sciences Undergraduate Research Grant, Spring 2000
Alan F. Blizi Scholarship in Environmental Science, Fall 1999 and Spring 2000
Dean's List (GPA of 3.5 or above) Spring 2002, Spring 2001, Fall 2000, Fall 1999, Fall 1998

Publications

Kogut, L. S. and T. Luxton. 2002. Collaborative learning in general chemistry with CQI monitoring and evaluation. Investigaçoes command post Ensino de Ciênci*as.* Online AT http://www.if.ufrgs.br/public/ensino/revista.htm

Abstracts

Tadanier, C.J., T. Luxton, and M. Eick. 2002. Competitive adsorption of oxyanions. Goldschmidt Conference, Davos, Switzerland.

Luxton, T.P. and M.J. Eick, 2001. Competitive adsorption of monosilicic acid and arsenite on goethite. Soil Science Society of America, Charlotte, NC.

Career Related Skills

- Skilled in the development and implementation of laboratory and field experiments
- Experience with maintaining complex laboratory instruments
- Proficient teaching and presentation verbal communication skills
- Strong data collection and manipulation skills
- Proficient in the use of spreadsheet (Excel and Lotus), data base (Access), graphic (Delta Graph and Sigma Plot), word processing (Word, Word Perfect, and Lotus), statistics programs (SAS)
- Skilled in the use of computer chemical solution modeling programs (MINTEQ and TK Solver) and the chemical surface complexation model program FITEQL